Stability of a single top layer of cubes

Master of Science thesis

September 2009

R. V. van Buchem

Graduation committee:

Prof. Dr. Ir. M.J.F. Stive
Prof. Dr. Ir. W.S.J. Uijttewaal
Ir. H.J. Verhagen
Ir. M. Caljouw

List of trademarks in this report:

- DASYLAB is a registered tradename of Daqpoint Benelux B.V., the Netherlands
- ACCROPODE is a registered trademark of Sogreah Consultants - France

PREFACE

To accomplish the Master of Science program in Civil Engineering, at Delft University of Technology, the stability of a breakwater's top layer armoured with a single layer of cubes was studied. Furthermore, the influence of different slopes and packing densities on the stability was investigated. The study is based on wave flume experiments performed in the Fluid Mechanics Laboratory of the Faculty of Civil Engineering and Geosciences. The preparation as well as the elaboration of the measurements was performed at Witteveen+Bos consulting engineers.

I would like to thank my graduation committee for their supervision and support during the whole process. Furthermore, I would like to thank Witteveen+Bos consulting engineers. for all the support I received. Also I would like to thank all the members of the support staff of the Fluid Mechanics Laboratory for their help and advice during the experiments.

Finally, I would like to thank everyone who assisted me in the realization of this report and helped achieving my goals.

Robin van Buchem

Delft, September 2009

ABSTRACT

In an attempt to reduce the cost of breakwaters, several elements have been developed. Examples are Accropodes, Tetrapods and concrete cubes. Previous tests were performed with armour layers consisting of a double layer of cubes. This study is based on a single layer of cubes. The great benefit of a single layer of cubes is that it reduces the total cost of concrete. Another benefit is that because of the shape, cubes are easy to prefabricate.

Three important aspects considering the stability of a single armour layer of a breakwater consisting of concrete cubes are addressed: The wave steepness, the influence of the slope on the stability of the single armour layer, and the influence of the packing density on the stability of the single armour layer. This study is based on a literature study and the results from a test program including a small-scale physical model tests. All conclusions in this thesis have been based on model tests, in which the cubes were placed by hand and placed in a stretching bond (half-steensverband).

In total eighteen tests were performed in the wave flume of the Fluid Mechanics Laboratory of the Faculty of Civil Engineering and Geosciences. Two different slopes were tested together with three different packing densities and three different wave steepness's. The complete test series are presented in the table below.

Test program of study

Test serie	n_p	cot α	s_{0p}
A	0.20	1.5	0.02-0.06
B	0.28	1.5	0.02-0.06
C	0.35	1.5	0.02-0.06
D	0.20	2.0	0.02-0.06
E	0.28	2.0	0.02-0.06
F	0.35	2.0	0.02-0.06

It was found that the gentler slope did not contribute to the stability in this setting using a stretching bond. In fact the model failed earlier than the model with a steeper slope in most cases. The best results were found using a slope of cotα = 1.5.

Secondly, the influence of the packing density showed varying failure mechanism. When applying a large packing density (n_p = 0.20) the damage occurred below SWL. Contrary to small packing densities (n_p = 0.35) where damage occurred higher than SWL. It was found that, from the tested packing densities, a packing density of 0.28 gives the best results for both slopes.

This conclusion is conform the findings of previous tests [Van Gent et al, 1999]. During these tests an optimum packing density of n_p = 0.25 – 0.30 was found. Although the cubes were placed randomly in the tests of Van Gent. In this study the cubes were placed in a stretching bond.

Finally it was found that a wave steepness of s_{0p} = 0.04-0.05 causes minimum stability for the armour layer.

The tests with a single armour layer of cubes placed in a stretching bond indicated that high stability numbers ($H_s/\Delta D_n$) can be reached before failure occurs (N_{od} > 0.2). the tests show that stability numbers as high as 4.5 can be realized before N_{od} > 0.2 is reached.

This study shows that the use of a single top layer of cubes is feasible. The top layer becomes very stable when placed in a stretching bond. In this configuration it is recommended to use a single top layer of cubes instead of a double top layer of cubes.

Nevertheless it is recommended to perform more tests in order to generate more data. Especially for the setting of n_p = 0.25 - 0.30 and with the cubes placed in a stretching bond. This configuration proves to be very promising and the maximum stability number for failure wasn't found during this study.

The results during the tests seem to have a strong correlation with pitched stones. Therefore the black box model as well as the analytical method for pitched stones (6-xi-rule) is treated in an attempt to optimize the design rules for different configurations.

Finally, in combination with an adjusted 6-xi-rule and the formulae from Van der Meer for loose rock, formulae were developed based on curve fitting. The formulae are valid for cubes placed in a stretching bond.

For plunging waves $\xi_p < \xi_{cr}$:

$$\frac{H_s}{\Delta D_n} = c_{pl} \cdot \xi_p^{-0.5} \cdot n_p^{0.18} \cdot \cot\alpha^{-0.5}$$

For surging waves $\xi_p \geq \xi_{cr}$:

$$\frac{H_s}{\Delta D_n} = c_s \cdot \xi_p^{2/3} \cdot n_p^{0.13} \cdot \cot\alpha^{0.5}$$

In which: c_s = coefficient for surging waves depending on packing density [-]
c_{pl} = coefficient for plunging waves depending on packing density [-]

The formulae use different coefficients for different breaker types. The coefficients for different wave conditions are found through curve fitting.

Coefficients for breaker types

Packing density [-]	n_p	0.20	0.28	0.35
Coefficient for plunging waves [-]	c_{pl}	8.5	15	10.5
Coefficient for surging waves [-]	c_s	1.1	1.5	1.25

TABLE OF CONTENTS

LIST OF FIGURES

LIST OF TABLES

LIST OF SYMBOLS

a	Accuracy	[mm]
B_{test}	Width of test area	[m]
d_l	Armour layer thickness	[m]
c_s	Coefficient for surging waves	[-]
c_{pl}	Coefficient for plunging waves	[-]
D	Diameter of armour element	[m]
D_n	Nominal diameter armour element	[m]
D_{n50}	Median nominal diameter	[m]
E	Variance density	[m^2s]
f	Frequency	[Hz]
F_D	Drag force	[N]
F_F	Friction force	[N]
F_G	Gravity force	[N]
F_L	Lift force	[N]
Fr	Froude number	[-]
F_S	Shear force	[N]
g	Gravitational acceleration	[m/s^2]
h	Water depth	[m]
h_c	water depth at toe of structure	[m]
$H_{1/10}$	Average of 10% highest waves	[m]
H_{m0}	Significant wave height calculated from the wave spectrum	[m]
H_s	Significant wave height	[m]
H_{so}	Significant wave height deep water	[m]
k_t	Layer thickness coefficient	[-]
K_D	Hudson stability coefficient	[-]
L	Wavelength	[m]
L_o	Deep-water wave length	[m]
M	Mass of an armour unit	[kg]
M_{50}	Median mass of armour element	[kg]
m_0	Zeroth moment of the wave spectrum	[m^2]
m_2	Second moment of the wave spectrum	[m^2/s^2]
n	Sampling range	[-]
n_p	Packing density	[-]
n_L	Prototype to model scale ratio of parameter L	[-]
n_v	Porosity	[%]
N	Number of waves	[-]
N_{cubes}	Number of cubes per m^2	[-]
N_s	Stability number	[-]
N_d	Percentage of displaced units	[%]
N_{od}	Damage number	[-]
P	Notional permeability parameter (loose rock)	[-]
R_c	Elevation of the crest above SWL	[m]
Re	Reynolds number	[-]
s	Wave steepness	[-]
s_m	Wave steepness based on T_m	[-]
s_{m0}	Wave steepness based on T_{m0}	[-]
s_{0p}	Wave steepness based on T_{0p}	[-]
S_d	Damage number (loose rock)	[-]
t	Storm duration	[hour]
T	Wave period	[s]

T_m	Mean wave period	[s]
T_{m0}	Mean wave period deep water	[s]
T_p	Spectral peak period	[s]
T_{0p}	Spectral peak period deep water	[s]
U	Flow velocity	[m/s]
$\bar{U}$	Average flow velocity	[m/s]
V	Volume armour unit	[m^3]
W_{50}	Weight of a unit with a diameter D_{n50}	[kg]
x_m	Model value	[-]
x_p	Prototype value	[-]
z	Reliability	[-]
α	Slope angle	[°]
Δ	Relative mass density	[-]
σ	Standard deviation	[mm]
υ	Kinematic viscosity	[m^2/s]
ρ_c	Mass density concrete armour elements	[kg/m^3]
ρ_w	Mass density water	[kg/m^3]
ξ	Iribarren number	[-]
ξ_{0p}	Iribarren number based on T_{0p}	[-]
ξ_{cr}	Critical value of the surf similarity parameter	[-]
ξ_m	Iribarren number based on T_m	[-]

1. INTRODUCTION

In order to get a better insight in the stability behaviour of cubes in a single armour layer of a breakwater, tests are performed in the Fluid Mechanics Laboratory of the Faculty of Civil Engineering and Geosciences at Delft University of Technology. this chapter gives a general introduction about a breakwater with a single armour layer consisting of concrete cubes.

1.1. Background

Breakwaters are used for protection against waves and flooding. In general breakwaters are used to protect ships and harbours against incoming waves. Furthermore, a breakwater can be applied to protect valuable habitats that are threatened by the destructive force from the sea. In addition, breakwaters are used to protect beaches from erosion. In some situations a breakwater is also used to prevent or reduce the siltation of navigation channels.

Breakwaters vary in shape and type of armour layer. This study focuses on conventional breakwaters. A conventional breakwater consists of different parts. It consists of an armour layer, a toe, one or more sub layers and a core. The armour layer is the main focus of this study. Different types of armour layers are known. It can consist of more than one armour layer. This makes the breakwater probably more expensive to build. This is simply because more elements are needed than using a single armour layer. In this report only one type of armour layer is considered. This is a single layer of concrete cubes.

Figure 1. Breakwater with armour layer consisting of concrete cubes

Single armour layers consisting of concrete cubes are relatively easy to produce and cost effective. However, an important aspect of a single armour layer is that if the single layer of armour fails, most likely the whole structure will fail. This is of course, because it has only one layer to protect the layer underneath. Abrupt failure occurs instead of progressive damage. This is a problem and a disadvantage compared to an armour layer consisting of two layers of cubes. This is the reason why for a single armour layer the stability is of greater importance.

Besides the disadvantage of abrupt failure, a breakwater with a single armour layer consisting of concrete cubes, is an interesting alternative to apply compared to, for instance, the more conventional double layer of cubes. The cost reduction is the most important aspect.

The packing density is of importance. It is found that if the packing density reaches a certain value, the single top layer becomes unstable. But the costs are very important. It would be convenient to reduce the amount of concrete that is necessary, by reducing the packing density. But too low packing density will allow the sub layer material to wash out. This means that there is an optimum packing density. Part of this study is to determine this optimum packing density.

For a further development of an armour layer consisting of a single layer of cubes, it is necessary to investigate the optimum packing density. Additional testing which focuses on the method of placement is desired as well. So far tests have been done with dropping cubes from the waterline [Van der Vliet, 2001][Bisschop, 2002] and placing the cubes randomly and by hand [Bhageloe ,1998] [Van Gent, 1999].

1.2. Content

This report describes the results of the hydraulic model tests performed in the wave flume which is located at the Fluid Mechanics Laboratory of the Faculty of Civil Engineering and Geosciences at the University of Technology in Delft.

Chapter two describes the previous studies done based on a single armour layer of cubes and presents the problem definitions.

Chapter three describes the theoretical background of this study. It focuses on stability of concrete cubes. The same chapter also treats the packing density, wave steepness and damage number. Furthermore, the method of placement is treated here.

The next chapter, chapter four, focuses on the model set up. Before starting the tests, scaling factors have to be determined. In the same chapter all parameters are treated. The parameters are separated in structural parameters and environmental parameters.

After chapter four, chapter five gives more insight in the performed experiments. The used cubes, materials and method of damage recording are presented here.

Chapter six presents the generated data from the performed tests. All performed tests are treated here. After that the analysis of the results is treated. Finally, chapter seven presents the conclusions and chapter eight the recommendations.

2. PROBLEM ANALYSIS

In this chapter a description of previous tests is given which involves a single armour layer of cubes. After that the problem definitions are presented. Followed by a short description about how the study fits into the previous studies, and what the new elements are.

2.1. Previous studies

In the case of an armour layer consisting of a single layer of cubes there has been done some research in The Netherlands [Van Gent and Spaan, 1998] [Bhageloe, 1998] [Van der Meer, 1987, 1988, 1999]. All used physical model tests. These tests showed that a single armour layer consisting of cubes could be more stable than a double armour layer of cubes. It can be seen as a good alternative for an armour layer to reduce building costs. The less concrete used, the less material costs.

Van der Meer (1987, 1988) did the most research in the Netherlands concerning this subject, a single armour layer of cubes. His work formed the basis on which Van Gent and Bhageloe (1998) proceeded. Bhageloe and Van Gent performed tests to study the feasibility of a single armour layer of cubes. They performed also tests involving other armour layer elements like tetrapods and rock. In addition, Van Gent (1999) extended the research on a single armour layer of cubes. Not only was the stability tested. Also the influence of packing density, sub layer material, and wave steepness was tested. Van Gent (2001) also did testing on high-density cubes.

Finally, research is performed considering the method of placement. Bhageloe (1998) and Van Gent (1999) have placed the cubes by hand. Additional studies are performed to find out what the influence is by dropping the cubes from, and just above the waterline [Van der Vliet, 2001][Bisschop, 2002].

A summary of the relevant conclusions found during the previous tests is given below.

- During these tests the sensitivity of single top-layers to the packing density (percentage of open space in the top-layer) for randomly placed cubes, was studied. It was found that packing densities of $n_p = 0.25$ and $n_p = 0.3$ (i.e. a porosity of n = 25% - 30% open space for a thickness of a top layer of one diameter) were appropriate. More cubes in the armour layer increase the costs.

- Research on the influence of wave steepness on stability showed that minimum stability will probably occur at $s_{0p} = 0.04 - 0.05$ [Bhageloe, 1998].

- The tests performed mentioned above all used a slope of 1:1.5. It is accepted as a standard slope for cubes.

- Different methods of placement of the cubes on the slope are applied. This means that the cubes were dropped from a certain distance from the waterline or placed by hand on the slope. Especially when the cubes are dropped, the cubes show a strong variation in orientation. Both methods show reasonable results, although the results using the placement by hand showed better results.

2.2. Research questions

The following problem descriptions are defined:

- What is the influence of the slope angle on the stability of a single armour layer of cubes.
- What is the influence of the packing density on the stability of a single armour layer of cubes.
- What is the influence of the wave steepness on the stability of a single armour layer of cubes.

During these tests the strength of a single armour layer of concrete cubes is examined using a different method of placement. All cubes are placed in a stretching bond (halfsteensverband).

2.3. Approach

In the present study new elements are introduced. The first new element is the method of placement. The placement occurred in a stretching bond. This means that the cubes were placed in a horizontal row perpendicular to the slope at a certain distance from each other in an attempt to reach different packing densities. Secondly the slope steepness as a variable is introduced. Besides the commonly accepted slope of 1:1.5, a slope of 1:2 is introduced. This is done to find out what the influence on the stability of the armour layer is.

The following comparison can be made based on the tests already performed.

- During this study the three different packing densities were tested, i.e. n_p = 0.20, 0.28, and 0.35. It covers the previous tested packing densities. The difference lies within the method of placement. In this study the cubes are placed in a horizontal stretching bond.
- The wave steepness was varied. In previous research was found that minimum stability of a single armour layer consisting of concrete cubes occurred with a wave steepness of 0.04-0.05 [Bhageloe, 1998]. Again the cubes were placed randomly and on a slope of 1:1.5
- The tests that were previously performed, involve that the influence of the slope was studied. All previous studies mentioned above used a slope of 1:1.5. An additional slope of 1:2 was tested during this study.
- During this study the cubes will be placed by hand. Contrary to previous studies the cubes are placed in horizontal rows called stretching bonds. This means that a constant distance between the cubes is applied.

3. THEORETICAL BACKGROUND

3.1. Stability

In this section the overall stability of an element is discussed. Since this study is based on stability of concrete cubes, the main focus will be on these armour units. In the following sections, the stability of coherent material in the form of concrete cubes will be treated. Also the importance of the packing density, placement method and damage definition will be treated.

3.1.1 Driving forces

In order to get a clear insight in stability it is necessary to know which forces make an armour element move. The units are on a slope, enduring cyclic wave attacks. These waves generate forces on the armour units.

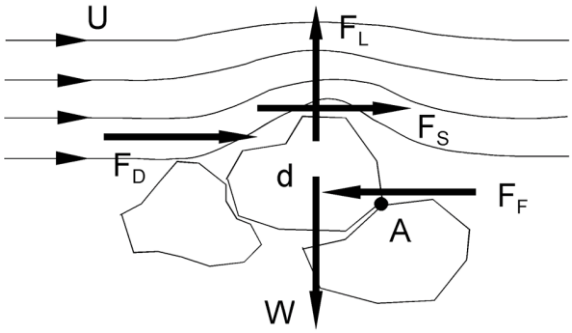

Figure 2. Driving forces (Schiereck, 2001)

The following driving forces are of importance:

Drag force F_D:
The wave induced water motion cause the drag force. It can be seen as the resisting force the material and the water experience from each other. A pressure difference is created between the front and the back of the cube. A lower pressure at the back is formed due the fact that the current detaches from the cube, creating a wake behind the cube.

$$F_D \approx C_D \cdot \rho_w \cdot A \cdot \bar{v} \cdot |v| \tag{3.1}$$

Lift force F_L:
In the direction normal to the drag F_D the lift force F_L is active. The lift force is a result of a pressure difference between the bottom and the topside of the cube. This pressure difference is caused by the curvature of the flow above the cubes. As a result the flow will be greater above of the cube than beneath the cube.

$$F_L \approx C_L \cdot \rho_w \cdot A \cdot \bar{v} \cdot |v| \tag{3.2}$$

It must be mentioned that in case of an armour layer of cubes used in this study the drag force F_D will be relative small compared to the lift force, $F_L >> F_D$.

Shear force F_S:
The shear force F_S is caused by the water which flows along the armour element. Often this shear force is expressed into the drag force.

$$F_S \approx C_S \cdot \rho_w \cdot A \cdot \bar{v} \cdot |v| \tag{3.3}$$

In every formula presented above is a coefficient present. In which the C_D, C_L, and C_S are empirical coefficients, related to the shape and orientation of the armour element.

Gravitational force F_G:
Of course there is also a gravitational force F_G active. The following equation presents the own weight of the cube under water.

$$F_G = (\rho_c - \rho_w) \cdot V \cdot g \tag{3.4}$$

Friction force F_F:
Finally there is the reaction force acting at the points of contact between the armour elements. When applying armour stones this friction will be much less than when applying cubes. Therefore friction among the cubes is of importance. When a cube is lifted by the pressure from below, it will lift other blocks as well, due this friction or clamping. The clamping of the cubes will be less when the gaps between the cubes increase. Therefore the friction is probably directly related to the packing density.

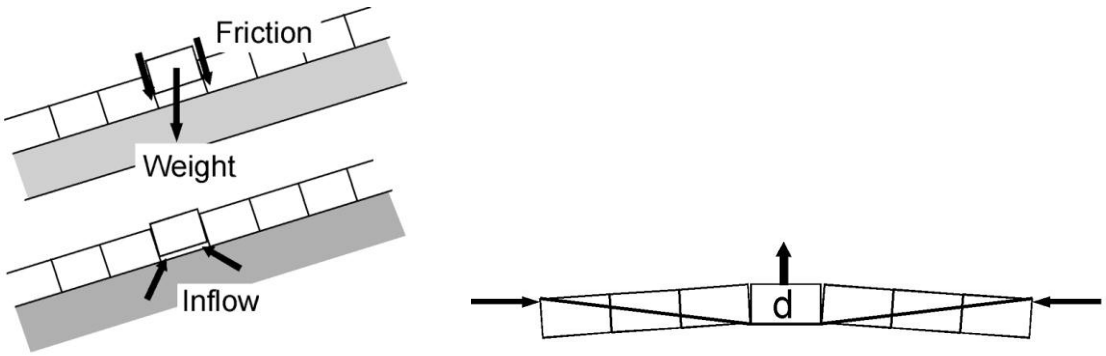

Figure 3. Friction (left) and clamping (right) (Schiereck, 2001)

As mentioned before the elements endure cyclic wave attacks. This means that the flow around the units is non-stationary in all directions. This makes it very hard to predict the forces. Therefore much of the stability rules are based on hydraulic model tests.

3.2. Stability number

It is obvious that the forces vary with the parameters, like the angle of the slope and the wave climate. Besides of the complexity of the flow field, also the shape of the armour element, the cube, is important. Since we are interested in de size of the elements to use for the armour layer, it seems logical to involve the diameter of the element. For stability the weight of the cube is an important parameter. This leads to the following expression, which is simply the nominal diameter of the cube with the same volume as the stone considered.

$$D_n = \left(\frac{M}{\rho_c} \right)^{1/3} \tag{3.5}$$

In which:

ρ_c	= mass density of cube	[kg/m^3]
M	= mass of the cube	[kg]
D_n	= nominal diameter of the cube	[m]

When assuming that the flow is quasi-stationair, the inertia forces can be neglected:

$$\frac{F_D + F_L}{F_G} \infty \left(\frac{\rho_c - \rho_w}{\rho_w} \right) \frac{gD_n}{v^2} = \frac{v^2}{\Delta g D_n} \tag{3.6}$$

In which v is the local characteristic flow velocity as induced by wave motion. By inserting wave velocity $v \approx \sqrt{g \cdot H}$ for wave height H, we find the well-known stability number:

$$N_s = \frac{H}{\Delta D} \tag{3.7}$$

This parameter is often used for breakwater design. The higher this number is the higher waves can be accommodated by the same stone size. By substituting the nominal diameter and the significant wave height, the stability parameter, $H/\Delta D$ or stability number, N_s takes the form of $H_s/\Delta D_n$.

3.3. Damage definition

In an attempt to define the recorded damage of an armour layer the damage number has been developed. The following applies for the damage number N_{od}:

$$N_{od} = \frac{n_{displ}}{B_{test} / D_n} \tag{3.8}$$

In which:

n_{displ}	= more than one D_n displaced cubes	[-]
B_{test}	= Width of test area (= 0.80 m.)	[m]
D_n	= nominal diameter cube	[m]

In case of failure of a single armour layer of cubes the following criterion is known, N_{od} = 0.2 [Bhageloe, 1998][Van Gent et al, 1999]. It can be discussed whether this is a just criterion. Cubes that are displaced more than one cube diameter could still contribute to the stability of the entire slope. This is because in some occasions the cubes will fall into gaps that were previously formed in the armour layer. In such a situation the cube is only relocated in the armour layer, and therefore the cube still contributes to the stability. In other situations the cube ends on the slope or at the toe of the structure. In these cases the cubes don't contribute to the stability. Nevertheless, during this study N_{od} = 0.2 is used as the criteria for failure.

Acceptable damage levels for cubes in a single layer are significantly less than for double layers (N_{od} = 2). The hydraulic stability as found in model tests can be described by the following equations for start of damage and failure respectively [Bhageloe, 1998]:

Start of damage, N_{od} = 0:

$$\frac{H}{\Delta D_n} = 2.9 - 3.0 \tag{3.9}$$

Failure, N_{od} = 0.2:

$$\frac{H}{\Delta D_n} = 3.5 - 3.75 \tag{3.10}$$

The difference between start of damage and failure is very small. Because there is no reserve in the form of a second layer, damage to the armour layer will immediately result in exposure of the sublayer to direct wave attack.

3.4. Packing density

The packing density is directly related to the placement pattern of the armour layer. It is a term mainly applied to artificial armour units. The basis of the definition of placing density or packing density is the number of elements (N) per m^2. The packing density is then given by the ratio of the size of the blocks by the thickness of the "equivalent layer thickness". In other words, the packing density is the percentage of the area of the surface covered by blocks, in case all blocks are placed flat on the surface. In reality, the blocks are not placed flat on the surface, see figure 4. There is also a hollow space between the blocks and the under layer. In addition, the defined top of the blocks is not exactly the upper side of the block. Here also is a space. If one calculates the volume of the layer and divides that by the volume of the concrete of the block, one gets the porosity of the layer.

$$d_l = \left(1 - n_p\right) D_n \tag{3.11}$$

$$N_{cubes} = \frac{d_l}{D_n^3} \tag{3.12}$$

In which:

d_l	= equivalent layer thickness	[m]
n_p	= packing density	[-]
D_n	= nominal diameter cube	[m]
N_{cubes}	= number of cubes per m^2	[-]

For nicely placed blocks, the packing density is equal to (1- porosity.)

$$n_v = 1 - \frac{D_n^3 N_{cubes}}{d} \tag{3.13}$$

In which:

n_v	= porosity	[-]
d	= measured layer thickness	[m]

[Van Gent, 2001] recommended to use a packing density for a single armour layer of cubes corresponding to a packing density of n_p of 0.25-0.30.

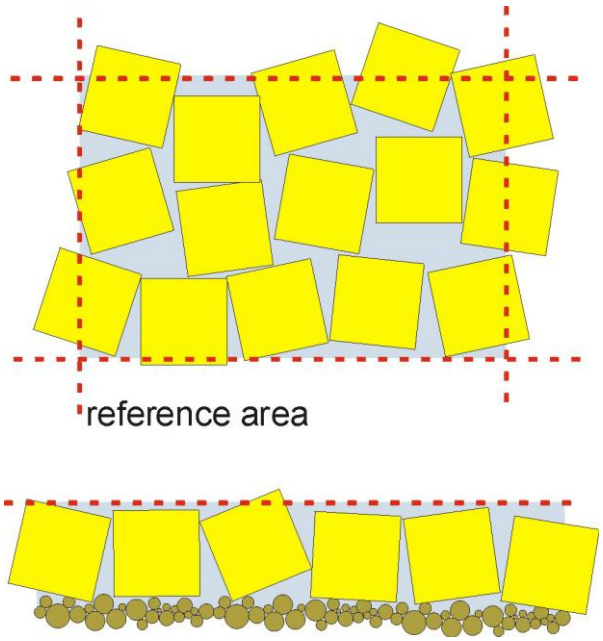

Figure 4. Placing density (top) and porosity

In figure 4 both porosity and packing density are illustrated. The packing density is given in the upper figure, and can be calculated by dividing the area of the blocks by the area of the control area. In the lower figure is indicated that also below and above the blocks there is an “empty” space. The volume not used by concrete divided by the total volume is the porosity. If one compares the measured porosity and the packing density with the values assuming a “flat” positioning of the cubes, a difference becomes apparent. This indicates that there is a small difference. [Verhagen, Van der Vliet, 2001]

3.5. Placement method

As mentioned before different methods of placement are possible. Controlled placement versus random placement. Previous studies used basically two different methods. Those are: Dropping the cubes from, or just above the waterline. The second method the cubes are placed by hand.

When the cubes are dropped from, or above, the waterline it is quite hard to direct the cube to exactly the wanted place. Therefore the cubes will fall randomly in place [Van der Vliet, 2001].
During the tests performed by Bhageloe (1998) and Van Gent (1999) the cubes were placed by hand, but still randomly.

The cubes during this study are placed in a stretching bond. This means that the cubes are placed in a horizontal row, starting at the toe of the structure, with a constant distance from each other. This way the packing density is constant for the whole slope. In practise this means that the cubes will be placed very carefully and need to be monitored whether the cubes are at the right place. This is controlled placement.

The cubes were placed carefully during this study and no pressure was applied on the cubes. Cubes that slightly moved due to the core material beneath were left that way. All layers were loosely placed to simulate a real situation. This means that no layer was compressed.

3.6. Van der Meer

For cubes in a double armour layer on a slope of 1:1.5, Van der Meer derived an relation between the stability number and the damage number, N_{od}, the wave conditions and the structural parameters [Van der Meer, 1988].

$$\frac{H_s}{\Delta D_n} = \left(6.7 \frac{N_{od}^{0.4}}{N^{0.3}} + 1.0 \right) s_{om}^{-0.1} \tag{3.14}$$

In which: N = number of waves at the toe of the structure [-]

For deep water conditions Van der Meer also derived formulae to predict the stability of armour stone on uniform slopes with crests above the maximum run-up level. These tests were based on a large amount of model tests. The formulae make use of a distinction between plunging waves and surging waves [Van der Meer, 1988].

For plunging waves $\xi_m < \xi_{cr}$:

$$\frac{H_s}{\Delta D_n} = c_{pl} \cdot P^{0.18} \cdot \left(\frac{S_d}{\sqrt{N}} \right)^{0.2} \cdot \xi_m^{-0.5} \tag{3.15}$$

For surging waves $\xi_m \geq \xi_{cr}$:

$$\frac{H_s}{\Delta D_n} = c_s \cdot P^{-0.13} \cdot \left(\frac{S_d}{\sqrt{N}} \right)^{0.2} \cdot \sqrt{\cot \alpha} \cdot \xi_m^P \tag{3.16}$$

In which: P = notional permeability parameter ($0.1 \leq P \leq 0.6$) [-]
S_d = damage number (loose rock) [-]

The critical value of the surf similarity parameter is given by:

$$\xi_{cr} = \left[6.2 P^{0.31} \sqrt{\tan \alpha} \right]^{\frac{1}{P+0.5}} \tag{3.17}$$

Although these formulae were designed based on armour stone, the basics can be used to develop a prediction in which the parameters used during this study play a role. In this study the number of waves is constant.

A permeability parameter P has been introduced and the value for different structures has been established by curve-fitting the results. The figure gives the values for various situations. A homogeneous structure (no core) gives P ≈ 0.6, a rock armour layer with a permeable core: P ≈ 0.5, an armour layer with filter on a permeable core: P ≈ 0.4 and an "impermeable" core: P ≈ 0.1.

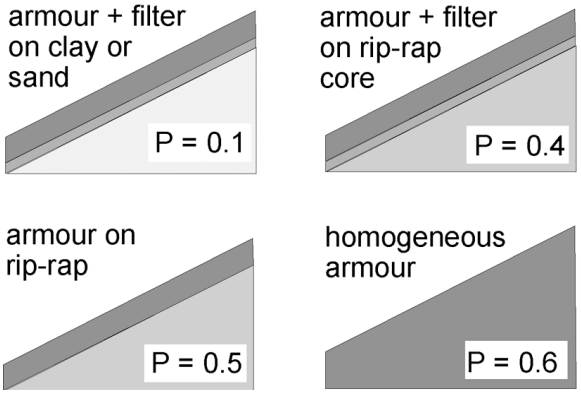

Figure 5. Notional permeability parameter

Both formulae, those of a double layer of cubes and the rip rap configuration, can be used here. At this point it is not clear yet which will be used for the analysis of the data.

3.7. Wave steepness

The nature of the water movement in waves on a slope is mostly dominated by the angle of the slope, the incoming wave height, and the wave period. The fictitious wave steepness is a parameter, which contains the wave height and the wavelength. The following equation is often applied to calculate the wave steepness:

$$s = \frac{2\pi}{g}\frac{H_s}{T_p^{\,2}} \tag{3.18}$$

In which: H_s = significant wave height [m]
T_p = peak wave period [s]
g = gravitational acceleration (= 9.81) [m/s^2]

The effect of the wave period is connected with the shape and intensity of breaking waves.
It must be noted that the value of H_s in the expression $H_s/\Delta D$ is measured at the location of the toe of the structure after elimination of any wave reflection [d'Angremond, 2001].

3.8. Iribarren number

For waves breaking on a slope, the dimensionless Iribarren number or surf similarity parameter is of importance. The parameter is defined as:

$$\xi = \frac{\tan\alpha}{\sqrt{s}} \tag{3.19}$$

In which: α = slope angle [°]
s = fictitious wave steepness [-]

The different shapes of waves breaking, depending on the surf similarity parameter are described. The transition between the breaker types is gradual and the values of the transition between them are just an indication [Battjes, 1974].

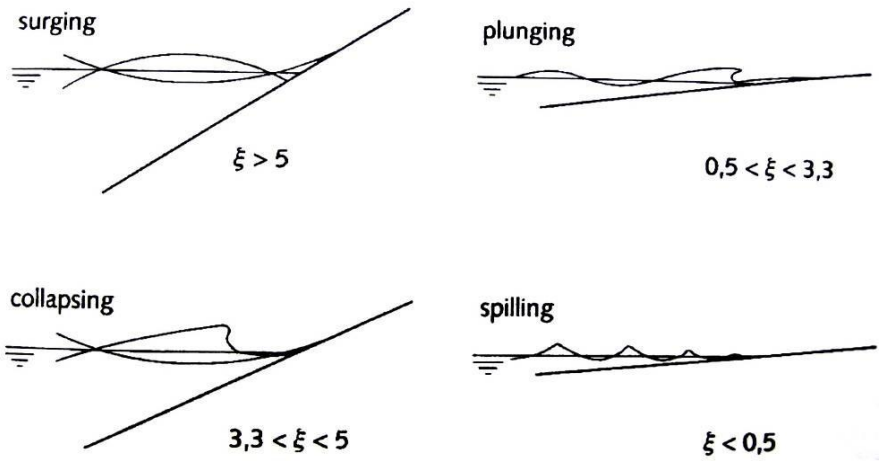

Figure 6. Breaker types as a function of ξ

3.9. Slope

Different armour elements often use different slopes. For instance, an armour layer that consists of Accropodes, uses a slope of 1:1.33. A commonly used slope for a breakwater with a single armour layer of cubes is 1:1.5. To find out what influence the slope has on the stability of the cubes another slope was added, cotα= 2. It is expected that this slope will be more stable.

4. MODEL SET-UP

Small scale model testing offers the opportunity to scale the prototype situation to a scaled model. The greatest benefit is that one can verify the structure in a controlled environment. Also the behaviour of the structure can be checked during design conditions. This chapter deals with scaling problems. First the principles of scaling are treated. After that the main objective of this study is treated.

4.1. Scaling law

In the ideal situation the laboratory model should behave in all respects like a controlled version of the prototype. Of course this is perhaps never the case. But this similar behaviour is achieved when all influential factors are in proportion between the prototype and the model, while those factors that are not in proportion are supposed to be so small that they are not significant to the process. Requirements of similitude will vary with the problem being studied and the degree of accuracy in model reproduction of prototype behaviour. In fluid mechanics, similarity generally includes three basic classifications: dynamic similarity geometric similarity, kinematic similarity and [De Vries, 1977] [Hughes, 1993].

Dynamic similarity
Dynamic similarity between two geometrically and kinematically similar systems requires that the ratios of all vectorial forces in the two systems are the same.

To achieve complete similarity all relevant dimensionless parameters must have the same corresponding values for model and prototype. A systematic procedure for forming a complete set of dimensionless products from a given set of variables is the Buckingham Pi Theorem, which means:

$$\pi_p = \pi_m = f(\pi_1, \pi_2, ..., \pi_r) \tag{4.1}$$

In which the π's are a complete set of dimensionless products.

Geometric similarity
When the ratios of all corresponding linear dimensions between the prototype and the model are equal the model is geometrically similar:

$$n_L = \frac{x_p}{x_m} = \frac{y_p}{y_m} = \frac{z_p}{z_m} \tag{4.2}$$

In which:	n_L =	prototype to model scale ratio of parameter L	[-]
	x_p =	value of the prototype	[-]
	x_m =	value of the model	[-]

The Froude number is a dimensionless number comparing inertial and gravitational forces in a hydraulic flow at free surface. It may be used to quantify the resistance of an object moving through water, and compare objects of different sizes. Named after William Froude, the Froude number is based on the speed/length ratio. To achieve similarity the Froude number must be equal in model and prototype.

$$Fr = \sqrt{\frac{inertial\_force}{gravity\_force}} = \sqrt{\frac{\rho L^2 U^2}{\rho L^3 g}} = \frac{U}{\sqrt{gL}} \tag{4.3}$$

In which: U = velocity [m/s]
L = length [m]

Based on the formula for the Froude number, the following scale rules are found:

Wave height H:	n_H	$= n_L$	[m]
Wave period T:	n_T	$= n_L^{1/2}$	[s]
Storm duration t:	n_t	$= n_L^{1/2}$	[s]
Mass M:	n_t	$= n_L^{3}$	[kg]

Stability number:
These tests involve stability of the armour layer. Therefore it is important that the stability number is scaled correctly. The following rule applies:

$$n_l = \left(\frac{H_s}{\Delta D_n} \right)_p = \left(\frac{H_s}{\Delta D_n} \right)_m \tag{4.4}$$

Reynolds number:
For practically all coastal engineering problems the forces associated with surface tension and elastic compression are relatively small, and can thus be safely neglected. To overcome scaling problems it is important that the Reynolds number is sufficiently large (turbulent flow). The following has to be obeyed [Dai and Kamel, 1969]:

$$\mathrm{Re} = \frac{\sqrt{gH_s} \cdot D_n}{\upsilon} > 3 \cdot 10^4 \tag{4.5}$$

In which: Re = velocity [m/s]
υ = kinematic viscosity (10^{-6}) [m^2/s]

Kinematic similarity
The science of kinematics studies the space-time relationship. Kinematic similarity consequently indicates a similarity of motion between particles in model and prototype. If the velocity at corresponding points in the model and prototype are in the same direction and differ by a constant scale factor, the model is regarded as kinematic similar to the prototype.

Scale differences
The permeability of the core material influences armour stability, wave run-up and wave overtopping. The mean problem related to the scaling of core material in models is that the hydraulic gradient and the pore velocity are varying in space and time. This makes it difficult to achieve fully correct scaling.

The use of Froude scaling in wave flume model tests causes incorrect scaling of viscosity, elasticity and surface tension. The linear geometric scaling of material diameters which follows from Froude scaling may lead to much too large viscous forces corresponding to too small Reynolds number, especially in sublayers and core of small scale models. The related increase in flow resistance reduces the flow in and out of sublayers and core. This again causes relatively larger uprush and down-rush velocities. As a result run-up levels will be too high and armour stability too low [Burcharth et al, 1999]. Appendix C treats the core scaling.

4.2. Governing parameters

In this section the governing parameters are treated. The armour layer is the main focus of the tests. Every part of the breakwater is treated separately. A conventional breakwater exists of a toe, core, armour layer and filter layer(s). The environmental parameters are of importance too. Since this study is performed in the Netherlands, the Dutch situations have been chosen to determine the dimensions and scale.

4.2.1 Environmental parameters

Everything of influence on the stability by its surroundings are environmental parameters. Every aspect will be treated separately. These are:

Table 1. Governing parameters

Type of the wave spectrum	JONSWAP	[-]
Characteristic wave heights	H_{m0}	[m]
Characteristic wave steepness	s	[-]
Number of waves	N	[-]
Water depth	h	[m]
Angle of incidence	α	[°]

Wave spectrum

During the test series a JONSWAP spectrum was used. In previous tests the Pierson Moskowitz spectrum was used [Bhageloe, 1998] [Van der Meer, 1999]. The JONSWAP spectrum is an enhanced Pierson Moskowitz spectrum. This spectrum is assumed to be especially representative for the North Sea. For further information about the JONSWAP spectrum see annex B. The significant wave height can be determined from the variance density spectrum using equation (4.6).

$$H_{m0} = 4\sqrt{m_0} \tag{4.6}$$

The total area of the spectrum equals to the total variance:

$$m_0 = \int_0^\infty E(f)\,df \tag{4.7}$$

Wave height

All the tests were performed with increasing wave height, starting with the lowest. This way a building storm was simulated by a sequence of test with increasing wave height. During the test instability could be visually detected. The corresponding wave height was measured. Instability is not the only factor. After that, failure of the construction is important.

Wave steepness

The tests were performed with constant wave steepness. The wave steepness is a parameter which includes the characteristic wave height and the wave length, also known as fictitious wave steepness:

$$s = \frac{H}{L} = \frac{2\pi}{g}\frac{H}{T^2} \tag{4.8}$$

It is recommended to use wave steepness between 3-3.5% for the peak period. This is similar to a wave steepness of 5% for the mean period. In general wind waves wave waves occur with a wave steepness between 0.02-0.06. During tests a wave steepness of 0.02, 0.04 and 0.06 were used.

Number of waves

The number of waves, N, was set on 1000 waves. This way, the wave series will be sufficiently long enough to analyze the wave spectra. After these 1000 the next test was started. Assuming that if no damage occurs after 1000 waves, more waves won't develop (more) damage [Van der Meer, 1986]. The number of waves simulates a storm duration of approximate three hours (prototype).

Water depth

The wave flume has restrictions. One is that the wave flume has a limited depth. To perform reliable tests the water depth should be:

$$h_{water} \geq 3 * H_s \tag{4.9}$$

Of course, when the waves get too high, the chance for overtopping increases. This means that an upper limit is of importance. With the maximum wave height set on 0.18 m, the water depth then becomes 0.50 m.

4.3. Structural parameters

In order to get a clear view that structural parameters are of some influence, they will be discussed in this paragraph. All parameters will be treated in this section. The structural parameters that are of influence are:

- Armour layer
- Sublayer (material and thickness)
- Core material
- Slope angle α
- Toe
- Foreshore
- Placing method armour layer
- Crest height

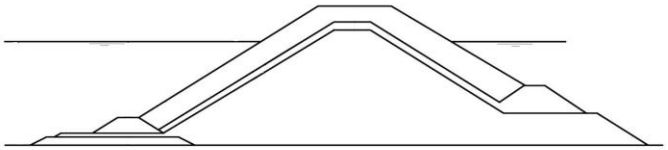

Figure 7. Conventional breakwater

Prototype dimensions

The design wave height H_s = 8.0 m is chosen. A realistic prototype cube size was set on 1.80 m. The following characteristics used for this study are presented in table 2.

Table 2. Prototype design characteristics

Wave height	H_s	[m]	8.00
Cube diameter	D_n	[m]	1.80
Sublayer material	D_{n50}	[m]	1.00
Core material	D_{n50}	[m]	0.60
Water density	ρ_w	[kg/m^3]	1025
Concrete density	ρ_c	[kg/m^3]	2500

Armour layer

The armour layer is the main focus of this study. The armour layer consists of a single layer of concrete cubes with a constant mass density.

In order to determine the model cube size, the model scale has to be used. When the model scale is chosen too large no damage will occur due to the maximum capabilities of the wave board. A very small scale will induce possible scale effects.

The following formula was used to determine the relative mass density:

$$\Delta = \left(\rho_c - \rho_w\right) / \rho_w \tag{4.10}$$

In which: ρ_c = mass density of cubes [kg/m^3]
ρ_w = mass density of water [kg/m^3]

By using the following equation the weight of the cubes can be determined.

$$D_n = \sqrt[3]{\frac{W}{\rho_s}} \tag{4.11}$$

For the prototype, the concrete will have a mass density of 2500 kg/m^3. In this case for the model scale a mass density of 1800 kg/m^3 is used. The following characteristics presented in table 3 are used. This lead to a scale factor, n_L, of 40.

Table 3. Characteristics model

Cube diameter	D_n	[m]	0.045
Cube density	ρ_c	[kg/m^3]	1800
Relative density	Δ	[-]	0.8
Water density	ρ_w	[kg/m^3]	1000

Sublayer

The sublayer is an important part of the breakwater. In case of low permeability of the sublayer, the waves are reflected against this sublayer and subsequently increase the lift forces on the armour layer. Contrary to low permeability, the size of the material cannot be too small. Otherwise it will wash away. This means that the size of the material is restricted to certain design rules. Different design rules are known. A well-known rule is based on material weight [Rock Manual, 2007].

$$10 < W_{toplayer} / W_{sublayer} < 20 \tag{4.12}$$

The second, and stricter, approach is based on the nominal diameter of the armour layer and the sublayer.

$$2 < D_{n,armour} / D_{n50,sublayer} < 2.5 \tag{4.13}$$

Applying the second rule leads to a sublayer material of 0.60 m.

Core

The necessary use of Froude scaling in model tests causes incorrect scaling for the permeability of the core and sublayer. The linear geometric scaling of material diameters which follows from Froude scaling may lead to much too large viscous forces corresponding to too small Reynolds numbers, especially in sublayers and core material of small scale models. The related increase in flow resistance reduces the flow in and out of under layer and core. This again causes relatively larger up-rush and down-rush velocities. To overcome this problem the core is scaled by a different approach. The result of this method is that larger core material is needed [Burcharth, 1999].

Slope

During this study two different slopes were tested. These are cotα= 1.5 and 2.0. Previous tests have been done for a single armour layer with random placed cubes. All test involved a slope of cotα= 1.5. To find out what influence the slope has on the stability of the cubes another slope was tested, cotα= 2.0.

Toe

The toe is a very important feature of the structure. In a way it is the starting point of the construction's stability. If the toe fails, it is most likely that the whole structure will fail. Therefore, in an attempt to secure the stability, the toe in the model was fixed in the form of a wooden beam. In this way the toe will not influence the result of the present study.

Foreshore

On the seaward profile, the tests were performed without a foreshore in front of the structure. This means that no foreshore was taken in account. This is done to minimize the effect on the waves.

Crest height

The tests are performed for a non-overtopped structure. The relative freeboard on the seaward side R_c/h_c should be about 1.6 [Van der Meer, 1987]. In which h_c is the water depth at toe of the structure and R_c is the relative crest height or freeboard. Therefore the crest height was set on 0.80 m. This way much of the wave energy will reach only the front side of the model. Especially for the less steeper slopes this crest height will be enough.

5. EXPERIMENTS

The tests were performed at the Fluid Mechanics Laboratory of the Faculty of Civil Engineering and Geosciences in Delft. In this chapter the experimental procedure is explained. As well as the facilities used.

5.1. Facilities

The following facilities at the Fluids Mechanics laboratory were used.

- Wave flume
- Wave gauges
- Software
- Concrete cubes
- Core material

5.1.1 Wave flume

At the University of Technology in Delft, the wave flume was used to perform the tests. The wave flume is located at the Fluid Mechanics Laboratory of the Faculty of Civil Engineering and Geosciences. The wave flume has the following dimensions:

- Length 42 [m]
- Width 0.80 [m]
- Maximum depth 0.85 [m]

Figure 8. Wave flume

The wave flume is presented in the figure above. At the beginning of the wave flume the wave board, with a wave reflection compensator, is positioned. The desired waves are generated by this hydraulic driven wave board. It can generate regular as well as irregular waves. To overcome the problem of reflection, the wave generator is equipped with an active reflection compensation system. This is done to minimize the waves that re-reflect from the wave paddle to be measures by the wave gauges. This system is called an active reflection compensation system, also known as ARC.

5.1.2 Wave gauges

In order to get reliable results a good preparation before performing the tests was needed. Six wave gauges were used. They were placed at two locations with three wave gauges each. This way it was possible to split incoming waves and reflected waves using a least squares method [Mansard and Funke, 1980].

Figure 9 presents the set-up of the wave flume and the six wave gauges.

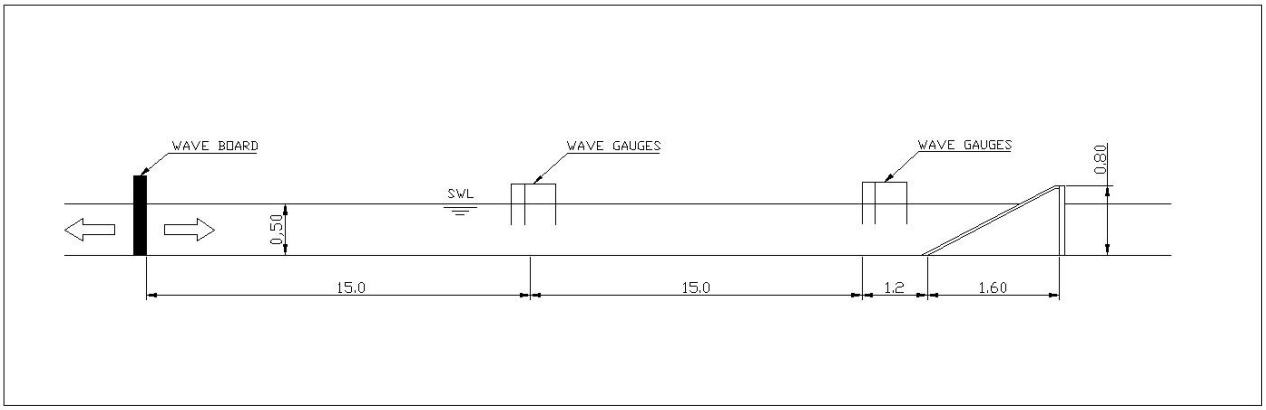

Figure 9. Set-up wave flume

The wave gauges are used to measure the incoming wave height caused by the wave board. The first set of wave gauges was placed at the toe of the structure trying to exclude the reflected waves from the structure. The distance between the second set of wave gauges and the first set was 15 meter. The distance between the wave gauges forming a set are for both configurations the same. The distance from the toe of the structure towards the first wave gauge was 50 cm. The next wave gauge was located 0.30 m. further. And the third was located at a distance of 0.4 m. All distances of the wave gauges are included in the next table which presents the calibration process. Pictures were taken from a fixed position. The pictures were taken at the start of a serie and after each serie of a thousand waves. The photos are presented in appendix G.

5.1.3 Software

The program DELFTAUKE/GENERATE was used to generate steering files. The signals of the wave gauges were stored by using the program DASYLAB. For analyzing the wave data the program DECOMP running under MATLAB was used. With three wave gauges placed at a certain distance from each other. This way the incoming and reflected wave could easily be separated.

5.2. Wave characteristics

To simulate a good wave climate in the wave flume a test program was created and inserted into the wave generator. In the previous chapter is explained that three different wave steepness's were tested. In the same chapter the maximum characteristic wave height H_s was determined and set on 18 cm. To simulate a storm built-up, wave heights were increased upon failure of the model. Together with the wave heights and the wave steepness, the correlated peak periods T_p were calculated and presented in the next table.

Table 4. Input wave periods model

H_{s0}		0.06	0.08	0.10	0.12	0.14	0.16	0.18	0.20
s_{0p}	0.02	1.39	1.60	1.79	1.96	2.12	2.26	2.40	2.53
	0.04	0.98	1.13	1.27	1.39	1.50	1.60	1.70	1.79
	0.06	0.80	0.92	1.03	1.13	1.22	1.31	1.39	1.46

The lowest wave height was set on 0.06 m. This is the starting point of the tests. Proceeding until the maximum wave height is employed which set on 20 cm.

5.2.1 Measurements

As mentioned before, wave gauges were used to measure the incoming wave height. The wave gauges have scale factors of 0.025 m/V. Before starting a test serie, the wave flume was filled with water and the gauges were calibrated. The next picture shows the set-up of the wave gauges.

Figure 10. Positioning wave gauges

Before starting the tests the waves gauges were calibrated. The results can be found in the next table. The gauges were calibrated by calibrated by putting them at a higher position and measuring the signal.

Table 5. Calibration wave gauges

Gauge	Distance [m]	Calibration [m/V]	-10 [cm]	0 [cm]	10 [cm]	Calibration [m/V]
w1	0	-0.025	3.933	0	-4.055	-0.025
w2	0.31	0.0243	-4.202	0	4.03	0.0243
w3	0.7	0.0234	-4.29	0	4.251	0.0234
w4	15	-0.0256	3.96	0	-3.864	-0.0256
w5	15.31	-0.0258	3.97	0	-3.77	-0.0258
w6	15.71	0.0245	-3.937	0	4.22	0.0245

5.3. Cubes

As stated in the previous chapter the cubes should have a nominal diameter of 45 mm. A mould was fabricated in which a hundred cubes of 45 mm could be produced. But the cubes needed to have a density of 1800 kg/m^3. Normal concrete cubes will have a density of around 2400 kg/m^3 to 2500 kg/m^3. Therefore the cubes were prepared in the laboratory itself. Concrete is made of cement gravel sand and water. To realize such a density, a lighter material was used. This material was vermiculite.

Figure 11. Cubes being produced

In total 548 cubes were used although 800 were produced. The best cubes were selected for the experiment. The cubes were a bit fragile especially at the corners. Nevertheless the cubes functioned very well during the experiments.

The following table presents the total amount of cubes used during the experiments. All the cubes used were weighted just before using them for the model. The following table presents the median weight and the median density.

Table 6. Cube characteristics

Cubes	W_{cube} [g]	ρ_{cube} [kg/m^3]	σ_w [g]	σ_ρ [kg/m^3]
548	170.9	1875	3.7	40

More information about the cubes and the sieve curve can be found in appendix D.

5.4. Core material

According to appendix C, a nominal diameter D_{n50} of 17 mm was needed. The chosen material, Basalt, is rubble stone and has sharp edges. Appendix E gives more information about the material. It was necessary to wash the core material first. This was done to guarantee that the water in the wave flume remained clear during the test series.


Figure 12. Core material

The number of stones that need to be handpicked from a sample to realize a certain accuracy can be found with [Buijs, 1984]:

$$n \geq \frac{z^2 \sigma^2}{a^2} \tag{5.1}$$

In which:	n	= sampling range	[-]
	σ	= standard deviation	[mm]
	z	= reliability	[-]
	a	= accuracy	[mm]

In this study the sampling range is 200 stones. Therefore 200 stones were measured.

Table 7 presents the characteristics of the core/sublayer material.

Table 7. Core material characteristics

W_{50} [g]	ρ_{stone} [kg/m^3]	D_{n50} [mm]	σ_w [g]
12.7	2960	15.5	4.1

5.5. Test procedure

Before starting the testing, a test program was developed. The method of placement is defined in the form of a stretching bond corresponding to certain packing densities. In this study, n_p = 0.20, 0.28 and 0.35. Once the damage occurred a procedure of damage recording had to be defined.

5.5.1 Test series

In the tests two different slopes were used, together with three packing densities, and three different kinds of wave steepness. This leads to a test program of eighteen series consisting of several individual test runs. Table 8 gives the test series.

Table 8. Test series

Test serie	Slope cot(α)	Wave steepness s_{mo}	Packing density n_p
A101-A104	1.5	0.02	0.20
A201-A206	1.5	0.02	0.28
A301-A307	1.5	0.02	0.35
B101-B104	1.5	0.04	0.20
B201-B206	1.5	0.04	0.28
B301-B307	1.5	0.04	0.35
C101-C105	1.5	0.06	0.20
C201-C206	1.5	0.06	0.28
C301-C306	1.5	0.06	0.35
D101-D105	2.0	0.02	0.20
D201-D206	2.0	0.02	0.28
D301-D306	2.0	0.02	0.35
E101-E104	2.0	0.04	0.20
E201-E205	2.0	0.04	0.28
E301-E306	2.0	0.04	0.35
F101-F104	2.0	0.06	0.20
F201-F205	2.0	0.06	0.28
F301-F307	2.0	0.06	0.35

Before placing the layers the length of the layers was calculated. For every series a standard procedure was followed. First the core was placed. After the core the toe was put in place. After this the cubes were placed. All layers were loosely placed to simulate a real situation. This means that no layer was compressed.

5.5.2 Placement method

An important aspect for the stability is the placement method. The slopes were drawn on the glass of the wave flume. Therefore it was rather easy to place the core. After the core the toe was fixed. The toe gives stability for the armour layer and prevents the armour layer from sliding down. The consequence is that the toe should be placed before the armour layer. Finally the armour layer was put in place. Since the study focuses on the stability of the armour layer this was done very carefully. All the cubes were placed by hand and placed at a certain distance from each other to obtain the desired packing density.

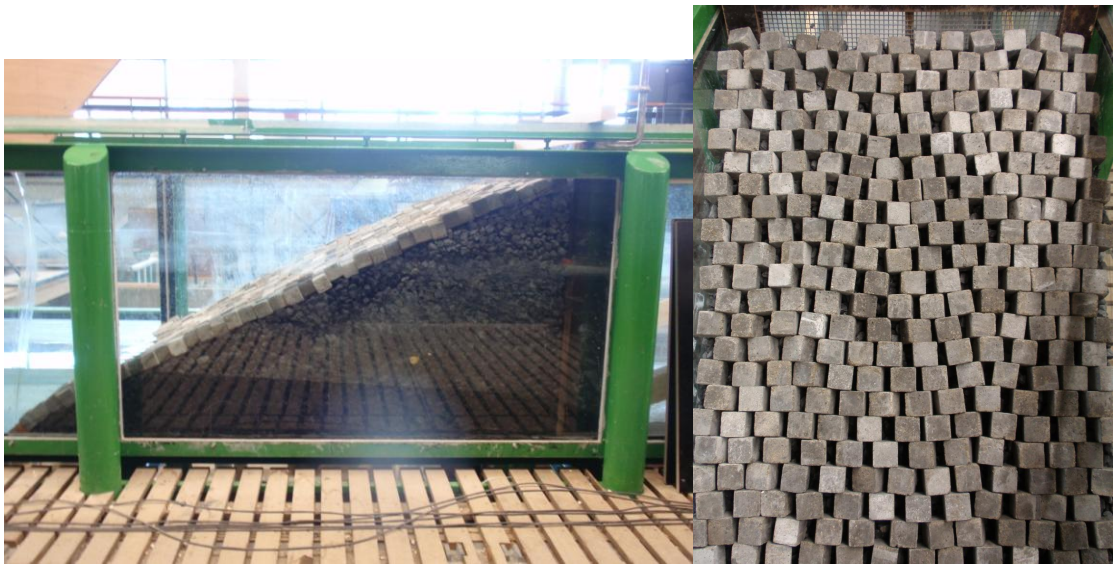
Figure 13. Top and side view model slope 1:2

Every single cube was placed by hand. First the amount of cubes per row was calculated needed to achieve the packing density. This resulted in a packing density with small deviations. This was conform the placement in practice, when the cubes are placed by crane. Cubes that slightly moved were left that way. This way a realistic placement method was achieved.

Three different packing densities are tested, n_p = 0.20, 0.28, 0.35. The packing density is defined as the open space in the armour layer. The maximum width of the wave flume was 0.80 m. This is considered to be width L. This means that with a packing density of 0.20, the total amount of cubes in one row (x-direction) then becomes 0.8L. Table 9 presents the corresponding distances between the cubes.

Table 9. Packing density of cubes and theoretical gaps

n_p	Cubes	Gap [m]
0.20	14-15	0.012
0.28	12-13	0.02
0.35	11-12	0.032

All cubes were placed row by row and in horizontal position. Because the cubes will have the intention of sliding down the slope, no packing density differences are used on the vertical axis (y-direction). Corresponding to table 10, for n_p = 0.2, a row of 15 cubes was placed. The next row consists of 14 cubes. Next row consists of 15, and so on.

5.5.3 Damage recording

The cubes were placed in horizontal rows. After each test the amount of displaced cubes (n_{disp} meaning displaced more than one nominal diameter) was counted. The damage after each test in the testing series was left as it was. This means that the cumulative damage was determined for every test serie. After counting the displaced cubes, the damage number N_{od} is determined.

After every test serie the construction is rebuilt. The corresponding value for failure of N_{od} for single layer cubes was set 0.2 [Bhageloe, 1998][Van Gent et al., 1999]. This means that the structure has failed when 4 cubes were displaced more than one nominal diameter D_n.

6. TEST RESULTS

A total of 18 test series and a total of 99 tests were performed. The tests were labelled starting with A101 and ending with F306. The complete test program together with the results is presented in annex A. In the same annex all the measured wave characteristics are presented. All pictures referred to can be found in Annex F.

6.1. Description of the damage

6.1.1 Test serie A

A slope of cotα = 1.5 and a packing density of n_p = 0.2 was used. Furthermore, three different kinds of wave steepness were tested. The damage numbers for the tests are presented in annex A.

Table 10. Test serie A

Serie	cotα	n_p	s_{0p}	Tests	Waves
A1	1.5	0.2	0.02	4	1000
A2	1.5	0.2	0.04	6	1000
A3	1.5	0.2	0.06	7	1000

During the first test series *A1*, a wave steepness s_{0p} = 0.02 in combination with the characteristics mentioned above gave a more or less unstable situation. There were four displaced cubes, which ended in front of the toe of the model. This gives a N_{od} = 0.2. According to previous testing this can be considered as failure of the model [Bhageloe, 1998][Van Gent et al., 1999]. Nevertheless, it was decided to continue with another test run. Picture A0 shows the model before starting the test, and picture A1 is the result after the test serie. The damage occurred just below SWL as can be seen on the picture. For incoming waves the packing density was very stable. But the damage occurred when there was maximum down rush. At that moment there is still much water standing in the sublayer. Due to pressure differences some cubes were pushed out. In addition some sublayer material washed out. Start of damage occurred at $H_s/\Delta D_n$ = 3.5.

During the second test serie *A2*, a wave steepness s_{0p} = 0.04 was used. The same damage pattern was found. Again the damage occurred just below SWL. This time it occurred even lower below SWL. This happened because of the increased wave steepness. Picture A2 presents the damage that appeared after the complete test serie. Start of damage occurred at $H_s/\Delta D_n$ = 2.9. In comparison to the previous discussed test, the damage begun earlier and was more severe. At the end, thirteen cubes were counted at the bottom of the wave flume. Again this model was considered to have failed. Since large gaps were present in the armour layer, some sublayer material washed out.

During the third test *A3*, a wave steepness of s_{0p} = 0.06 was used as input for the wave board. After the test serie it was concluded that the model failed again. This time a total of eight cubes were displaced. All the displaced cubes ended at the bottom of the wave flume. Picture A3 shows the final result of the test serie. Start of damage occurred at $H_s/\Delta D_n$ = 3.2. The total of displaced cubes was less than the total amount of displaced cubes in the precedence test serie. The damage occurred this time even lower beneath SWL compared to the predeceasing test.

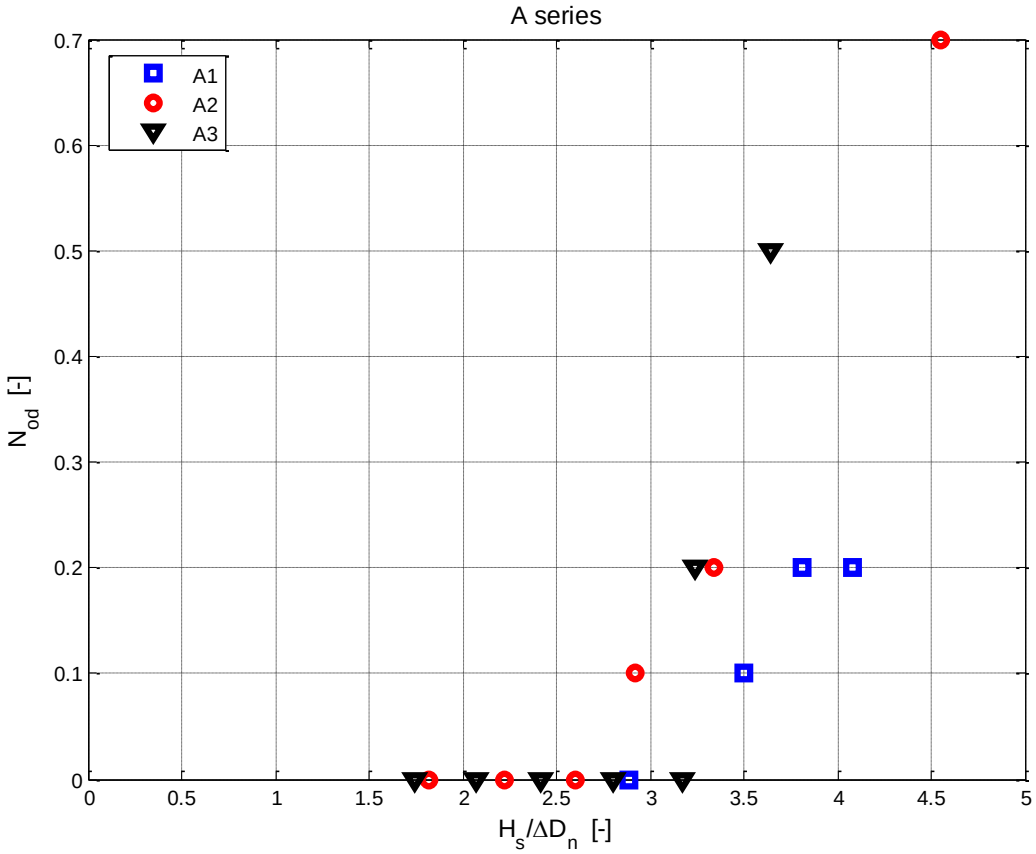

Figure 14. Test results A series, n_p = 0.20, cotα = 1.5

6.1.2 Test serie B

A slope of cotα = 1.5 and three different kinds of wave steepness were tested. Furthermore, a different packing density of n_p = 0.28, different than previous tests, was used. The damage numbers for the tests are presented in annex A.

Table 11. Test serie B

Serie	cotα	n_p	s_{0p}	Tests	Waves
B1	1.5	0.28	0.02	5	1000
B2	1.5	0.28	0.04	6	1000
B3	1.5	0.28	0.06	7	1000

During test serie *B1*, a wave steepness s_{0p} = 0.02 was used. A picture was taken before starting the test serie, picture B0. Picture B1 shows the result after the test serie. Both pictures are almost similar. No damage occurred and just some of the cubes slightly moved.

During the second test serie *B2*, a wave steepness s_{0p} = 0.04 was used. After the tests, picture B2 shows the result. Again no damage was recorded. Some cubes slightly moved due to the wave attack. This is because of resettlement of the cubes.

During the third test *B3*, a wave steepness of s_{0p} = 0.06 was used. No damage was recorded. Some cubes were moving. But it never seemed that a cube would leave the armour layer. After the tests picture B3 was taken.

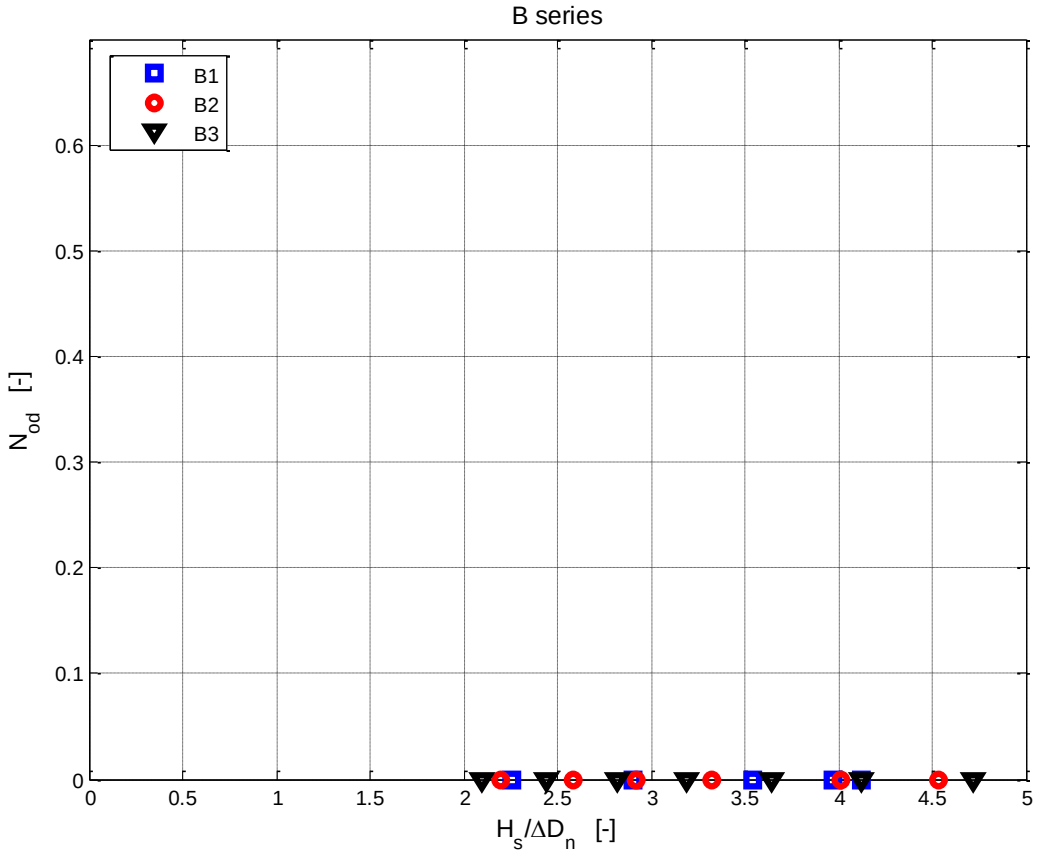

Figure 15. Test results B series, n_p = 0.28, cotα = 1.5

6.1.3 Test serie C

A slope of cotα = 1.5 and three different kinds of wave steepness were tested. Furthermore, a packing density of n_p = 0.35, different than previous tests, was used. The damage numbers for the tests are presented in annex A.

Table 12. Test serie C

Serie	cotα	n_p	s_{0p}	Tests	Waves
C1	1.5	0.35	0.02	5	1000
C2	1.5	0.35	0.04	6	1000
C3	1.5	0.35	0.06	6	1000

During the first test series *C1* some adjustments were made. In the original study a packing density of n_p = 0.40 was included. It was very hard to build an armour layer of cubes applying a n_p = 0.40. Therefore the packing density was changed to n_p = 0.35. Still, it took quite some effort to put the cubes in place. Perhaps unexpected, once in place, it turned out to be rather stable. Using the wave steepness s_{0p} = 0.02, no damage was recorded. Some cubes rotated a bit at $H_s/\Delta D_n$ = 3.4. Picture C0 was taken at the start of the test serie. And picture C1 was taken after.

During the second test serie *C2*, a wave steepness s_{0p} = 0.04 was used. Some damage occurred. In total two cubes were found on the bottom of the wave flume. The damage occurred above SWL. The waves collapsing on the slope is the primary cause of damage, contrary to a low packing density where pressure differences are the cause of the start of damage. Cubes started to rotate at $H_s/\Delta D_n$ = 2.9. Due to the smaller packing density, and therefore larger open space be-

tween the cubes, the cubes tend to subside as a group. Once close together the difference in pressure starts to play a role again. Locally the packing density has changed. Subsequently cubes get lifted out. Start of damage occurred at $H_s/\Delta D_n$ = 4.0. Because this process repeats itself, in time, more damage will occur. This test, only two cubes were found at the toe of the model. Several cubes were rotated. Picture C2 was taken after the test serie was completed. No sublayer material was washed out.

During the third test *C3*, a wave steepness of s_{0p} = 0.06 was used. Only one cube was found on the bottom of the wave flume. Picture C3 shows the results of the test. Again some cubes were rotated. There was no recording of moving sublayer material.

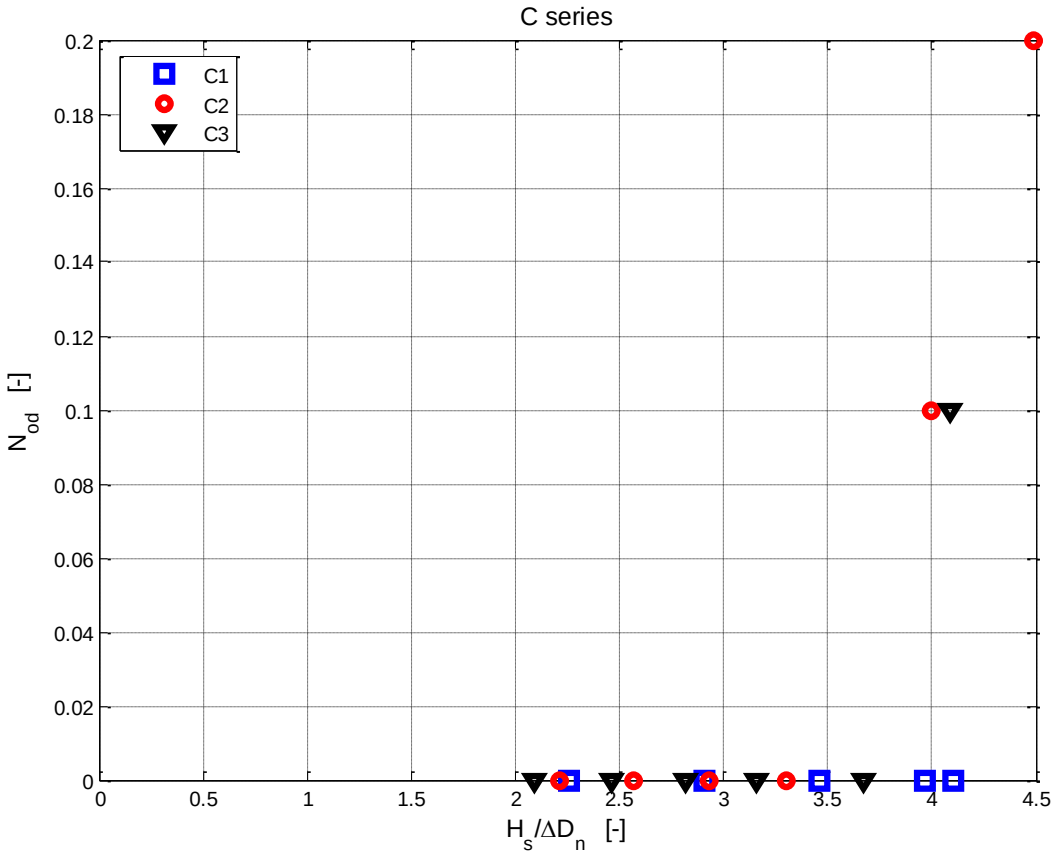

Figure 16. Test results C series, n_p = 0.35, cotα = 1.5

6.1.4 Test serie D

A slope of cotα = 2.0 and a packing density of n_p = 0.2 was used. Furthermore, three different kinds of wave steepness were tested. The damage numbers for the tests are presented in annex A.

Table 13. Test serie D

Serie	cotα	n_p	s_{0p}	Tests	Waves
D1	2.0	0.2	0.02	5	1000
D2	2.0	0.2	0.04	6	1000
D3	2.0	0.2	0.06	6	1000

During the first test series *D1*, a wave steepness s_{0p} = 0.02 in combination with the characteristics mentioned above were tested. The slope was changed to 1:2. A picture before the start of the

test was taken (picture D0). Early damage was recorded (test D102). Start of damage occurred at $H_s/\Delta D_n$ = 2.8. Two cubes were found at the bottom of the wave flume. Damage was recorded just beneath SWL. After those two cubes no more damage was recorded. There were some cubes lifted and returned to their original position. Picture D0 shows the model before the start of the tests. Picture D1 shows the model after the tests

During the second test serie *D2*, a wave steepness s_{0p} = 0.04 was used. There was a lot of damage recorded. Equal to test *serie A* many cubes were displaced due to pressure differences. Damage occurred beneath SWL. In total 21 cubes were found near the toe of the model. Picture D2 presents the end result. Because of the large gaps some sublayer material washed out. More damage would happen when the test wasn't stopped after 1000 waves (full test run).

During the third test *D3*, a wave steepness of s_{0p} = 0.06 was used. Even more damage occurred than test *D2*. A total of 24 cubes were displaced and found at the bottom of the wave flume. Start of damage occurred at $H_s/\Delta D_n$ = 2.8. Nearly all the cubes originated from beneath SWL. A little bit of core material washed out. Picture D3 was taken after 1000 waves. More damage would occur when the test wasn't stopped after the test run of 1000 waves.

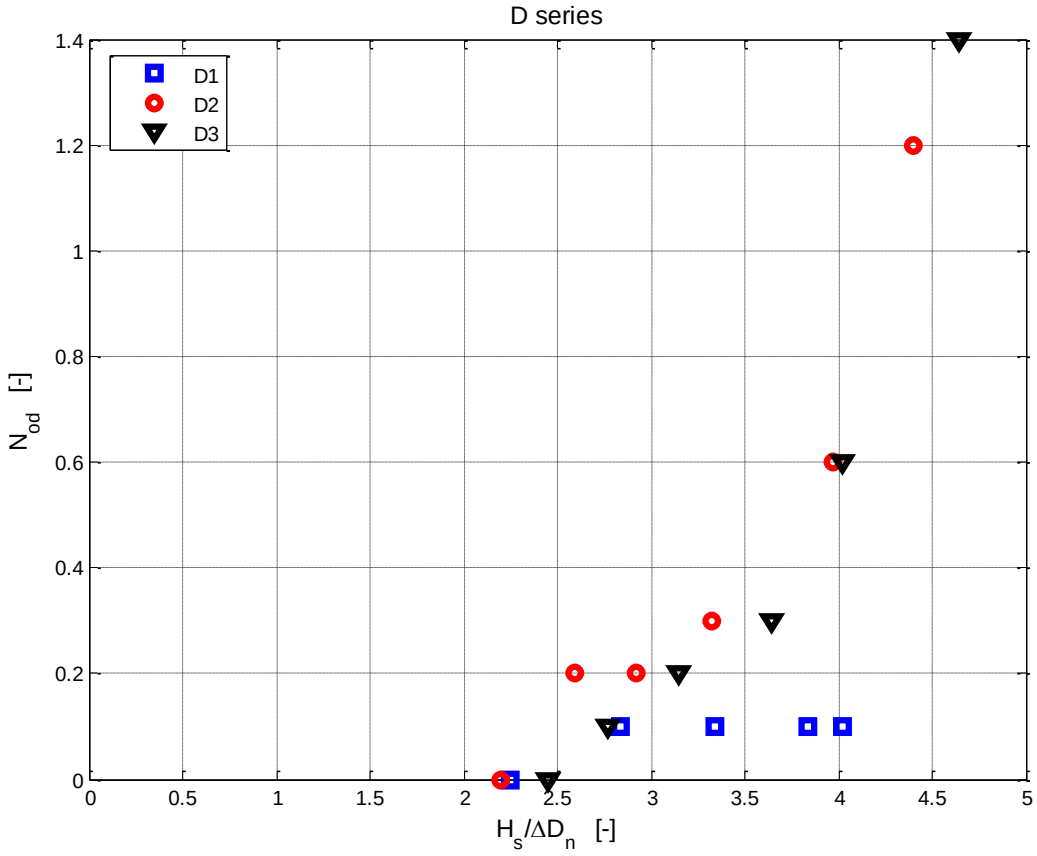

Figure 17. Test results D series, n_p = 0.20, cotα = 2.0

6.1.5 Test serie E

A slope of cotα = 2.0 and a packing density of n_p = 0.28 was used. Furthermore, three different kinds of wave steepness were tested. The damage numbers for the tests are presented in annex A.

Table 14. Test serie E

Serie	cotα	n_p	s_{0p}	Tests	Waves
E1	2.0	0.28	0.02	4	1000
E2	2.0	0.28	0.04	5	1000
E3	2.0	0.28	0.06	6	1000

During the first test series *E1*, a wave steepness s_{0p} = 0.02 in combination with the characteristics mentioned above were tested. There was no damage recorded. Two pictures were taken. Picture E0 shows the model before the test. Picture E1 shows the result.

During the second test serie *E2*, a wave steepness s_{0p} = 0.04 was used. This packing density proofed to be very stable in combination with these characteristics. No damage occurred. During the highest wave heights there were only slightly moving cubes. Picture E2 presents the slope after the test serie.

During the third test *E3*, a wave steepness of s_{0p} = 0.06 was used. Still no damage occurred. Picture E3 was taken afterwards. The cubes were moving slightly during the test with the largest wave height.

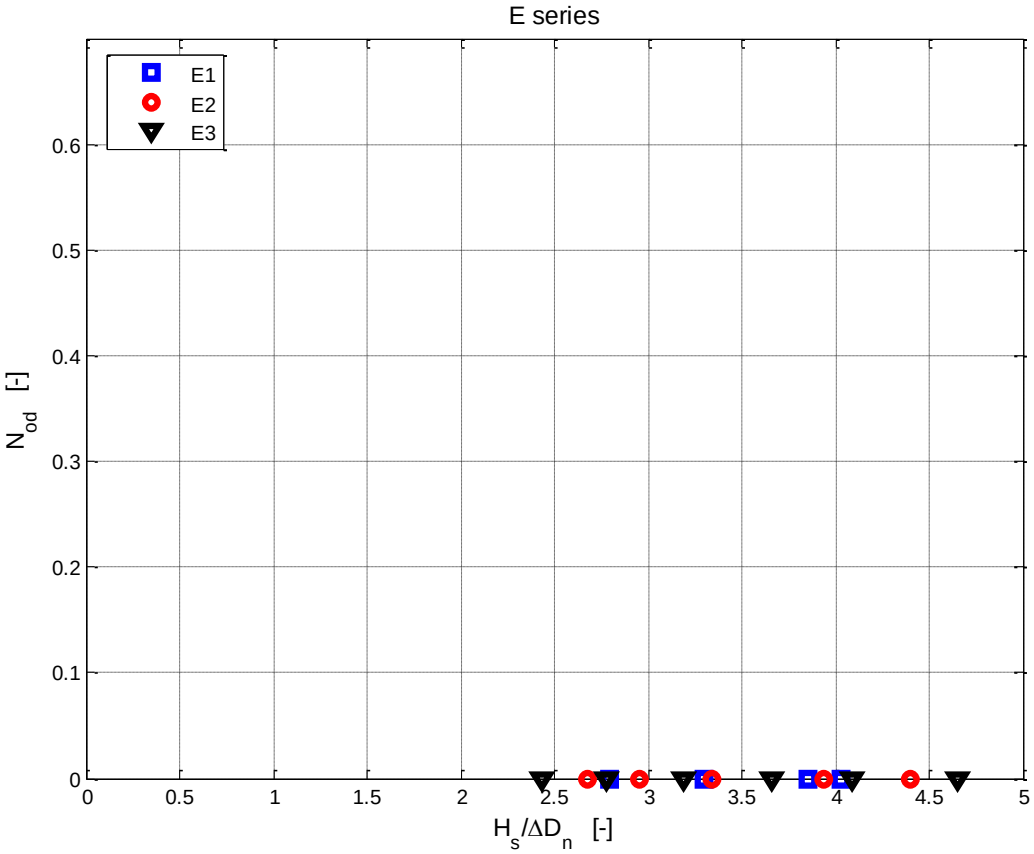

Figure 18. Test results E series, n_p = 0.28, cotα = 2.0

6.1.6 Test serie F

A slope of cotα = 2.0 and a packing density of n_p = 0.35 was used. Furthermore, three different kinds of wave steepness were tested. The damage numbers for the tests are presented in annex A.

Table 15. Test serie F

Serie	cotα	n_p	s_{0p}	Tests	Waves
F1	2.0	0.35	0.02	4	1000
F2	2.0	0.35	0.04	5	1000
F3	2.0	0.35	0.06	7	1000

During the first test series *F1*, a wave steepness s_{0p} = 0.02 in combination with the characteristics mentioned above were tested. A picture before the start of the test was taken (picture F0). During the improving wave heights more cubes started to rotate. Start of rotating of the cubes occurred at $H_s/\Delta D_n$ = 2.5. Finally 8 cubes were rotated forming a local greater packing density. Still, no damage was recorded. Picture F0 shows the model before the start of the tests. Picture F1 shows the slope after the test.

During the second test serie *F2*, a wave steepness s_{0p} = 0.04 was used. Quite a lot of settling occurred. Cubes that started to rotate and ended up lower in the armour layer. Large gaps arise but only one cube left the armour layer. Nevertheless, the model showed gaps that large that the model could be considered to have failed. Start of damage occurred at $H_s/\Delta D_n$ = 3.9. A picture F2 was taken after the test. In total 12 cubes subsided more than 1 D_n.

During the third test *F3*, a wave steepness of s_{0p} = 0.06 was used. Again, cubes started to rotate. Start of rotating of the cubes occurred at $H_s/\Delta D_n$ = 2.8. Picture F3 shows the end result. No cubes were found at the toe of the breakwater. Conform the previous test some cubes ended up lower in the armour layer without leaving the armour layer and within the criteria of one D_n.

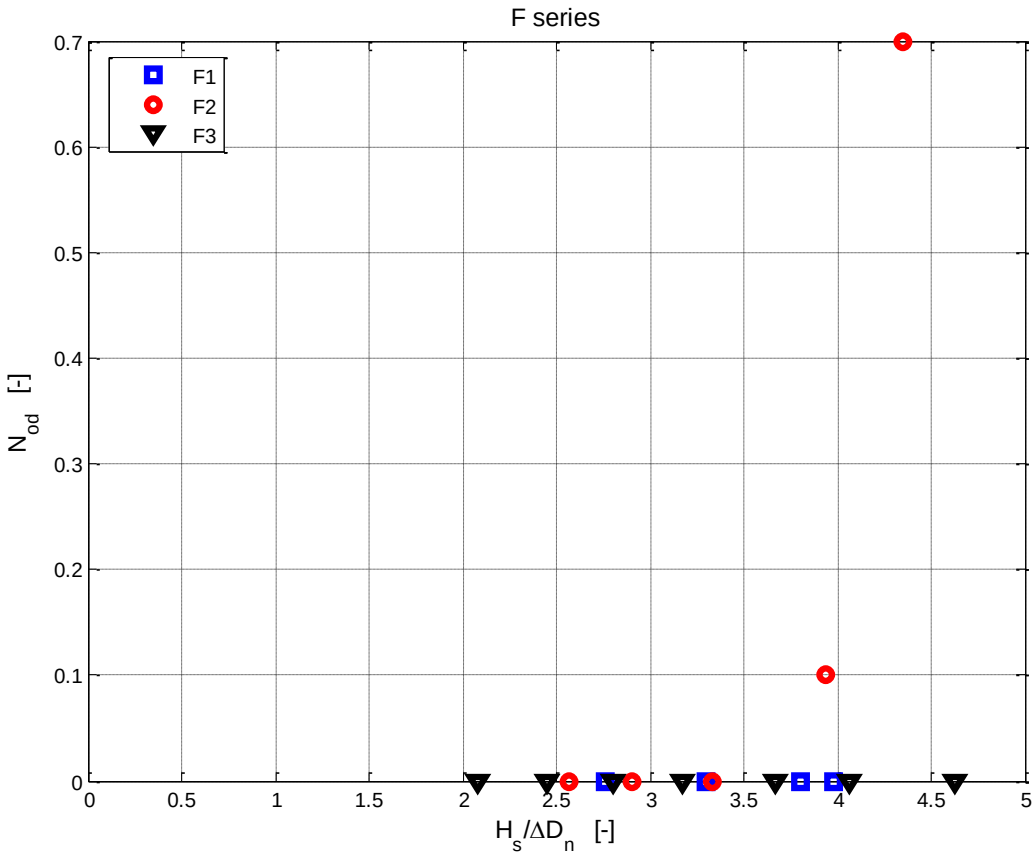

Figure 19. Test results F series, n_p = 0.35, cotα = 2.0

6.2. Discussion of test results

Using the measured data, and trying to find a line that fits the measured data offers some insight on what the influence is of the different parameters. The following parameters are of importance for this study and linked to $H_s/\Delta D_n$:

s_{p0}, cotα and n_p.

6.2.1 Influence of the wave steepness

During the test program, every complete test serie, used three different kinds of wave steepness as input for the wave board. Those are s_{0p} = 0.02, 0.04 and 0.06.

All the used wave steepness's are plotted in a single graph presented in appendix J. In the same graph all points from a data set of a single serie are connected by a line through curve fitting.

Wave steepness s_{0p} = 0.02
A wave steepness of s_{op} = 0.02 didn't do a lot of damage during testing. The only damage recorded is in combination with a small packing density (n_p = 0.2). All other tests show no damage.

Wave steepness s_{0p} = 0.04
Different outcomes are found. A total of 13 cubes are displaced after test A2, none after test B2 and just 2 after test C2. For a different slope other conditions apply. A total of 21 cubes were displaced after test D2. No cubes are displaced after test E2 and 4 after F2.

Wave steepness s_{0p} = 0.06
Again, different outcomes are found. A total of 8 cubes are displaced after test A3, none after test B3 and only 1 after test C3. For a different slope (1:2) other conditions apply. A total of 24 cubes were displaced after test D3. No cubes are displaced after test E3 and none after F3.

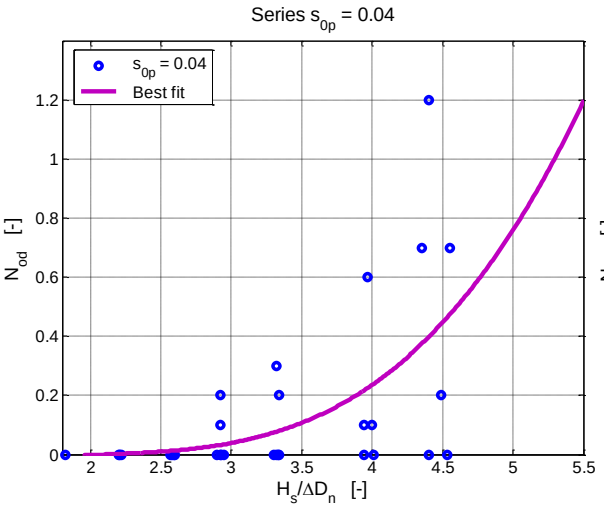

Figure 20. All series with s_{0p} = 0.04

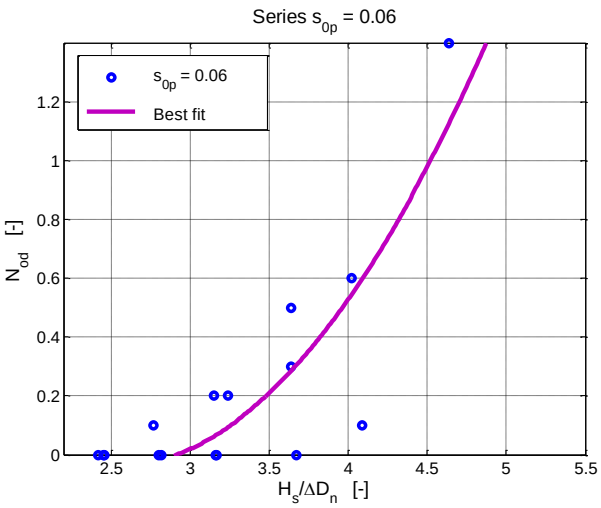

Figure 21. All series with s_{0p} = 0.06

There are large scatters in the result for the wave steepness as can be seen in the graphs above. In an attempt to find the influence of the wave steepness no clear results were found. Nevertheless some remarks can be made. When looking at the two figures above it can be said that damage occurred sooner with a wave steepness of 0.04. But the damage that occurs is more severe and increases more rapidly with a wave steepness of 0.06. Failure occurs for s_{0p} = 0.04 at N_{od} = 0.2 with a stability number of 3.9. And for s_{0p} = 0.06 already at 3.5.

6.2.2 Influence of the packing density

For tests A and D a packing density of $n_p = 0.20$ was applied. Test B and E used a $n_p = 0.28$. A packing density $n_p = 0.35$ was applied to test C and F. All the used wave packing densities are plotted in a single graph and presented in appendix J. In the same graph all points from a data set of a single serie are connected by a line through curve fitting

Packing density $n_p = 0.2$
The tests showed that when applying the packing density of $n_p = 0.2$, the armour layer will fail due increasing flow in the core of the breakwater. When the down rush reaches the maximum, the breakwater will be unable to reduce the pressure inside due to lack of porosity. Due this interaction the cubes will be lifted and will be pushed out the armour layer. This could happen very rapidly depending on the incoming wave height and wavelength, hence the wave steepness. This packing density is very stable when only considering wave force impact.

The process of placing the cubes using this packing density $n_p = 0.2$, is very easy. The cubes can be placed almost randomly keeping in mind that the cubes should be placed parallel to the slope. The damage occurs beneath SWL.

Packing density $n_p = 0.28$
The tests performed using a packing density of $n_p = 0.28$ showed that, within the boundaries of the test program, no damage occurred. The cubes were stable. When placing the cubes in a stretching bond (halfsteensverband), the armour layer gains strength due the interaction of the cubes. The cubes use the weight of the cubes above to be more stable. At the same time the porosity is sufficiently large to release the pressure inside the breakwater that has been build up by the water inside the core. The placing method is of importance. This packing density could be realized fairly easy.

Packing density $n_p = 0.35$
For a packing density of $n_p = 0.35$ a different process occurs. Contrary to the packing density of $n_p = 0.28$ this packing density fails due the wave force impact. The cubes will rotate because of the waves collapsing on the slope. The cubes subside and will form locally a lower porosity. This way the local pressure will increase again, subsequently the cubes will be lifted again.

The process of placing the cubes when applying this packing density is rather difficult. This is because of the big gaps between the cubes. In practice this will be almost impossible to realize. Even with assistance from a diver. Damage occurred above SWL.

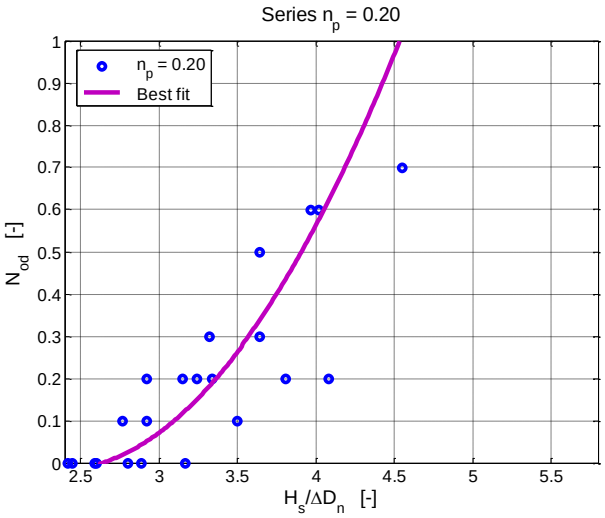

Figure 22. All series with $n_p = 0.20$

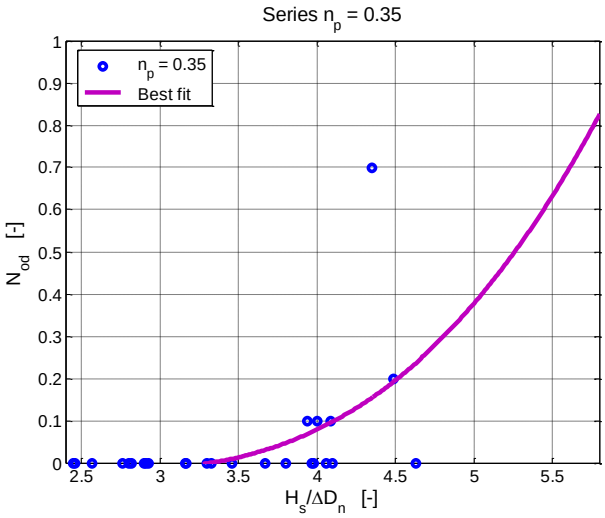

Figure 23. All series with $n_p = 0.35$

Obvious the series with a packing density of n_p = 0.28 is the most stable configuration. Since no damage occurred no graph is drawn. Graphs are presented for the packing densities of n_p = 0.20 and n_p = 0.35. For the packing density of n_p = 0.20 the damage happened the fastest and increased rapidly. Early damage was recorded at a stability number of 2.7.

6.2.3 Influence of the slope

Tests A, B and C used a slope of cotα = 1.5. Tests D, E, and F used a slope of cotα = 2.0. Since tests B and E didn't produce any damage, it's hard to use the data for the analysis. All the test series with different slopes are plotted and presented in appendix J.

Slope cotα = 1.5
The tests involving a slope of cotα = 1.5 showed that a larger stability was reached than using a slope of cotα = 2.0. Although some tests with this slope showed one or two more displaced cubes (A1/D1, see table beneath). This is attributed to the placement. Another benefit is the lesser material needed for the armour layer, sublayer material, core material, and the usage of surface.

Slope cotα = 2.0
In some tests a considerable amount of cubes were displaced. Especially when a slope of cotα = 2.0 was applied. The stability of the cubes is less. This is probably due the lack of interlocking. Furthermore, contrary to the slope of cotα = 1.5, more material is needed for the armour layer, sublayer material, core material. Also the usage of surface increases when applying a gentler slope.

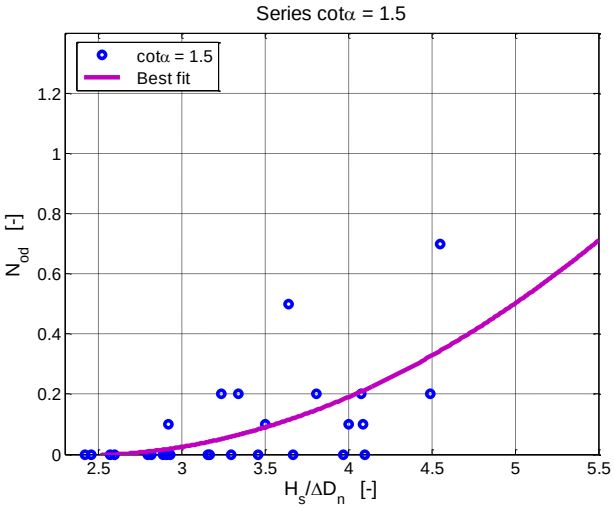

Figure 24. Series cotα = 1.5

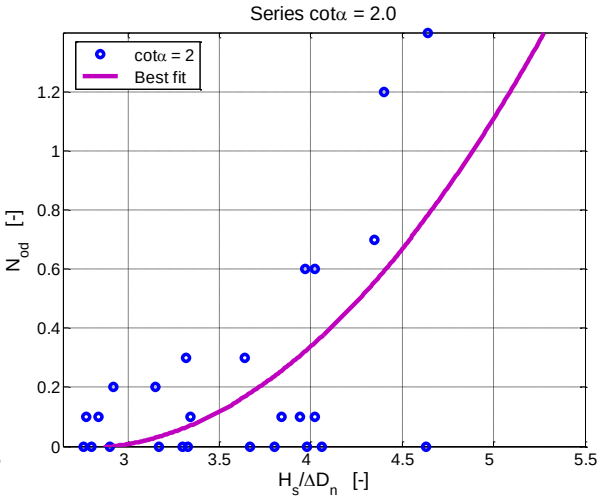

Figure 25. Series cotα = 2.0

The figures above present the series with the same slope. Start of damage is roughly the same. But the damage of the model occurred faster with a slope of cotα = 2.0. It can be said that the starting point of failure is the same but the damage increases with a factor 2 in this configuration.

6.2.4 Individual test series

In an attempt to find the most stable configuration all the series were plotted in one figure and connected with a line through curve fitting.

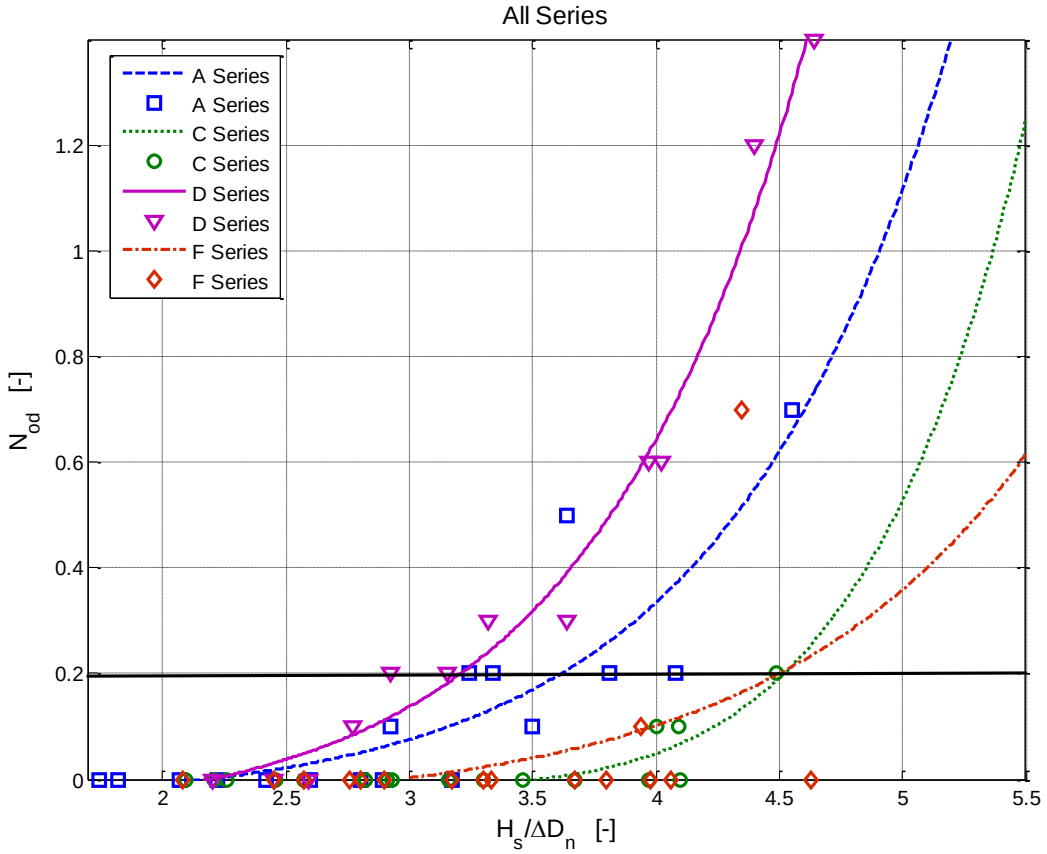

Figure 26. All Series

It must be mentioned that test series B and E aren't included because these tests didn't show any damage. Therefore those tests are the most stable configurations. Nevertheless, these tests use different slopes and different wave steepness's. That's why in this paragraph the other series are discussed.

Looking at the figure above, it shows that earliest failure occurs with the D-series. The D-series use a slope of cotα = 2 and a packing density of n_p = 0.20. Test series A doesn't look stable either, as well as test series F. The later shows an explosive growth on the damage. This is unacceptable. Finally, test series C gives very good results. Failure occurs at a stability number of 4.5. This is very high.

Still, as mentioned before the results of test series B and E are excellent. Both use a packing density of n_p = 0.28 but use different slopes.

The following table presents the stability numbers that correspond with a damage number N_{od} of 0.2.

Table 16. Stability numbers for all test at N_{od} = 0.2 (failure)

Serie	A	B	C	D	E	F
$H_s/\Delta D_n$	3.6	> 4.7	4.5	3.2	> 4.6	4.5

All test results previously plotted in this chapter show a large scatter of the data. Therefore in the next paragraph a different approach is introduced.

6.2.5 Data comparison Bhageloe

Bhageloe used during his tests with a single armour layer of cubes a constant slope of 1:1.5. furthermore, a packing density of n_p = 0.28 and different kinds of wave steepness was applied. The same configuration was applied during test series B. The difference again lies within the placement method. The next graph presents the data from Bhageloe together with the data generated from test series B.

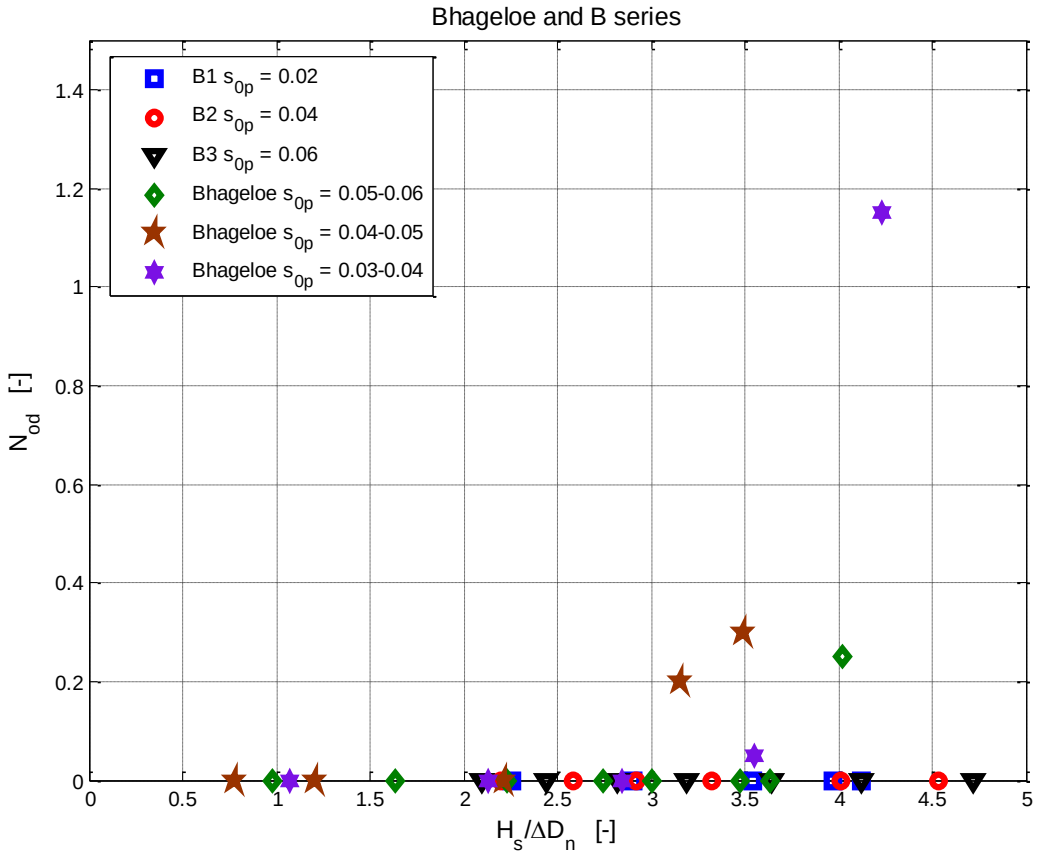

Figure 27. Bhageloe and B series

Since the data generated during the B series didn't gave any damage and the data from Bhageloe did, it can be stated that the configuration use in this study is more stable than the configuration used by Bhageloe.

6.2.6 Influences

Attempts to optimize an equation in which the influence of all the test parameters are considered weren't very successful. Therefore an attempt is made with a limited amount of variables. Formulae for artificial units were derived in the past. A well known formula was derived by Van der Meer (1988) for a double armour layer of cubes is already presented and has the following form:

$$\frac{H_s}{\Delta D_n} = \left(6.7 \frac{N_{od}^{0.4}}{N^{0.3}} + 1.0 \right) s_{m0}^{-0.1} \qquad (6.1)$$

This formula forms the basis for the for the formula found and presented below.

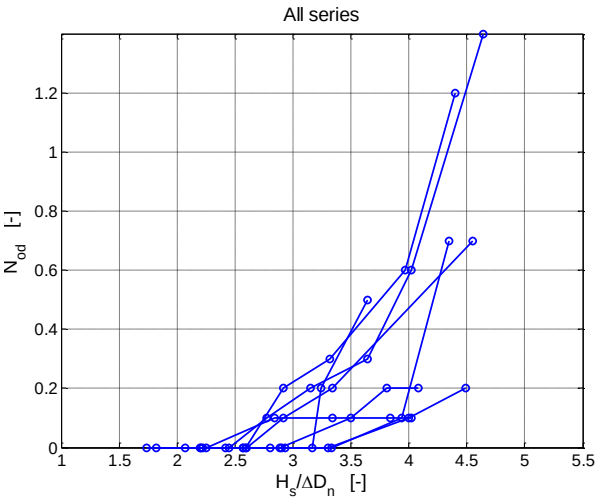

Figure 28. All series

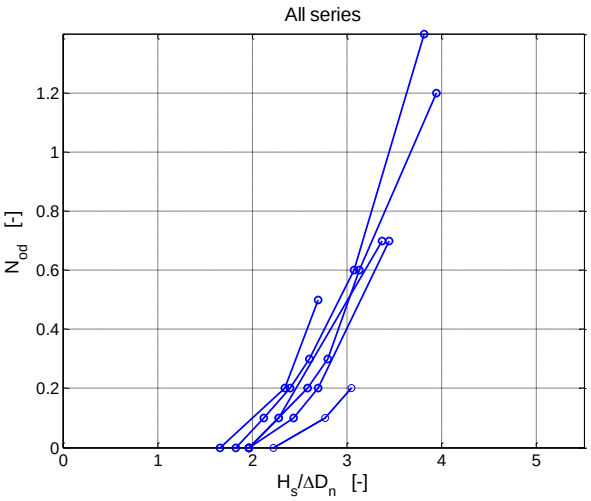

Figure 29. Applied formula

The amount of waves was kept constant during all test series and therefore this parameter isn't directly used in this equation.

$$\frac{H_s}{\Delta D_n} = \left(1.0 N_{od}^{0.6} + 1.1\right) s_{0p}^{-0.18} \tag{6.2}$$

6.3. Analysis of the test results

The results found in the previous chapters seem so have strong a correlation with pitched stones. This setting has a relative small permeability and large friction force between the armour elements. This is also the case with concrete cubes. Therefore the black box model as well as the analytical method for pitched stones is treated in an attempt to optimize the design rules for different configurations. First the black box method and the analytical method is explained. After that the individual series are presented. Finally an attempt is made to find a general stability rule in which the packing density, the slope and the wave steepness is involved regarding a single layer of cubes placed in a stretching bond.

6.3.1 Black-box model

The black-box model was developed for the need of a first global design of the top layer stability. Subsequently it can be used as a criterion for armour layer stability to which it simply can be tested with the use of a computer. The simplicity however, has as downside that the area of uncertainty is rather large. The black-box method is often used as design method for a stable armour layer.

The black-box model has kept it's original form during the past years. The breaker parameter ξ_{0p} was placed on the horizontal axis, while the stability number $H_s/\Delta D_n$ was placed on the vertical axis. The figures show two lines. These lines represent a boundary for a certain area. The following areas are represented.

- The stability of the armour layer is good (beneath the lowest line).
- The stability of the armour layer is uncertain (between the two lines).
- The stability of the armour layer is insufficient (above the highest line).

Previous black-box models are based on hydraulic model tests. The first test results were published in 1992. Since then, the method is improved. Two improvements are of importance. Those are, an increasing breaker parameter ξ_{0p} and irregular waves instead of only regular waves.

Early graphs showed that the lines kept descending. Recently is discovered that the stability of the armour layer as function of the breaker parameter ξ_{0p} could increase if $\xi_{0p} > 3$. It should be mentioned that under normal Dutch circumstances the ξ_{0p} varies between one and two. Nevertheless in this study $\xi_{0p} > 3$ will be included.

6.3.2 Analytical method

For the calculations of the failure mechanism armour layer instability the so-called analytical method can be used. The method was formed in such a way that the armour layer can be checked on stability. The following criteria are used for the analytical method.

- The armour layer element may not move despite wave attack.
- The armour layer element can move only 10%.
- The general stability boundary should hold (6-xi-rule)

When using the analytical method as design method, the armour layer should be tested on all three criteria. In some combinations of parameters, unrealistic high stability calculations are the result (for example with very fine sub layer material in combination with low packing density). Therefore a general upper rule was developed known as the 6-xi-rule. The mean focus regarding the analytical method will lie on the 6-xi-rule

$$\frac{H_s}{\Delta D_n} \leq 6\xi^{-2/3} \tag{6.3}$$

The following graph gives an indication of the 6-xi-rule. The rule is founded on extended hydraulic tests [TAW, 2003]

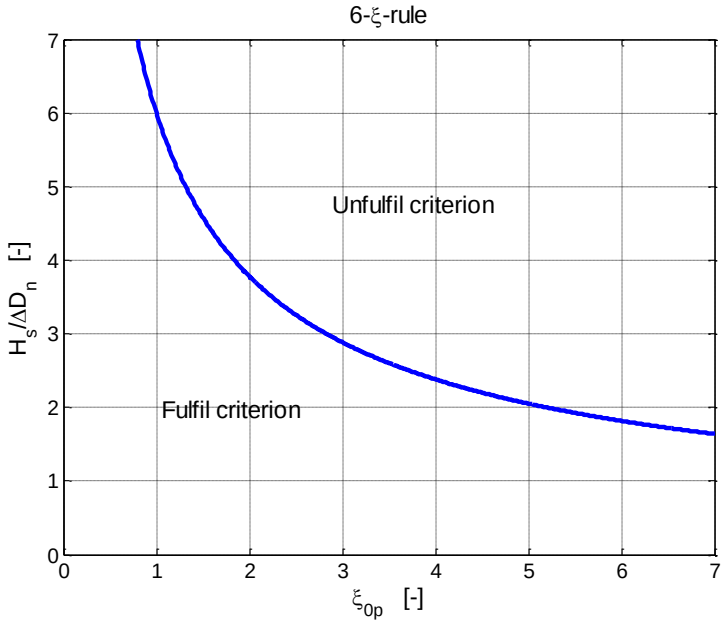

Figure 30. 6-xi-rule

6.3.3 Test results based on black-box model and analytical method

All the performed series are plotted in graphs based on the black-box model and analytical method. The analytical method is used to find an optimum xi-rule per test serie. Subsequently the lines that indicate the 'uncertain' area, according to the black box model, is plotted. This way the optimum xi-rule is found. All individual graphs are presented in appendix H.

6.3.4 Test series

The data from all the series is plotted in a total of six graphs presented in appendix H. The graphs plotted have three different values. The damage number N_{od} is used in the graphs to indicate three different situations. No damage, start of damage and failure indicated by triangles and circles.

- $N_{od} = 0$
- $0 < N_{od} < 0.2$
- $N_{od} \geq 0.2$

The table beneath presents the different xi-values found by using the lowest line. Above this line the uncertainty starts playing a role.

Table 17. Xi-rules found

Serie	A	B	C	D	E	F
n_p	0.2	0.28	0.35	0.2	0.28	0.35
cotα	1.5	1.5	1.5	2.0	2.0	2.0
Best fit	$6.5\xi^{-2/3}$	$12\xi^{-2/3}$	$8\xi^{-2/3}$	$5\xi^{-2/3}$	$9.5\xi^{-2/3}$	$6.5\xi^{-2/3}$

6.3.5 Slope and packing density

The two graphs below present the two slopes with the three packing densities in two graphs. The graphs show that the packing density of $n_p = 0.28$ on a slope of 1:1.5 is the most stable configuration.

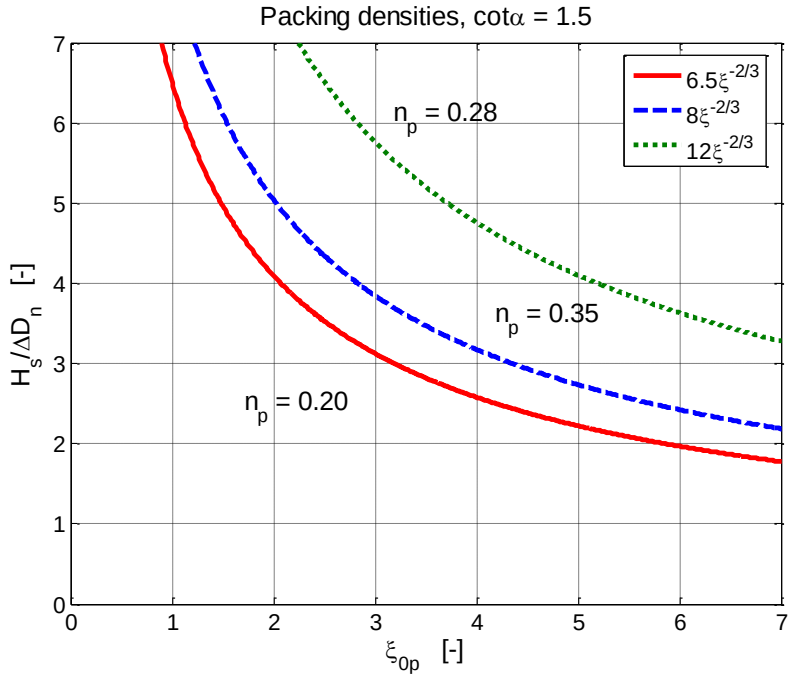

Figure 31. Packing densities on slope cotα = 1.5

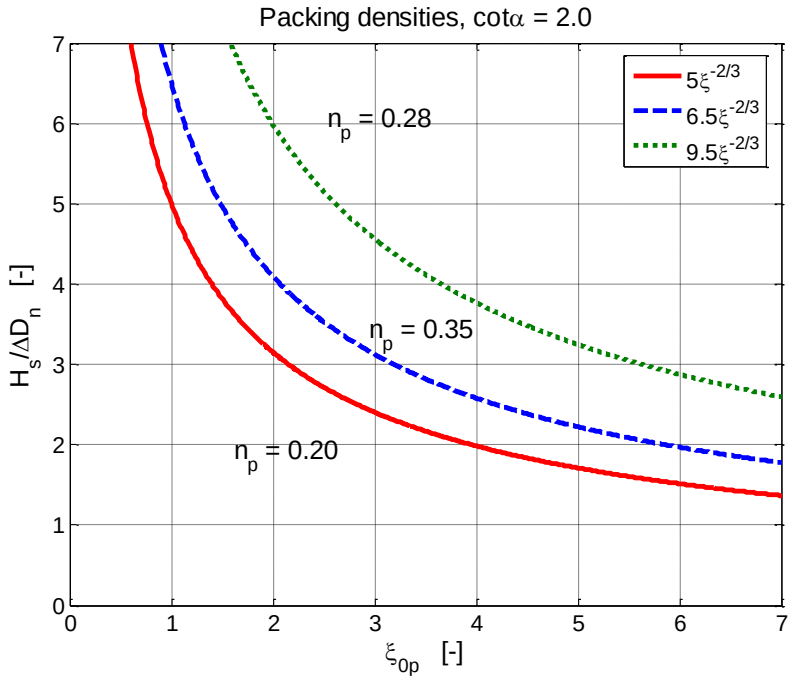

Figure 32. Packing densities on slope cotα = 2.0

Furthermore, the slope of cotα = 1.5 is more stable than cotα = 2.0, when applying this configuration. The graphs do support this analysis. It most be mentioned that the packing density of $n_p = 0.28$ could be more stable than presented in the graphs above. This is due the fact that during testing no damage was reported when a packing density of $n_p = 0.28$ was applied.

6.4. Cubes in a stretching bond

In this paragraph an attempt is made to realize formulae in which the influence of the packing density and the influence of the slope are combined. The formulae by Van der Meer are used as a starting point to develop formulae which include the packing density. The formula for a double layer of cubes doesn't involve the surf similarity parameter. Therefore no distinguish is made for surging and plunging waves. Looking at the plotted results from the test series this it seems unjustified. Therefore the formulae for loose rock is used as a starting point.

Since we have a different configuration than riprap, the permeability parameter is not applicable here. As well as the form of the damage number. The waves were kept constant in this study. Still the formulae by Van der Meer is used as a starting point to develop formulae which include the packing density and slope variation.

6.4.1 Formulae

Van der Meer used the distinction between surging waves and plunging waves. Therefore, and based on the fact that the stability probably increases when $\xi_{0p} > 3$, The same is done here. The plotted data does show an increased stability when $\xi_{0p} > 3$ occurs. The following formulae are developed that can be applied for cubes that are placed in a stretching bond.

For plunging waves $\xi_p < \xi_{cr}$:

$$\frac{H_s}{\Delta D_n} = c_{pl} \cdot \xi_p^{-0.5} \cdot n_p^{0.18} \cdot \cot \alpha^{-0.5} \tag{6.4}$$

For surging waves $\xi_p \geq \xi_{cr}$:

$$\frac{H_s}{\Delta D_n} = c_s \cdot \xi_p^{\,2/3} \cdot n_p^{\,0.13} \cdot \cot \alpha^{0.5} \tag{6.5}$$

In which: c_s = coefficient for surging waves depending on packing density [-]
c_{pl} = coefficient for plunging waves depending on packing density [-]

The formulae use different coefficients for different breaker types. The coefficients for different wave conditions are found through curve fitting. For different packing densities different processes play a role. In the next paragraph this will be discussed. For now the different coefficients are presented in the next table.

Table 18. Coefficients for breaker types

Packing density [-]	n_p	0.2	0.28	0.35
Coefficient for plunging waves [-]	c_{pl}	8.5	15	10.5
Coefficient for surging waves [-]	c_s	1.1	1.5	1.25

It must be mentioned that this is a careful estimation in case of test series B and E, since with this packing densities no damage occurred. Similar to Van der Meer's equations there is a point of transition. This point of transition can be found by:

$$\xi_{cr} = \left[\frac{c_{pl}}{c_s} \cdot n_p^{0.05} \cdot \tan\alpha \right]^{6/7} \tag{6.6}$$

When applying the formulae on the test serie A, the following results are plotted.

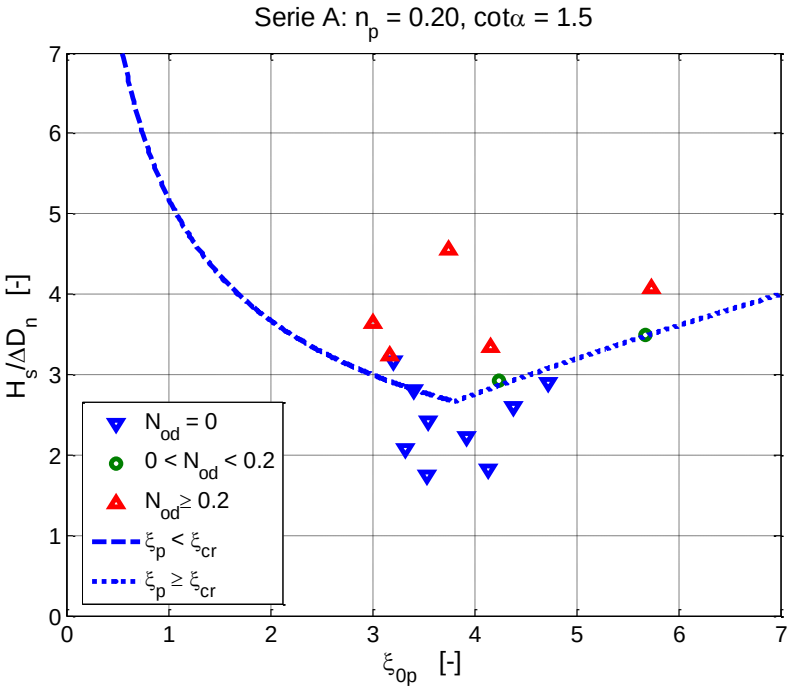

Figure 33. A Series with formulae

All other test series are plotted using the formulae above and presented in appendix I.

6.4.2 Physical process

In this paragraph an attempt is made to specify the physical processes which form the basis for the behaviour of the different results found in the previous chapters.

For an armour layer basically two different failure mechanism can be distinguished. Those are:

- The situation in which the wave has maximum withdraw.
- The situation in which the wave hits the armour layer.

The first situation, in which the wave has it's maximum withdraw is a complex dynamic progress. This process has it's maximum at the lowest point of the waterline. At this point, a flow occurs in the direction of the armour layer elements from within the sub layers and core. The flow will result in a pressure difference that can lift the armour layer elements from the top layer. For the stability of the armour layer it is important that the water easily flows through the armour layer but, at the same time, it has difficulties flowing through the sub layer.

This process, elevation of the cubes out of the armour layer, happened when the packing density of n_p = 0.20 was applied. Therefore this mechanism is the cause of failure for this configuration. But the packing density of n_p = 0.35 didn't have the problem of cubes that got lifted.

The second process is more or less the reverse mechanism. At the moment of impact a pressure peak occurs at the top of the armour layer elements, which subsequently penetrates the sublayer. Although this happened for all packing densities, the packing density of $n_p = 0.35$ suffered the most from this failure mechanism. Due to the large gaps the cubes couldn't interlock enough to withstand the wave impact and started to rotate and finally subsided.

Although the packing density of $n_p = 0.20$ failed because of the pressure difference which was formed during the wave trough, it was capable resisting the wave force.

Based on the tests it can be said that the packing density of $n_p = 0.28$ was the most stable configuration. It seems to be the optimum packing founded on the facts that is capable of releasing the pressure and withstand the wave attack at the same time.

The test results show that a slope of $\cot\alpha = 1.5$ is more stable than a slope of $\cot\alpha = 2.0$. The steeper slope seems to benefit more from the gravity in the form of friction between the armour elements. When the slope gets steeper the cubes seem to rely more on the neighbouring cubes. The more gentler slope therefore relies less on the friction between the elements and therefore get lifted easier when packing density of $n_p = 0.20$ is applied. Also when a packing density of $n_p = 0.35$ was used in combination with a slope of 1:2, the cubes started to rotate sooner than on a slope of 1:1.5.

The findings in this paragraph seem to justify the surging and plunging coefficients found through curve fitting.

7. CONCLUSIONS

The main objectives of this study are to assess the influence of the slope, packing density and wave steepness on the stability of an armour layer consisting of concrete cubes placed in a stretching bond. The study consists of hydraulic testing performed in a wave flume from the Fluid Mechanics laboratory of the Faculty of Civil Engineering and Geosciences at Delft University of Technology. A total of eighteen tests were performed. During these tests three different wave steepness were tested, as well as three different packing densities and two different slopes.

The following test program was realized.

Table 19. Test program of the study

Test series	n_p	cot α	s_{0p}
A	0.20	1.5	0.02-0.06
B	0.28	1.5	0.02-0.06
C	0.35	1.5	0.02-0.06
D	0.20	2.0	0.02-0.06
E	0.28	2.0	0.02-0.06
F	0.35	2.0	0.02-0.06

Additional, the placement method is an important parameter. The cubes were placed by hand in a stretching bond configuration.

7.1. Slope angle

The test results showed that the slope of 1:1.5 gave better results than the slope of 1:2. Failure of the armour layer occurred sooner when applying a slope of cotα = 2.0.

Cubes that are placed on the steeper slope do interlock better than the cubes on the milder slope. Gravity contributes to the stability more than with the less steeper slope. The cubes rely more on the sublayer material when using the less steeper slope. This is coherent with the reason that a steeper slope leads to more stability. Also cost wise is the steeper slope more attractive.

- Based on the performed tests, the slope of cotα = 1.5 gives the best results.

7.2. Packing density

The best results were achieved using a packing density of 0.28. As a matter of fact, stability numbers as high as 4.5 were no exception. This is very high. The porosity is good to overcome the pressure problem and, at the same time, the armour layer is consistent to withstand the wave forces. It saves concrete compared to the packing density of n_p = 0.20. Furthermore, it is easier to realize than n_p = 0.35. This conclusion is conform the findings of previous tests although the cubes during this study were placed in a stretching bond. [Van Gent et al, 1999].

- Based on the performed tests the packing density n_p = 0.28 gives the best results.

7.3. Wave steepness

The tests all showed a similar process. The wave steepness of 2% didn't do much damage. Most damage occurred when a wave steepness of 4% - 5% was applied. The following conclusions can be drawn:

- Minimum stability will occur at s_{0p} = 0.04-0.05.

This is conform the earlier findings [Bhageloe, 1998].

7.4. Placement method

The cubes were placed in a stretching bond. Horizontal rows were formed with every cube at the same distance from each other. The results are very promising and more stable than random placement like dropping the cubes from above the waterline.

7.5. Overall conclusion

Based on the findings above the following combination of slope and packing density can be seen as the most stable combination.

- A slope of cotα = 1.5 and the cubes placed in a stretching bond with a packing density of n_p =0.28, is the most stable configuration that is tested.

Using the data that is found from the tests results, a set of equations is developed to predict the behaviour of the armour layer's stability. The equations involve the wave steepness, slope and packing density and is valid for a single armour layer consisting of concrete cubes and the placement method tested in this study, e.g. a stretching bond.

For plunging waves $\xi_p < \xi_{cr}$:

$$\frac{H_s}{\Delta D_n} = c_{pl} \cdot \xi_p^{-0.5} \cdot n_p^{0.18} \cdot \cot\alpha^{-0.5} \tag{7.1}$$

For surging waves $\xi_p \geq \xi_{cr}$:

$$\frac{H_s}{\Delta D_n} = c_s \cdot \xi_p^{2/3} \cdot n_p^{0.13} \cdot \cot\alpha^{0.5} \tag{7.2}$$

With the transition from plunging waves to surging waves which can be derived using the critical value of the surf similarity parameter ξ_{cr}:

$$\xi_{cr} = \left[\frac{c_{pl}}{c_s} \cdot n_p^{0.05} \cdot \tan\alpha \right]^{6/7} \tag{7.3}$$

For the coefficients for plunging waves and surging waves the following coefficients have been found through curve fitting and presented in the next table.

Table 20. Coefficients for breaker types

Packing density [-]	n_p	0.2	0.28	0.35
Coefficient for plunging waves [-]	c_{pl}	8.5	15	10.5
Coefficient for surging waves [-]	c_s	1.1	1.5	1.25

The formulae derived show a significantly more stable situation that the formulae derived by Van der Meer. As mentioned before this is due the placement pattern. The placement method, in a stretching bond, is an attractive solution to save concrete and at the same time gain on stability.

8. RECOMMENDATIONS

The overall results show that a single armour layer of cubes placed in a stretching bond is very stable when using a packing density of $n_p = 0.28$. The high stability number that is reached looks very promising.

- The results treated in de conclusions show that more tests are recommended. As found in earlier tests a packing density of $n_p = 0.28$ gives the best results. The difference lies in the fact that the method of placement differs. Nevertheless it is comprehensive with the studies before [Van Gent en Spaan, 1998] [Bhageloe, 1998] [Van der Meer, 1999]. All tests are based on a single test serie. It is recommended to repeat the same test serie to verify the results.

- The steeper slope with the stretching bond placing method seems to be the best alternative. Most breakwaters with a single layer of cubes as armour layers are built with a slope of 1:1.5. For the test series using a different slope, it is recommended to do more tests with more slopes. For instance, what would be the influence on the stability when applying a slope of 1:3, or 1:1.33 even.

- The packing density of $n_p = 0.28$ and a slope of 1:1.5 needs further testing. Basically the wave flume wasn't able to create waves that were capable of doing any damage on this configuration. An even greater stability number can be achieved. Greater than the already reached $H_s/\Delta D = 4.5$. This looks very promising.

- During the present study the experiments were performed with the number of waves set on N = 1000. It is advisable to perform tests with more than 1000 waves.

9. REFERENCES

BATTJES, J.A. (1998) Collegedictaat “korte golven” CT4320. Technische universiteit Delft, Faculteit Civiele Techniek en Geowetenschappen (Reader Short Waves)

BHAGELOE, G.S. (1998) Golfbrekers met een enkele toplaag (Breakwaters with a single toplayer), Master’s Thesis, *Delft University of Technology, Delft*

BISSCHOP, C. (2002) Modelonderzoek naar het aanbrengen van kubussen in de toplaag van een golfbreker met een zijschuifstorter (Model investigation into the placement of cubes on a breakwater using a side-stone dumping vessel), Master’s Thesis, *Delft University of Technology, Delft*

BUIJS, A. (1984) Statistiek om mee te werken (Statistict in practice); second, revised edition, H.E. Stenfert Kroese B.V. Leiden

BURCHARTH, H.F., LIU, Z. AND TROCH, P. (1999) Scaling of core material in rubble mound breakwater model tests, *Proceedings of COPEDEC V, Cape Town,* 1518-1528

CIRIA; CUR; CETMEFT (2007) The Rock Manual, The use of rock in hydraulic engineering (2nd edition)

DAI, Y.B. and KAMEL, A.M. (1969), Scale effect tests for rubble-mound breakwaters, U.S. Army Engineer Waterways Experiment Station, Corps of engineers, December 1969, Vicksburg, Mississippi

D'ANGREMOND, K., VAN ROODE, F.C. (2001) Breakwaters and closure dams, *Delft University Press, Delft*

D'ANGREMOND, K., BERENDSEN, E., BHAGELOE, G.S., VAN GENT, M.R.A. AND VAN DER MEER, J.W. (1999) Breakwaters with a single armour layer, *Proceedings of COPEDEC V, Cape Town,* 1441-1449

DE VRIES, M. (1977) Waterloopkundig onderzoek: collegehandleiding b80 (Hydraulic model investigation: college manual b80); second edition, *Technische Hogeschool Delft, Delft* (in Dutch)

HOLTHUIJSEN, L.H. (2002) Waves in Oceanic and Coastal Waters, *Delft University of Technology, Delft*

HUGHES, S.A. (1993) Physical models and laboratory techniques in coastal engineering, *World Scientific Publishing Co. Pte. Ltd., Singapore*

MANSARD, E. and FUNKE, E. (1980), ‘The measurement of incident and reflected spectra using a least-square method, Proc. ICCE’80, ASCE, pp.154-172, Sydney

TAW (2003), Technisch rapport steenzettingen, Achtergronden. Verkeer en Waterstaat

VAN DER MEER, J.W. (1987) Stability of breakwater armour layers – Design formulae, *Coastal Engineering 11,* 219-239

VAN DER MEER, J.W. (1988) Stability of cubes, tetrapods and accropode, *Proceedings of the International Conference on Breakwaters ’88, Eastbourne, ICE,* 71-80

VAN DER MEER, J.W. (1999) Design of concrete armour layers, *Proceedings of the International Conference on Coastal Structures '99, Santander,* 213-221

VAN DER VLIET, C. (2001) Praktisch haalbare plaatsingsdichtheid van betonnen kubussen in de afdeklaag van een golfbreker (Practically achievable placing density of cubes in the armour layer of a breakwater), Master's Thesis, *Delft University of Technology, Delft*

VAN GENT, M.R.A. AND SPAAN, G.B.H. (1998) Golfbrekers met een enkele toplaag van kubussen (Breakwaters with a single layer of cubes), Delft Hydraulics report H3387, Delft Hydraulics, Delft

VAN GENT, M.R.A., D'ANGREMOND, K. AND TRIEMSTRA, R. (2001) Rubble mound breakwaters: Single armour layers and high-density units, *Proceedings of the International Conference on Coastlines, Structures and Breakwaters, London, ICE,* 307-318

APPENDIX A; TEST RESULTS

Deep water									Near construction						
Test	cotα	n_v	H_{s0}	s_{p0}	T_p	H_{m0}	T_{m0}	s_{m0}	H_s	T_m	s_m	$H_s/\Delta D_n$	N_0	N_{od}	Tijd
A101	1.5	0.20	0.12	0.02	1.96	0.082	1.95	0.01	0.104	1.83	0.02	2.89	0	0	32.7
A102	1.5	0.20	0.14	0.02	2.12	0.104	2.02	0.02	0.126	2.42	0.01	3.50	2	**0.1**	35.3
A103	1.5	0.20	0.16	0.02	2.26	0.126	2.28	0.02	0.137	2.58	0.01	3.81	4	**0.2**	37.7
A104	1.5	0.20	0.165	0.02	2.30	0.154	2.36	0.02	0.147	2.64	0.01	4.08	4	**0.2**	38.3
A201	1.5	0.20	0.10	0.04	1.27	0.067	1.25	0.03	0.066	1.27	0.03	1.82	0	0	21.1
A202	1.5	0.20	0.12	0.04	1.39	0.081	1.34	0.03	0.080	1.33	0.03	2.22	0	0	23.1
A203	1.5	0.20	0.14	0.04	1.50	0.094	1.47	0.03	0.094	1.61	0.02	2.60	0	0	25.0
A204	1.5	0.20	0.16	0.04	1.60	0.108	1.56	0.03	0.105	1.65	0.02	2.92	2	**0.1**	26.7
A205	1.5	0.20	0.18	0.04	1.70	0.122	1.76	0.03	0.120	1.73	0.03	3.34	4	**0.2**	28.3
A206	1.5	0.20	0.20	0.04	1.79	0.165	1.77	0.03	0.164	1.82	0.03	4.55	13	**0.7**	29.8
A301	1.5	0.20	0.10	0.06	1.03	0.064	1.01	0.04	0.062	1.06	0.04	1.74	0	0	17.2
A302	1.5	0.20	0.12	0.06	1.13	0.076	1.13	0.04	0.075	1.09	0.04	2.07	0	0	18.9
A303	1.5	0.20	0.14	0.06	1.22	0.089	1.20	0.04	0.087	1.26	0.04	2.42	0	0	20.4
A304	1.5	0.20	0.16	0.06	1.31	0.102	1.31	0.04	0.101	1.30	0.04	2.80	0	0	21.8
A305	1.5	0.20	0.18	0.06	1.39	0.115	1.36	0.04	0.114	1.30	0.04	3.17	0	0	23.1
A306	1.5	0.20	0.16	0.06	1.31	0.119	1.31	0.04	0.117	1.30	0.04	3.24	4	**0.2**	21.8
A307	1.5	0.20	0.18	0.06	1.39	0.134	1.41	0.04	0.131	1.31	0.05	3.64	8	**0.5**	23.1

Table A 1. Results serie A

Deep water									Near construction						
Test	cotα	n_v	H_{s0}	s_{p0}	T_p	H_{m0}	T_{m0}	s_{m0}	H_s	T_m	s_m	$H_s/\Delta D_n$	N_0	N_{od}	Tijd
B101	1.5	0.28	0.12	0.02	1.96	0.082	1.95	0.01	0.081	1.83	0.02	2.26	0	0	32.7
B102	1.5	0.28	0.12	0.02	1.96	0.105	2.02	0.02	0.104	1.83	0.02	2.90	0	0	32.7
B103	1.5	0.28	0.14	0.02	2.12	0.127	2.28	0.02	0.127	2.44	0.01	3.54	0	0	35.3
B104	1.5	0.28	0.16	0.02	2.26	0.147	2.36	0.02	0.143	2.50	0.01	3.97	0	0	37.7
B105	1.5	0.28	0.165	0.02	2.30	0.155	2.36	0.02	0.148	2.58	0.01	4.12	0	0	38.3
B201	1.5	0.28	0.12	0.04	1.39	0.080	1.36	0.03	0.079	1.31	0.03	2.20	0	0	23.1
B202	1.5	0.28	0.14	0.04	1.50	0.094	1.47	0.03	0.093	1.55	0.02	2.58	0	0	25.0
B203	1.5	0.28	0.16	0.04	1.60	0.108	1.57	0.03	0.105	1.65	0.02	2.92	0	0	26.7
B204	1.5	0.28	0.18	0.04	1.70	0.121	1.76	0.02	0.120	1.73	0.03	3.32	0	0	28.3
B205	1.5	0.28	0.18	0.04	1.70	0.145	1.71	0.03	0.144	1.71	0.03	4.01	0	0	28.3
B206	1.5	0.28	0.20	0.04	1.79	0.170	1.81	0.03	0.163	1.82	0.03	4.53	0	0	29.8

All series performed with N = 1000 waves.

Deep water									Near construction						
Test	cotα	n_v	H_{s0}	s_{p0}	T_p	H_{m0}	T_{m0}	s_{m0}	H_s	T_m	s_m	$H_s/\Delta D_n$	N_0	N_{od}	Tijd
B301	1.5	0.28	0.12	0.06	1.13	0.077	1.11	0.04	0.076	1.09	0.04	2.10	0	0	18.9
B302	1.5	0.28	0.14	0.06	1.22	0.089	1.21	0.04	0.088	1.25	0.04	2.44	0	0	20.4
B303	1.5	0.28	0.16	0.06	1.31	0.103	1.31	0.04	0.102	1.3	0.04	2.82	0	0	21.8
B304	1.5	0.28	0.18	0.06	1.39	0.116	1.36	0.04	0.115	1.33	0.04	3.19	0	0	23.1
B305	1.5	0.28	0.18	0.06	1.39	0.135	1.36	0.05	0.131	1.33	0.05	3.65	0	0	23.1
B306	1.5	0.28	0.20	0.06	1.46	0.149	1.47	0.04	0.148	1.39	0.05	4.12	0	0	24.4
B307	1.5	0.28	0.235	0.06	1.58	0.175	1.56	0.05	0.170	1.69	0.04	4.72	0	0	26.4

Table A 2. Results serie B

Deep water									Near construction						
Test	cotα	n_v	H_{s0}	s_{p0}	T_p	H_{m0}	T_{m0}	s_{m0}	H_s	T_m	s_m	$H_s/\Delta D_n$	N_0	N_{od}	Tijd
C101	1.5	0.35	0.12	0.02	1.96	0.082	1.96	0.01	0.081	1.86	0.02	2.26	0	0	32.7
C102	1.5	0.35	0.12	0.02	1.96	0.104	2.02	0.02	0.105	1.82	0.02	2.91	0	0	32.7
C103	1.5	0.35	0.14	0.02	2.12	0.125	2.27	0.02	0.124	2.41	0.01	3.46	0	0	35.3
C104	1.5	0.35	0.16	0.02	2.26	0.148	2.36	0.02	0.143	2.64	0.01	3.97	0	0	37.7
C105	1.5	0.35	0.165	0.02	2.30	0.154	2.36	0.02	0.148	2.70	0.01	4.10	0	0	38.3
C201	1.5	0.35	0.12	0.04	1.39	0.08	1.34	0.03	0.080	1.34	0.03	2.21	0	0	23.1
C202	1.5	0.35	0.14	0.04	1.50	0.094	1.47	0.03	0.093	1.53	0.03	2.57	0	0	25.0
C203	1.5	0.35	0.16	0.04	1.60	0.106	1.57	0.03	0.106	1.65	0.02	2.93	0	0	26.7
C204	1.5	0.35	0.18	0.04	1.70	0.12	1.76	0.02	0.119	1.73	0.03	3.30	0	0	28.3
C205	1.5	0.35	0.18	0.04	1.70	0.144	1.72	0.03	0.144	1.71	0.03	4.00	1	**0.1**	28.3
C206	1.5	0.35	0.2	0.04	1.79	0.169	1.80	0.03	0.162	1.82	0.03	4.49	3	**0.2**	29.8
C301	1.5	0.35	0.12	0.06	1.13	0.076	1.13	0.04	0.075	1.08	0.04	2.09	0	0	18.9
C302	1.5	0.35	0.14	0.06	1.22	0.089	1.23	0.04	0.089	1.26	0.04	2.46	0	0	20.4
C303	1.5	0.35	0.16	0.06	1.31	0.103	1.31	0.04	0.101	1.3	0.04	2.82	0	0	21.8
C304	1.5	0.35	0.18	0.06	1.39	0.114	1.36	0.04	0.114	1.31	0.04	3.16	0	0	23.1
C305	1.5	0.35	0.18	0.06	1.39	0.134	1.39	0.04	0.132	1.32	0.05	3.67	0	0	23.1
C306	1.5	0.35	0.20	0.06	1.46	0.148	1.47	0.04	0.147	1.32	0.05	4.09	1	**0.1**	24.4

Table A 3. Results serie C

All series performed with N = 1000 waves.

		Deep water							Near construction						
Test	cotα	n_p	H_{s0}	s_{0p}	T_p	H_{m0}	T_{m0}	s_{m0}	H_s	T_m	s_m	$H_s/\Delta D_n$	N_{displ}	N_{od}	Time
E101	2.0	0.28	0.12	0.02	1.96	0.099	2.02	0.02	0.100	1.86	0.02	2.79	0	0	32.7
E102	2.0	0.28	0.14	0.02	2.12	0.119	2.10	0.02	0.119	2.52	0.01	3.30	0	0	35.3
E103	2.0	0.28	0.16	0.02	2.26	0.139	2.34	0.02	0.139	2.58	0.01	3.85	0	0	37.7
E104	2.0	0.28	0.165	0.02	2.3	0.150	2.36	0.02	0.145	2.58	0.01	4.03	0	0	38.3
E201	2.0	0.28	0.14	0.04	1.50	0.094	1.47	0.03	0.096	1.56	0.03	2.68	0	0	25.0
E202	2.0	0.28	0.16	0.04	1.60	0.107	1.56	0.03	0.106	1.62	0.03	2.95	0	0	26.7
E203	2.0	0.28	0.18	0.04	1.70	0.121	1.76	0.02	0.120	1.73	0.03	3.34	0	0	28.3
E204	2.0	0.28	0.18	0.04	1.70	0.142	1.71	0.03	0.142	1.71	0.03	3.94	0	0	28.3
E205	2.0	0.28	0.20	0.04	1.79	0.157	1.79	0.03	0.158	1.80	0.03	4.40	0	0	29.8
E301	2.0	0.28	0.14	0.06	1.22	0.089	1.23	0.04	0.088	1.24	0.04	2.43	0	0	20.4
E302	2.0	0.28	0.16	0.06	1.31	0.101	1.31	0.04	0.100	1.29	0.04	2.78	0	0	21.8
E303	2.0	0.28	0.18	0.06	1.39	0.115	1.36	0.04	0.115	1.30	0.04	3.19	0	0	23.1
E304	2.0	0.28	0.18	0.06	1.39	0.13	1.36	0.04	0.132	1.30	0.05	3.66	0	0	23.1
E305	2.0	0.28	0.20	0.06	1.46	0.148	1.47	0.04	0.147	1.59	0.04	4.09	0	0	24.4
E306	2.0	0.28	0.235	0.06	1.58	0.169	1.56	0.04	0.168	1.67	0.04	4.65	0	0	26.4

Table A 4. Results serie D

		Deep water							Near construction						
Test	cotα	n_p	H_{s0}	s_{0p}	T_p	H_{m0}	T_{m0}	s_{m0}	H_s	T_m	s_m	$H_s/\Delta D_n$	N_{displ}	N_{od}	Time
E101	2.0	0.28	0.12	0.02	1.96	0.099	2.02	0.02	0.100	1.86	0.02	2.79	0	0	32.7
E102	2.0	0.28	0.14	0.02	2.12	0.119	2.10	0.02	0.119	2.52	0.01	3.30	0	0	35.3
E103	2.0	0.28	0.16	0.02	2.26	0.139	2.34	0.02	0.139	2.58	0.01	3.85	0	0	37.7
E104	2.0	0.28	0.165	0.02	2.30	0.15	2.36	0.02	0.145	2.58	0.01	4.03	0	0	38.3
E201	2.0	0.28	0.14	0.04	1.50	0.094	1.47	0.03	0.096	1.56	0.03	2.68	0	0	25.0
E202	2.0	0.28	0.16	0.04	1.60	0.107	1.56	0.03	0.106	1.62	0.03	2.95	0	0	26.7
E203	2.0	0.28	0.18	0.04	1.70	0.121	1.76	0.02	0.12	1.73	0.03	3.34	0	0	28.3
E204	2.0	0.28	0.18	0.04	1.70	0.142	1.71	0.03	0.142	1.71	0.03	3.94	0	0	28.3
E205	2.0	0.28	0.20	0.04	1.79	0.157	1.79	0.03	0.158	1.8	0.03	4.40	0	0	29.8

All series performed with N = 1000 waves.

		Deep water							Near construction						
Test	cotα	n_p	H_{s0}	s_{0p}	T_p	H_{m0}	T_{m0}	s_{m0}	H_s	T_m	s_m	$H_s/\Delta D_n$	N_{displ}	N_{od}	Time
E301	2.0	0.28	0.14	0.06	1.22	0.089	1.23	0.04	0.088	1.24	0.04	2.43	0	0	20.4
E302	2.0	0.28	0.16	0.06	1.31	0.101	1.31	0.04	0.100	1.29	0.04	2.78	0	0	21.8
E303	2.0	0.28	0.18	0.06	1.39	0.115	1.36	0.04	0.115	1.30	0.04	3.19	0	0	23.1
E304	2.0	0.28	0.18	0.06	1.39	0.130	1.36	0.04	0.132	1.30	0.05	3.66	0	0	23.1
E305	2.0	0.28	0.20	0.06	1.46	0.148	1.47	0.04	0.147	1.59	0.04	4.09	0	0	24.4
E306	2.0	0.28	0.235	0.06	1.58	0.169	1.56	0.04	0.168	1.67	0.04	4.65	0	0	26.4

Table A 5. Results serie E

		Deep water							Near construction						
Test	cotα	n_p	H_{s0}	s_{0p}	T_p	H_{m0}	T_{m0}	s_{m0}	H_s	T_m	s_m	$H_s/\Delta D_n$	N_{displ}	N_{od}	Time
F101	2.0	0.35	0.12	0.02	1.96	0.099	2.02	0.02	0.099	1.86	0.02	2.76	0	0	32.7
F102	2.0	0.35	0.14	0.02	2.12	0.119	2.10	0.02	0.119	2.52	0.01	3.30	0	0	35.3
F103	2.0	0.35	0.16	0.02	2.26	0.136	2.29	0.02	0.137	2.64	0.01	3.80	0	0	37.7
F104	2.0	0.35	0.165	0.02	2.3	0.148	2.36	0.02	0.143	2.64	0.01	3.98	0	0	38.3
F201	2.0	0.35	0.14	0.04	1.50	0.093	1.47	0.03	0.092	1.53	0.03	2.57	0	0	25.0
F202	2.0	0.35	0.16	0.04	1.60	0.106	1.57	0.03	0.104	1.65	0.02	2.90	0	0	26.7
F203	2.0	0.35	0.18	0.04	1.70	0.121	1.75	0.03	0.12	1.71	0.03	3.33	0	0	28.3
F204	2.0	0.35	0.18	0.04	1.70	0.141	1.72	0.03	0.142	1.71	0.03	3.94	1	**0.1**	28.3
F205	2.0	0.35	0.20	0.04	1.79	0.161	1.79	0.03	0.157	1.83	0.03	4.35	12	**0.7**	29.8
F301	2.0	0.35	0.12	0.06	1.13	0.077	1.13	0.04	0.075	1.16	0.04	2.08	0	0	18.9
F302	2.0	0.35	0.14	0.06	1.22	0.089	1.23	0.04	0.088	1.24	0.04	2.45	0	0	20.4
F303	2.0	0.35	0.16	0.06	1.31	0.102	1.31	0.04	0.101	1.27	0.04	2.80	0	0	21.8
F304	2.0	0.35	0.18	0.06	1.39	0.114	1.41	0.04	0.114	1.30	0.04	3.17	0	0	23.1
F305	2.0	0.35	0.18	0.06	1.39	0.134	1.35	0.05	0.132	1.30	0.05	3.67	0	0	23.1
F306	2.0	0.35	0.20	0.06	1.46	0.147	1.47	0.04	0.146	1.52	0.04	4.06	0	0	24.4
F307	2.0	0.35	0.235	0.06	1.58	0.168	1.56	0.04	0.167	1.67	0.04	4.63	0	0	26.4

Table A 6. Results serie F

All series performed with N = 1000 waves.

APPENDIX B; WAVE SPECTRUM

When using a model for testing in a wave flume, the best and most accurate results are wanted. To get the best result a realistic wave field is a must. In the flume is a wave board, which can generate irregular waves. An irregular wave field is best described with a variance-density spectrum. This type of spectrum provides a statistical description of the fluctuating wave height caused by wind. One of such a spectrum is the JONSWAP-spectrum. This spectrum is representative for not fully developed sea states, like the North Sea. That is why it was used for these experiments. The spectrum does not represent a fully developed sea (fetch limited to about 100 km). The JONSWAP-spectrum was generated by enhancing the Pierson-Moskowitz spectrum with a peak-enhancement function [Holthuijsen, 2002]. The spectrum is represented in the following equation:

$$E_{JONSWAP}(f) = \alpha g^2 (2\pi)^{-4} f^{-5} \exp\left\{\frac{5}{4}\left(\frac{f}{f_{peak}}\right)^{-4}\right\} \gamma^{\exp\left[-\frac{1}{2}\left(\frac{f-f_{peak}}{\sigma \cdot f_{peak}}\right)^2\right]} \quad \text{(B.1)}$$

With:

	E	= variance density	[m^2s]
	f	= frequency	[Hz]
	α	= energy scale coefficients	[-]
	γ,σ	= shape parameters	[-]

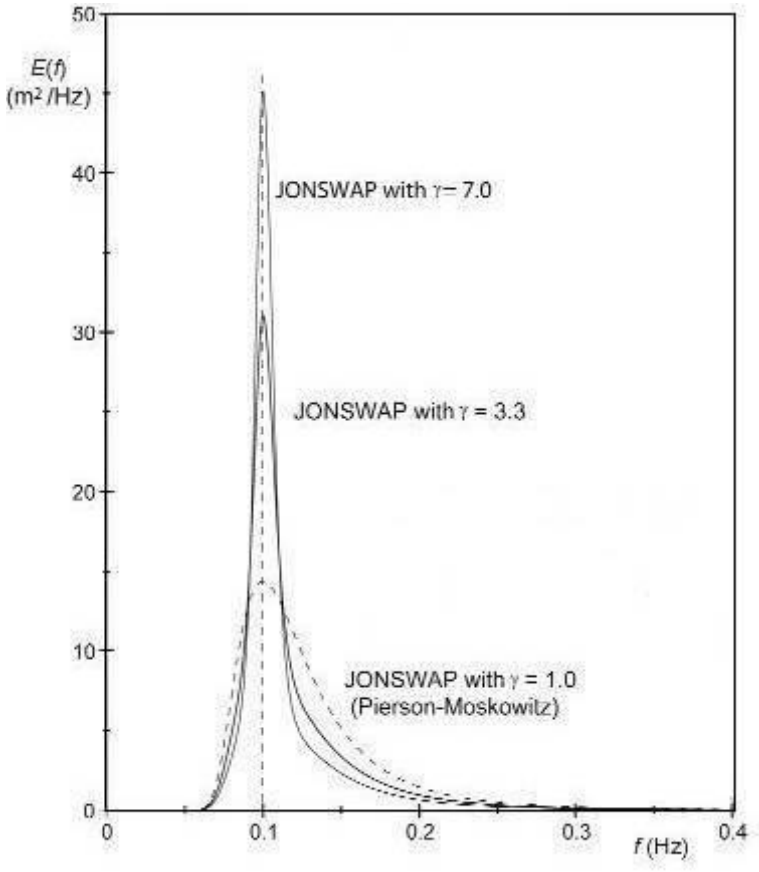

Figure B 1. JONSWAP spectrum

The shape parameters were defined as following. The γ is a peak-enhancement factor and σ is a peak-width parameter. With $\sigma = \sigma_a$ for $f \leq f_{peak}$ and $\sigma = \sigma_b$ for $f > f_{peak}$ to account for the slightly different widths on the two sides of the spectral peak. In JONSWAP, the scatter in the values of the shape parameters γ, σ_a and σ_b was so large that no dependence on the dimensionless fetch could be discerned. The average values were γ = 3.3, σ_a = 0.07 and σ_b =0.09 [Holthuijsen, 2002]

APPENDIX C; SCALING OF CORE MATERIAL

It is recommended that the diameter of the core material in the model is chosen in such a way that the Froude scale law holds for a characteristic pore velocity. The characteristic pore velocity can be chosen as the average velocity of the six points. The characteristic pore velocity is averaged with respect to time (one wave period) and space (6 points).

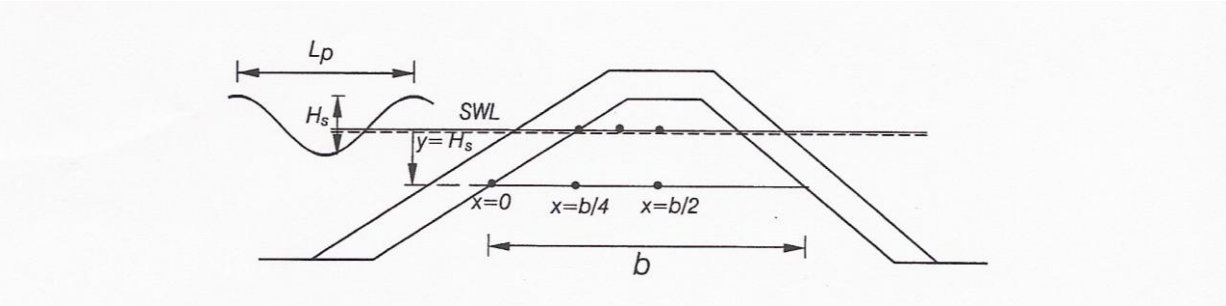

Figure C 1. Location for characteristic flow in the core

First, a reasonable estimate of the reference pressure was used.

$$p_{0,\max} = \rho_w g \frac{H_s}{2} \tag{C.1}$$

In order to determine the scale of the core material, the damping coefficient was used. The damping coefficient is found by curve fitting and is a function of the reference pressure.

$$\delta = 0.0141 \frac{n^{1/2} L_p^2}{H_s b} \tag{C.2}$$

In which:			
	n	= porosity of the core	[m]
	L_p	= wave length deep water	[m]
	H_s	= wave height	[m]
	b	= width as a function of y	[m]

Next, the horizontal pressure gradient, I_x, was calculated by applying formula (C.3).

$$I_x = -\frac{\pi H_s}{L'} e^{-\delta \frac{2\pi}{L'} x} \left[\delta \cos\left(\frac{2\pi}{L'} x + \frac{2\pi}{T_p} t \right) + \sin\left(\frac{2\pi}{L'} x + \frac{2\pi}{T_p} t \right) \right] \tag{C.3}$$

In which:				
	L' =	wave length in the core (L'= L/√1.4)	[m]
	T_p =	Wave period	[s]

From the horizontal pressure gradient, the pore velocity, U, in the six points, could be determined using formula (C.4).

$$I_x = \alpha \left(\frac{1-n}{n} \right)^2 \frac{\upsilon}{g d_{50}^2} \left(\frac{U}{n} \right) + \beta \frac{1-n}{n} \frac{1}{g d_{50}^2} \left(\frac{U}{n} \right)^2 \tag{C.4}$$

In which:	α,β	= Coefficients	[-]
	n	= porosity of the core	[-]
	v	= Kinematic viscosity (1.1 10^{-6})	[m^2/s]
	U	= pore velocity	[m/s]

The values of the coefficients α and β are dependent of the Reynolds number and the grain shape and grading [Burchart, et al, 1995]

Pressure gradient and pore velocity at different points and different times were calculated from equations (C.3) and (C.4), respectively. For example, at point (x=0, y=0) was obtained:

Table C 1. Pressure gradient and pore velocity

y_1	0	$0.1T_p$	$0.2T_p$	$0.3T_p$	$0.4T_p$	$0.5T_p$
t	0	1.15	2,3	3,45	4.6	5.75
I_x	-0.071	-0.178	-0.216	-0.172	-0.062	0.071
U_{abs}	0.102	0.160	0.177	0.158	0.095	0.102

The time average pore velocity of the prototype is given as:

Table C 2. Time averaged pore velocity D_n = 0.60 m

y [m]	0			8		
b [m]	36			60		
x	0	b/4	b/2	0	b/4	b/2
U [m/s]	0.139	0.130	0.114	0.133	0.122	0.101

Therefore the characteristic pore velocity in the prototype is $\bar{U}^p$ = 0.120 m/s. The Reynolds number then becomes, $Re^p = \bar{U}^p/\sqrt{40} = 67\ 10^3$. The waves and dimensions were scaled according to the Froude scaling law. The question rises whether the core material could be perhaps the same size as the sublayer material.

The next step was to determine the nominal diameter of the core material in the model. According to the Froude scaling law the characteristic pore velocity in the model should be $\overline{U}^m = \overline{U}^p / \sqrt{n}$ = 0.018 m/s.

As a trial for the core material let D_{50}^m = 0.015. The calculation of the characteristic core velocity is the same as the previous calculation. Following the same steps as before.

Table C 3. Time averaged pore velocity D_n = 0.015 m

y [m]	0			8		
b [m]	0,9			1,5		
x	0	b/4	b/2	0	b/4	b/2
U [m/s]	0.113	0.097	0.084	0.087	0.075	0.065

The characteristic pore velocity in the model for this nominal diameter $\bar{U}^m$, then became 0.014 m/s. This value is a bit smaller than the previous calculated 0.018 m/s. It was concluded that the core material is not scaled correctly based on the Froude scale rules. The core material should be larger. Therefore larger core material was used for another calculation.

A calculation was performed with a Nominal diameter of D_{n50} = 0.017 m. Table C4 gives the results.

Table C 4. Time averaged pore velocity D_n = 0.017 m

y [m]	0			8		
b [m]	0.9			1.5		
x	0	b/4	b/2	0	b/4	b/2
U [m/s]	0.130	0.112	0.097	0.101	0.087	0.075

The following characteristic pore velocity in the model for this nominal diameter $\bar{U}^m$ = 0.017 m/s was found. This gives as a result that based on the length scale of the core material a ratio of 1:35 holds.

Finally, the option of a vertical backside was investigated.

Table C 5. Time averaged pore velocity vertical backside

y [m]	0			8		
b [m]	0.45			0.75		
x	0	b/4	b/2	0	b/4	b/2
U [m/s]	0.159	0.138	0.119	0.123	0.107	0.092

The results do not differ that much. The average core velocity in that case becomes $\bar{U}^m$ = 0.018 m/s. Therefore it is very convenient to apply the same sublayer material as the core material and a vertical backside.

APPENDIX D; CUBE CHARACTERISTICS

Cube	W_{cube} [g]	ρ_{cube} [kg/m^3]	Cube	W_{cube} [g]	ρ_{cube} [kg/m^3]	Cube	W_{cube} [g]	ρ_{cube} [kg/m^3]
1	166,2	1824	**41**	175,3	1924	**81**	170,2	1868
2	177,1	1943	**42**	172,3	1891	**82**	173,4	1903
3	177	1942	**43**	169	1855	**83**	172,5	1893
4	176,6	1938	**44**	160	1756	**84**	174	1909
5	162,7	1785	**45**	174,8	1918	**85**	171,5	1882
6	173,8	1907	**46**	164,6	1806	**86**	164,8	1809
7	168,4	1848	**47**	166,4	1826	**87**	172,7	1895
8	167,7	1840	**48**	167,4	1837	**88**	170,7	1873
9	176	1931	**49**	168,3	1847	**89**	166,8	1830
10	168,5	1849	**50**	173,7	1906	**90**	170,4	1870
11	165,6	1817	**51**	171,8	1885	**91**	169	1855
12	173	1898	**52**	177,7	1950	**92**	167,6	1839
13	165,7	1818	**53**	171,5	1882	**93**	167,5	1838
14	176,4	1936	**54**	172,1	1889	**94**	176,6	1938
15	168,8	1852	**55**	172,5	1893	**95**	166,9	1832
16	167	1833	**56**	172,2	1890	**96**	172,7	1895
17	178,1	1954	**57**	173,7	1906	**97**	170,1	1867
18	168,9	1853	**58**	172,1	1889	**98**	164,7	1807
19	171,7	1884	**59**	172,2	1890	**99**	165,7	1818
20	167,5	1838	**60**	171,3	1880	**100**	173,3	1902
21	164,4	1804	**61**	171,1	1878	**101**	164,3	1803
22	166,6	1828	**62**	172,9	1897	**102**	169,3	1858
23	167,3	1836	**63**	172,2	1890	**103**	165	1811
24	175,9	1930	**64**	161,5	1772	**104**	167,5	1838
25	172,8	1896	**65**	157,2	1725	**105**	175,6	1927
26	169,3	1858	**66**	171,1	1878	**106**	170,4	1870
27	170,1	1867	**67**	166,8	1830	**107**	176,4	1936
28	167,5	1838	**68**	174,5	1915	**108**	170	1866
29	161,6	1773	**69**	169,8	1863	**109**	170	1866
30	171	1877	**70**	166,3	1825	**110**	169,3	1858
31	170,6	1872	**71**	167,9	1843	**111**	173,4	1903
32	175,6	1927	**72**	165,8	1819	**112**	168,2	1846
33	167,3	1836	**73**	172	1888	**113**	165,6	1817
34	177,2	1945	**74**	166	1822	**114**	164,1	1801
35	171,5	1882	**75**	167,9	1843	**115**	169,5	1860
36	169,7	1862	**76**	171,2	1879	**116**	165,8	1819
37	171,9	1886	**77**	168,1	1845	**117**	168	1844
38	166,4	1826	**78**	165,4	1815	**118**	169,2	1857
39	161	1767	**79**	167,4	1837	**119**	173,1	1900
40	167,9	1843	**80**	170,9	1875	**120**	173,1	1900

Cube	W_{cube} [g]	ρ_{cube} [kg/m^3]	Cube	W_{cube} [g]	ρ_{cube} [kg/m^3]	Cube	W_{cube} [g]	ρ_{cube} [kg/m^3]
121	167,7	1840	**161**	170,1	1867	**201**	165,9	1821
122	165,2	1813	**162**	174,4	1914	**202**	172,9	1897
123	165,5	1816	**163**	165,2	1813	**203**	170,3	1869
124	171,2	1879	**164**	176,2	1934	**204**	174,4	1914
125	171,4	1881	**165**	166,2	1824	**205**	177,1	1943
126	172,7	1895	**166**	177,5	1948	**206**	172,1	1889
127	167,1	1834	**167**	174,5	1915	**207**	165,5	1816
128	171,8	1885	**168**	170,7	1873	**208**	167	1833
129	168,1	1845	**169**	171,4	1881	**209**	165,6	1817
130	171,5	1882	**170**	169,4	1859	**210**	158,9	1744
131	173,6	1905	**171**	174,9	1919	**211**	165,5	1816
132	172,4	1892	**172**	170,3	1869	**212**	170,3	1869
133	164,3	1803	**173**	175,1	1922	**213**	170,7	1873
134	174,2	1912	**174**	173,8	1907	**214**	173,9	1908
135	172,4	1892	**175**	162,7	1785	**215**	172,6	1894
136	171,4	1881	**176**	171,1	1878	**216**	167,3	1836
137	172	1888	**177**	172,7	1895	**217**	172,7	1895
138	172,4	1892	**178**	174,2	1912	**218**	173	1898
139	174,5	1915	**179**	168,8	1852	**219**	173,4	1903
140	171,9	1886	**180**	170,6	1872	**220**	171,1	1878
141	173,3	1902	**181**	169,8	1863	**221**	167,5	1838
142	171,9	1886	**182**	173,4	1903	**222**	176,7	1939
143	165,6	1817	**183**	165,3	1814	**223**	176,8	1940
144	169,8	1863	**184**	168,9	1853	**224**	169	1855
145	168,6	1850	**185**	174,4	1914	**225**	172,5	1893
146	169,5	1860	**186**	170,8	1874	**226**	168,8	1852
147	167,4	1837	**187**	173,4	1903	**227**	174,8	1918
148	159,2	1747	**188**	170	1866	**228**	170,3	1869
149	164,7	1807	**189**	165,4	1815	**229**	166	1822
150	169	1855	**190**	171,1	1878	**230**	166	1822
151	168,8	1852	**191**	170	1866	**231**	174,6	1916
152	168,2	1846	**192**	173	1898	**232**	169,8	1863
153	167,1	1834	**193**	171,2	1879	**233**	172,8	1896
154	166,7	1829	**194**	166,3	1825	**234**	175,9	1930
155	167,6	1839	**195**	167,7	1840	**235**	173	1898
156	166,7	1829	**196**	170,9	1875	**236**	167,6	1839
157	163,5	1794	**197**	167,5	1838	**237**	167,8	1841
158	166,6	1828	**198**	168,7	1851	**238**	166,3	1825
159	168,1	1845	**199**	170,3	1869	**239**	170,3	1869
160	166,8	1830	**200**	167,4	1837	**240**	162,4	1782

Cube	W_{cube} [g]	ρ_{cube} [kg/m^3]	Cube	W_{cube} [g]	ρ_{cube} [kg/m^3]	Cube	W_{cube} [g]	ρ_{cube} [kg/m^3]
241	173,4	1903	**281**	168,6	1850	**321**	174,3	1913
242	172,7	1895	**282**	175,8	1929	**322**	169,8	1863
243	165,3	1814	**283**	179	1964	**323**	170,6	1872
244	169,5	1860	**284**	165,6	1817	**324**	173,2	1901
245	167,4	1837	**285**	173,6	1905	**325**	164,6	1806
246	168,5	1849	**286**	169,3	1858	**326**	170,7	1873
247	164,7	1807	**287**	172,4	1892	**327**	170	1866
248	171,3	1880	**288**	171,9	1886	**328**	169	1855
249	170,3	1869	**289**	170,9	1875	**329**	171,9	1886
250	168,2	1846	**290**	170	1866	**330**	171,4	1881
251	168,5	1849	**291**	171,4	1881	**331**	169,2	1857
252	169,5	1860	**292**	173	1898	**332**	164	1800
253	175,7	1928	**293**	171,9	1886	**333**	177	1942
254	161	1767	**294**	178,5	1959	**334**	175,7	1928
255	167,8	1841	**295**	170,8	1874	**335**	177,1	1943
256	172,8	1896	**296**	177,9	1952	**336**	172,6	1894
257	167,5	1838	**297**	172,8	1896	**337**	168,6	1850
258	167,1	1834	**298**	170	1866	**338**	168,8	1852
259	175,6	1927	**299**	173,6	1905	**339**	169,4	1859
260	165,7	1818	**300**	171	1877	**340**	171,9	1886
261	174	1909	**301**	169,2	1857	**341**	173,6	1905
262	170,6	1872	**302**	166,8	1830	**342**	167,6	1839
263	174,5	1915	**303**	172,6	1894	**343**	171,7	1884
264	166,9	1832	**304**	165,8	1819	**344**	171,8	1885
265	166,3	1825	**305**	171,9	1886	**345**	172,2	1890
266	170,3	1869	**306**	166,3	1825	**346**	172,3	1891
267	171,4	1881	**307**	170,4	1870	**347**	166,9	1832
268	174,4	1914	**308**	174,1	1911	**348**	171,2	1879
269	169,9	1864	**309**	169	1855	**349**	169,8	1863
270	172,5	1893	**310**	170,7	1873	**350**	160,3	1759
271	168,6	1850	**311**	169,2	1857	**351**	167,4	1837
272	173,6	1905	**312**	172	1888	**352**	173,5	1904
273	169,3	1858	**313**	176,6	1938	**353**	172,3	1891
274	172,4	1892	**314**	168	1844	**354**	172,5	1893
275	169,8	1863	**315**	175	1920	**355**	175,1	1922
276	170,7	1873	**316**	174	1909	**356**	170	1866
277	167,1	1834	**317**	171,8	1885	**357**	173,3	1902
278	165,9	1821	**318**	172,2	1890	**358**	164,8	1809
279	167,5	1838	**319**	176,6	1938	**359**	172,9	1897
280	179,2	1967	**320**	171,3	1880	**360**	167	1833

Cube	W_{cube} [g]	ρ_{cube} [kg/m^3]	Cube	W_{cube} [g]	ρ_{cube} [kg/m^3]	Cube	W_{cube} [g]	ρ_{cube} [kg/m^3]
361	165,3	1814	**401**	171,8	1885	**441**	169,3	1858
362	171,9	1886	**402**	170,2	1868	**442**	175,3	1924
363	171,9	1886	**403**	171	1877	**443**	174,3	1913
364	171,8	1885	**404**	169	1855	**444**	170	1866
365	164,4	1804	**405**	173,3	1902	**445**	172,9	1897
366	173,2	1901	**406**	173,4	1903	**446**	168,8	1852
367	171,9	1886	**407**	174	1909	**447**	177	1942
368	172,1	1889	**408**	178	1953	**448**	173,3	1902
369	167,9	1843	**409**	175,4	1925	**449**	170,2	1868
370	170,7	1873	**410**	174,1	1911	**450**	175,1	1922
371	168,4	1848	**411**	172,6	1894	**451**	173,1	1900
372	170	1866	**412**	171,5	1882	**452**	176,2	1934
373	166,9	1832	**413**	176,6	1938	**453**	177,6	1949
374	168,8	1852	**414**	176,6	1938	**454**	168,8	1852
375	176,3	1935	**415**	165	1811	**455**	175,9	1930
376	171,3	1880	**416**	174,2	1912	**456**	177,9	1952
377	172,2	1890	**417**	174,3	1913	**457**	172,8	1896
378	170,3	1869	**418**	173,1	1900	**458**	174,1	1911
379	168,9	1853	**419**	164,9	1810	**459**	168,3	1847
380	171,8	1885	**420**	175,1	1922	**460**	175,4	1925
381	172	1888	**421**	173,1	1900	**461**	170,2	1868
382	169,8	1863	**422**	167,7	1840	**462**	166,4	1826
383	172,9	1897	**423**	172,2	1890	**463**	166,6	1828
384	169,8	1863	**424**	172	1888	**464**	169,8	1863
385	167	1833	**425**	172,8	1896	**465**	173,8	1907
386	174,9	1919	**426**	175,2	1923	**466**	170,5	1871
387	170	1866	**427**	173	1898	**467**	166,4	1826
388	173,8	1907	**428**	174,8	1918	**468**	171,6	1883
389	170	1866	**429**	171,5	1882	**469**	172,3	1891
390	169,3	1858	**430**	176	1931	**470**	172,7	1895
391	170,4	1870	**431**	176,3	1935	**471**	166	1822
392	171,9	1886	**432**	171	1877	**472**	168,5	1849
393	164	1800	**433**	170,9	1875	**473**	162,3	1781
394	171,8	1885	**434**	171,3	1880	**474**	173,5	1904
395	171,1	1878	**435**	175,8	1929	**475**	170,6	1872
396	172,5	1893	**436**	175,4	1925	**476**	172,8	1896
397	175,4	1925	**437**	174,3	1913	**477**	170,2	1868
398	170,3	1869	**438**	176,7	1939	**478**	174,2	1912
399	169,3	1858	**439**	173,5	1904	**479**	168	1844
400	166	1822	**440**	174,5	1915	**480**	170,5	1871

Cube	W_{cube} [g]	ρ_{cube} [kg/m^3]	Cube	W_{cube} [g]	ρ_{cube} [kg/m^3]
481	167,9	1843	**521**	167,4	1837
482	169,8	1863	**522**	165,5	1816
483	168,2	1846	**523**	174	1909
484	171,7	1884	**524**	170	1866
485	173,3	1902	**525**	173,7	1906
486	165,8	1819	**526**	170	1866
487	171,9	1886	**527**	176,8	1940
488	171,6	1883	**528**	170,9	1875
489	167,8	1841	**529**	171,5	1882
490	171,7	1884	**530**	178,8	1962
491	168	1844	**531**	174,9	1919
492	168	1844	**532**	175,5	1926
493	170,4	1870	**533**	175,7	1928
494	166,2	1824	**534**	168,4	1848
495	171,2	1879	**535**	173,8	1907
496	169,1	1856	**536**	175,1	1922
497	172	1888	**537**	176,5	1937
498	172,3	1891	**538**	170,3	1869
499	168,1	1845	**539**	173,4	1903
500	164,4	1804	**540**	166,6	1828
501	169,3	1858	**541**	170	1866
502	165,1	1812	**542**	166,2	1824
503	165,9	1821	**543**	170,5	1871
504	171,1	1878	**544**	173,2	1901
505	171,9	1886	**545**	176,7	1939
506	166,1	1823	**546**	170,7	1873
507	172,9	1897	**547**	171,1	1878
508	176,3	1935	**548**	169	1855
509	168,4	1848			
510	176,2	1934			
511	169,3	1858			
512	168,8	1852			
513	177,4	1947			
514	179,9	1974			
515	172,2	1890			
516	168,1	1845			
517	171,4	1881			
518	171,4	1881			
519	175,6	1927			
520	173	1898			

APPENDIX E; CORE MATERIAL CHARACTERISTICS

For the core an sublayer an amount of 1.0 m^3 was needed. The material needed should have a nominal diameter of about 17 mm. as shown in appendix C. Therefore Basalt was chosen with a Nominal diameter of D_{n50} = 15.5 mm.

The following figure shows the distribution of the nominal diameter of the core material.

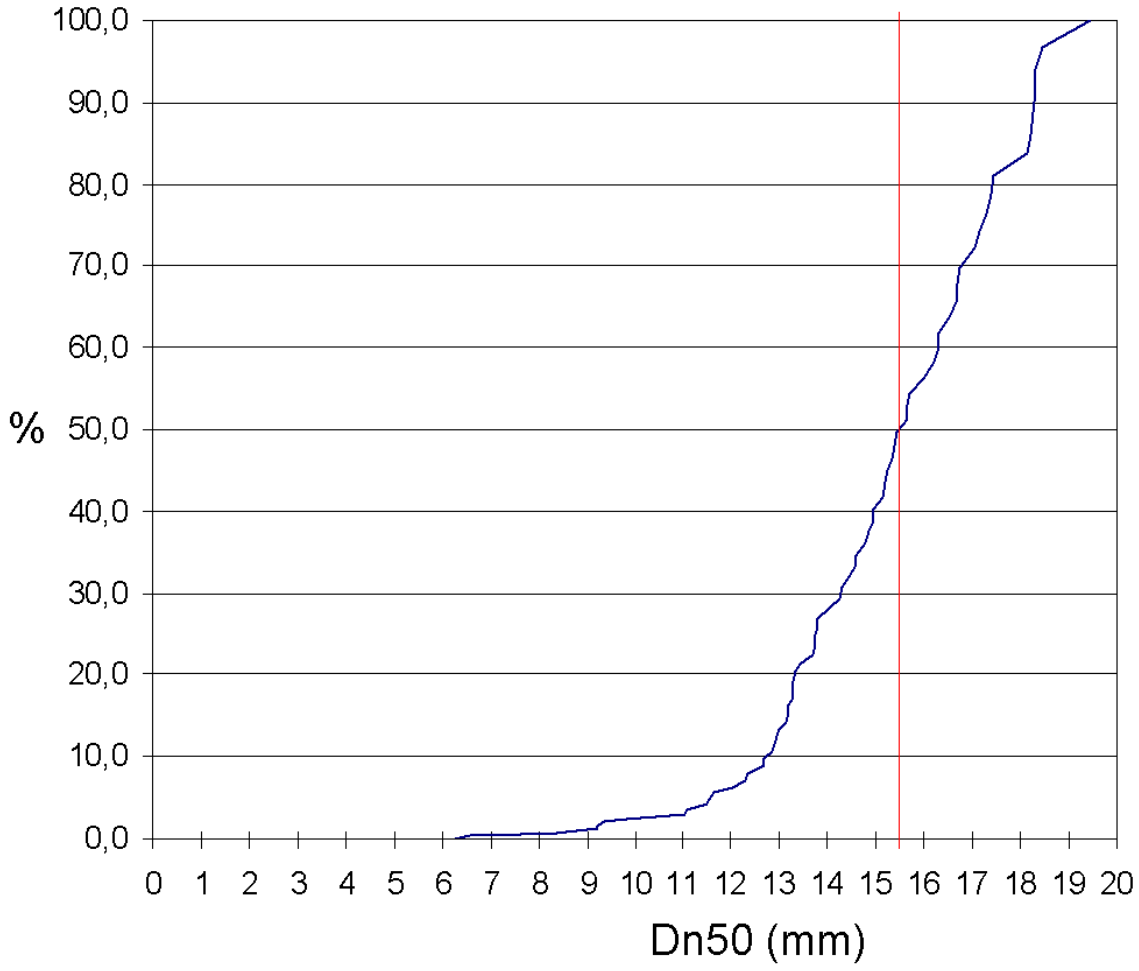

Figure E 1. Distribution of the nominal diameter of the core material

APPENDIX F; QUALITATIVE DESCRIPTION OF TESTS

A10X: The model consists of 30 rows of cubes (15 rows of 15 cubes, 15 rows of 14 cubes). A total of 435 cubes were used.

The following characteristics were applied during the test serie:

- **cotα = 1.5**
- **n_p = 0.2**
- **s_{0p} = 0.02**

A101
- T = 32.7 min. H_{s0} = 0.12 m.
- No damage occurred.

A102
- T = 32.7 min. H_{s0} = 0.12 m.
- No damage occurred.
- No anti reflection compensation (ARC).

A103
- T = 35.3 min. H_{s0} = 0.14 m.
- Damage recorded. One cube row 10, one cube row 14 (total of 2 cubes displaced).
- Some filter material on slope.
- No anti reflection compensation (ARC).

A104
- T = 37.7 min. H_{s0} = 0.16 m.
- Damage recorded. One cube row 9, one cube row 12 (total of 2 cubes displaced).
- Some filter material on slope.
- No anti reflection compensation (ARC).

A105
- T = 38.7 min. H_{s0} = 0.165 m.
- No extra damage.
- No anti reflection compensation (ARC).

The model was rebuild after this test serie.

A20X: The following characteristics were applied during the test serie:

- **cotα = 1.5**
- **n_p = 0.2**
- **s_{0p} = 0.04**

A201
- T = 21.1 min. H_{s0} = 0.10 m.
- No damage occurred.

A202
- T = 23.1 min. H_{s0} = 0.12 m.
- No damage occurred.

A203
- T = 25.0 min. H_{s0} = 0.14 m.
- Several cubes are lifted and returned to their original position.

A204
- T = 26.7 min. H_{s0} = 0.16 m.
- Damage recorded. One cube row 15, one cube row 14 (total of 2 cubes displaced).

A205
- T = 28.3 min. H_{s0} = 0.18 m.
- Damage recorded. One cube row 12, one cube row 13 (total of 2 cubes displaced).
- Some filter material on slope.

A206
- T = 29.8 min. H_{s0} = 0.14 m.
- Damage recorded. One cube row 10, three cubes row 11, one cube row 12, one cube row 13, one cube row 14, one cube row 15, one cube row 16 (total of 9 cubes displaced).
- Model has failed.
- Some filter material on slope.
- No anti reflection compensation (ARC).

The model was rebuild after this test serie.

A30X: The following characteristics were applied during the test serie:

- **$\cot\alpha$ = 1.5**
- **n_p = 0.2**
- **s_{0p} = 0.06**

A301
- T = 17.2 min. H_{s0} = 0.10 m.
- No damage occurred.

A302
- T = 18.9 min. H_{s0} = 0.12 m.
- No damage occurred.

A303
- T = 20.4 min. H_{s0} = 0.14 m.
- No damage occurred.

A304
- T = 21.8 min. H_{s0} = 0.16 m.
- No damage occurred.

A305
- T = 23.1 min. H_{s0} = 0.18 m.
- Several cubes are lifted and returned to their original position.

A306
- T = 21.8 min. H_{s0} = 0.16 m.
- Damage recorded. One cube row 12, one cube row 13, one cube row 14, one cube row 15 (total of 4 cubes displaced).
- No anti reflection compensation (ARC).

A307

- T = 23.1 min. H_{s0} = 0.18 m.
- Damage recorded. One cube row 11, one cube row 14, one cube row 15, one cube row 16 (total of 4 cubes displaced).
- Model has failed.
- No anti reflection compensation (ARC).

The model was rebuild after this test serie.

B10X: The model consists of 30 rows of cubes (15 rows of 12 cubes, 15 rows of 13 cubes). A total of 375 cubes were used.

The following characteristics were applied during the test serie:

- **cotα = 1.5**
- **n_p = 0.3**
- **s_{0p} = 0.02**

B101
- T = 32.7 min. H_{s0} = 0.12 m.
- No damage occurred.

B102
- T = 35.3 min. H_{s0} = 0.12 m.
- No damage occurred.
- No anti reflection compensation (ARC).

B103
- T = 37.7 min. H_{s0} = 0.14 m.
- No damage occurred.
- No anti reflection compensation (ARC).

B104
- T = 38.7 min. H_{s0} = 0.16 m.
- No damage occurred.
- No anti reflection compensation (ARC).

B105
- T = 38.7 min. H_{s0} = 0.165 m.
- No damage occurred.
- Several moving cubes.
- No anti reflection compensation (ARC).

The model was rebuild after this test serie.

B20X: The following characteristics were applied during the test serie:

- **cotα = 1.5**
- **n_p = 0.3**
- **s_{0p} = 0.04**

B201
- T = 23.1 min. H_{s0} = 0.12 m.
- No damage occurred.

B202
- T = 25.0 min. H_{s0} = 0.14 m.
- No damage occurred.

B203
- T = 26.7 min. H_{s0} = 0.16 m.
- No damage occurred.

B204
- T = 28.3 min. H_{s0} = 0.18 m.
- No damage occurred.

B205
- T = 28.3 min. H_{s0} = 0.18 m.
- Several moving cubes.
- No anti reflection compensation (ARC).

B206
- T = 29.8 min. H_{s0} = 0.20 m.
- Several moving cubes.
- No anti reflection compensation (ARC).

Model was rebuild after this test serie.

B30X: The following characteristics were applied during the test serie:

- **$\cot\alpha$ = 1.5**
- **n_p = 0.3**
- **s_{0p} = 0.06**

B301
- T = 18.9 min. H_{s0} = 0.12 m.
- No damage occurred.

B302
- T = 20.4 min. H_{s0} = 0.14 m.
- No damage occurred.

B303
- T = 21.8 min. H_{s0} = 0.16 m.
- No damage occurred.

B304
- T = 23.1 min. H_{s0} = 0.18 m.
- No damage occurred.

B305
- T = 23.1 min. H_{s0} = 0.18 m.
- Several moving cubes.
- No anti reflection compensation (ARC).

B306
- T = 24.4 min. H_{s0} = 0.20 m.
- Several moving cubes.
- No anti reflection compensation (ARC).

B307
- T = 26.4 min. H_{s0} = 0.235 m.
- Several cubes are lifted and returned to their original position.
- No anti reflection compensation (ARC).

Model was rebuild after this test serie.

C10X: The model consists of 30 rows of cubes (15 rows of 11 cubes, 15 rows of 12 cubes). A total of 345 cubes were used.

The following characteristics were applied during the test serie:

- **cotα = 1.5**
- **n_p = 0.35**
- **s_{0p} = 0.02**

C101
- T = 32.7 min. H_{s0} = 0.12 m.
- No damage occurred.

C102
- T = 32.7 min. H_{s0} = 0.12 m.
- No damage occurred.
- No anti reflection compensation (ARC).

C103
- T = 35.3 min. H_{s0} = 0.14 m.
- No damage occurred.
- Some slightly rotating cubes.
- No anti reflection compensation (ARC).

C104
- T = 37.7 min. H_{s0} = 0.16 m.
- No damage occurred.
- Some slightly rotating cubes.
- No anti reflection compensation (ARC).

C105
- T = 38.3 min. H_{s0} = 0.165 m.
- No damage occurred.
- Some rotating cubes. A bit of settling occurred.
- No anti reflection compensation (ARC).

The model was rebuild after this test serie.

C20X: The following characteristics were applied during the test serie:

- **cotα = 1.5**
- **n_p = 0.35**
- **s_{0p} = 0.04**

C201
- T = 23.1 min. H_{s0} = 0.12 m.
- No damage occurred.

C202
- T = 25.0 min. H_{s0} = 0.14 m.
- No damage occurred.

C203
- T = 26.7 min. H_{s0} = 0.16 m.
- Some rotating cubes. A bit of settling occurred.
- No damage occurred.

C204
- T = 28.3 min. H_{s0} = 0.18 m.
- Some rotating cubes. A bit of settling occurred.
- No damage occurred.

C205
- T = 28.3 min. H_{s0} = 0.18 m.
- Several moving cubes.
- Damage recorded. One cube row 11 (total of 1 cube displaced).
- No anti reflection compensation (ARC).

C206
- T = 29.8 min. H_{s0} = 0.20 m.
- Several moving cubes.
- No extra damage occurred.
- No anti reflection compensation (ARC).

Model was rebuild after this test serie.

C30X: The following characteristics were applied during the test serie:

- **$\cot\alpha$ = 1.5**
- **n_p = 0.35**
- **s_{0p} = 0.06**

C301
- T = 18.9 min. H_{s0} = 0.12 m.
- No damage occurred.

C302
- T = 20.4 min. H_{s0} = 0.14 m.
- No damage occurred.

C303
- T = 21.8 min. H_{s0} = 0.16 m.
- No damage occurred.

C304
- T = 23.1 min. H_{s0} = 0.18 m.
- No damage occurred.

C305
- T = 23.1 min. H_{s0} = 0.18 m.
- Several slightly rotating cubes.
- No anti reflection compensation (ARC).

C306
- T = 24.4 min. H_{s0} = 0.20 m.
- Several rotating cubes.
- Damage recorded. One cube row 14 (total of 1 cube displaced).
- No anti reflection compensation (ARC).

Model was rebuild after this test serie.

D10X: The model consists of 37 rows of cubes (18 rows of 14 cubes, 19 rows of 15 cubes). A total of 537 cubes were used.

The following characteristics were applied during the test serie:

- **$\cot\alpha$ = 2.0**
- **n_p = 0.2**
- **s_{0p} = 0.02**

D101
- T = 32.7 min. H_{s0} = 0.12 m.
- No damage occurred.

D102
- T = 32.7 min. H_{s0} = 0.12 m.
- Damage recorded. One cube row 12, one cube row 15 (total of 2 cubes displaced).
- No anti reflection compensation (ARC).

D103
- T = 35.3 min. H_{s0} = 0.14 m.
- No extra damage.
- Some moving cubes.
- No anti reflection compensation (ARC).

D104
- T = 37.7 min. H_{s0} = 0.16 m.
- No extra damage.
- Some moving cubes.
- No anti reflection compensation (ARC).

D105
- T = 38.7 min. H_{s0} = 0.165 m.
- No extra damage.
- Some moving cubes.
- No anti reflection compensation (ARC).

The model was rebuild after this test serie.

D20X: The following characteristics were applied during the test serie:

- **$\cot\alpha$ = 2.0**
- **n_p = 0.2**
- **s_{0p} = 0.04**

D201
- T = 23.1 min. H_{s0} = 0.12 m.
- No damage occurred.

D202
- T = 25.0 min. H_{s0} = 0.14 m.
- Several cubes are lifted and returned to their original position.
- Damage recorded. One cube row 15, one cube row 16 (total of 2 cubes displaced).
- Cubes were found on slope.

D203
- T = 26.7 min. H_{s0} = 0.16 m.
- Several cubes are lifted and returned to their original position.
- No extra damage.

D204
- T = 28.3 min. H_{s0} = 0.18 m.
- Damage recorded. One cube row 14, one cube row 20 (total of 2 cubes displaced).

D205
- T = 28.3 min. H_{s0} = 0.18 m.
- Damage recorded. One cube row 13, one cube row 17 (total of 2 cubes displaced).
- No anti reflection compensation (ARC).

D206
- T = 29.8 min. H_{s0} = 0.20 m.
- Damage recorded (total of 11 cubes displaced).
- Model has failed.
- Some filter material on slope.
- No anti reflection compensation (ARC).

The model was rebuild after this test serie.

D30X: The following characteristics were applied during the test serie:

- **$\cot\alpha$ = 2.0**
- **n_p = 0.2**
- **s_{0p} = 0.06**

D301
- T = 20.4 min. H_{s0} = 0.14 m.
- No damage occurred.

D302
- T = 21.8 min. H_{s0} = 0.16 m.
- Damage recorded. One cube row 17 (total of 1 cube displaced).

D303
- T = 23.1 min. H_{s0} = 0.18 m.
- Damage recorded. One cube row 17, one cube row 18 (total of 2 cubes displaced).

D304
- T = 23.1 min. H_{s0} = 0.18 m.
- Damage recorded. One cube row 16, one cube row 17 (total of 2 cubes displaced).
- No anti reflection compensation (ARC).

D305
- T = 24.4 min. H_{s0} = 0.20 m.
- Damage recorded. One cube row 14, two cubes row 15, two cubes row 16, one cube row 17 (total of 6 cubes displaced).
- No anti reflection compensation (ARC).

D306
- T = 26.4 min. H_{s0} = 0.235 m.
- Damage recorded (total of 13 cubes displaced).
- Model failed.
- No anti reflection compensation (ARC).

The model was rebuild after this test serie.

E10X: The model consists of 37 rows of cubes (18 rows of 12 cubes, 19 rows of 13 cubes). A total of 463 cubes were used.

The following characteristics were applied during the test serie:

- **cotα = 2.0**
- **n_p = 0.3**
- **s_{0p} = 0.02**

E101
- T = 32.7 min. H_{s0} = 0.12 m.
- No damage occurred.
- No anti reflection compensation (ARC).

E102
- T = 35.3 min. H_{s0} = 0.14 m.
- No damage occurred.
- No anti reflection compensation (ARC).

E103
- T = 37.7 min. H_{s0} = 0.16 m.
- No damage occurred.
- Slightly moving cubes.
- No anti reflection compensation (ARC).

E104
- T = 38.7 min. H_{s0} = 0.165 m.
- No damage occurred.
- Slightly moving cubes.
- No anti reflection compensation (ARC).

The model was rebuild after this test serie.

E20X: The following characteristics were applied during the test serie:

- **cotα = 2.0**
- **n_p = 0.3**
- **s_{0p} = 0.04**

E201
- T = 25.0 min. H_{s0} = 0.14 m.
- No damage occurred.

E202
- T = 26.7 min. H_{s0} = 0.16 m.
- No damage occurred.

E203
- T = 28.3 min. H_{s0} = 0.18 m.
- No damage occurred.

E204
- T = 28.3 min. H_{s0} = 0.18 m.
- Several moving cubes.
- No anti reflection compensation (ARC).

E205
- T = 29.8 min. H_{s0} = 0.20 m.
- Several moving cubes.
- No anti reflection compensation (ARC).

Model was rebuild after this test serie.

E30X: The following characteristics were applied during the test serie:

- **cotα = 2.0**
- **n_p = 0.3**
- **s_{0p} = 0.06**

E301
- T = 20.4 min. H_{s0} = 0.14 m.
- No damage occurred.

E302
- T = 21.8 min. H_{s0} = 0.16 m.
- No damage occurred.

E303
- T = 23.1 min. H_{s0} = 0.18 m.
- No damage occurred.

E304
- T = 23.1 min. H_{s0} = 0.18 m.
- Several moving cubes.
- No anti reflection compensation (ARC).

E305
- T = 24.4 min. H_{s0} = 0.20 m.
- Several moving cubes.
- No anti reflection compensation (ARC).

E306
- T = 26.4 min. H_{s0} = 0.235 m.
- Several cubes are lifted and returned to their original position.
- No anti reflection compensation (ARC).

Model was rebuild after this test serie.

F10X: The model consists of 37 rows of cubes (18 rows of 11 cubes, 19 rows of 12 cubes). A total of 426 cubes were used.

The following characteristics were applied during the test serie:

- **cotα = 2.0**
- **n_p = 0.35**
- **s_{0p} = 0.02**

F101
- T = 32.7 min. H_{s0} = 0.12 m.
- No damage occurred.
- Some slightly rotating cubes (2).
- No anti reflection compensation (ARC).

F102
- T = 35.3 min. H_{s0} = 0.14 m.
- No damage occurred.
- Some slightly rotating cubes (3).
- No anti reflection compensation (ARC).

F103
- T = 37.7 min. H_{s0} = 0.16 m.
- No damage occurred.
- Some rotating cubes (8).
- No anti reflection compensation (ARC).

F104
- T = 38.7 min. H_{s0} = 0.165 m.
- No damage occurred.
- Rotating cubes (8).
- No anti reflection compensation (ARC).

The model was rebuild after this test serie.

F20X: The following characteristics were applied during the test serie:

- **cotα = 2.0**
- **n_p = 0.35**
- **s_{0p} = 0.04**

F201
- T = 25.0 min. H_{s0} = 0.14 m.
- Three slightly rotating cubes.
- No damage occurred.

F202
- T = 26.7 min. H_{s0} = 0.16 m.
- Some rotating cubes.
- A bit of settling occurred.
- No damage occurred.

F203
- T = 28.3 min. H_{s0} = 0.18 m.
- Settling cubes (7).
- No real damage occurred.

F204
- T = 28.3 min. H_{s0} = 0.18 m.
- Several moving cubes.
- Damage recorded. One cube out of armour layer.
- No anti reflection compensation (ARC).

F205
- T = 29.8 min. H_{s0} = 0.20 m.
- Several moving cubes.
- Damage recorded. More cubes out of armour layer (total of 3 cubes displaced).
- Twelve cubes subsided more than one cube diameter.
- Model failed.
- No anti reflection compensation (ARC).

Model was rebuild after this test serie.

F30X: The following characteristics were applied during the test serie:

- **$\cot\alpha$ = 2.0**
- **n_p = 0.35**
- **s_{0p} = 0.06**

F301
- T = 18.9 min. H_{s0} = 0.12 m.
- No damage occurred.

F302
- T = 20.4 min. H_{s0} = 0.14 m.
- No damage occurred.

F303
- T = 21.8 min. H_{s0} = 0.16 m.
- No damage occurred.

F304
- T = 23.1 min. H_{s0} = 0.18 m.
- No damage occurred.

F305
- T = 23.1 min. H_{s0} = 0.18 m.
- No damage occurred.
- No anti reflection compensation (ARC).

F306
- T = 24.4 min. H_{s0} = 0.20 m.
- Several rotating cubes.
- No damage occurred.
- No anti reflection compensation (ARC).

This was the final test serie.

APPENDIX G; PHOTOS OF TEST SERIES

Figure G 1. Test serie A0

Figure G 2. Test serie A1

Figure G 3. Test serie A2

Figure G 4. Test serie A3

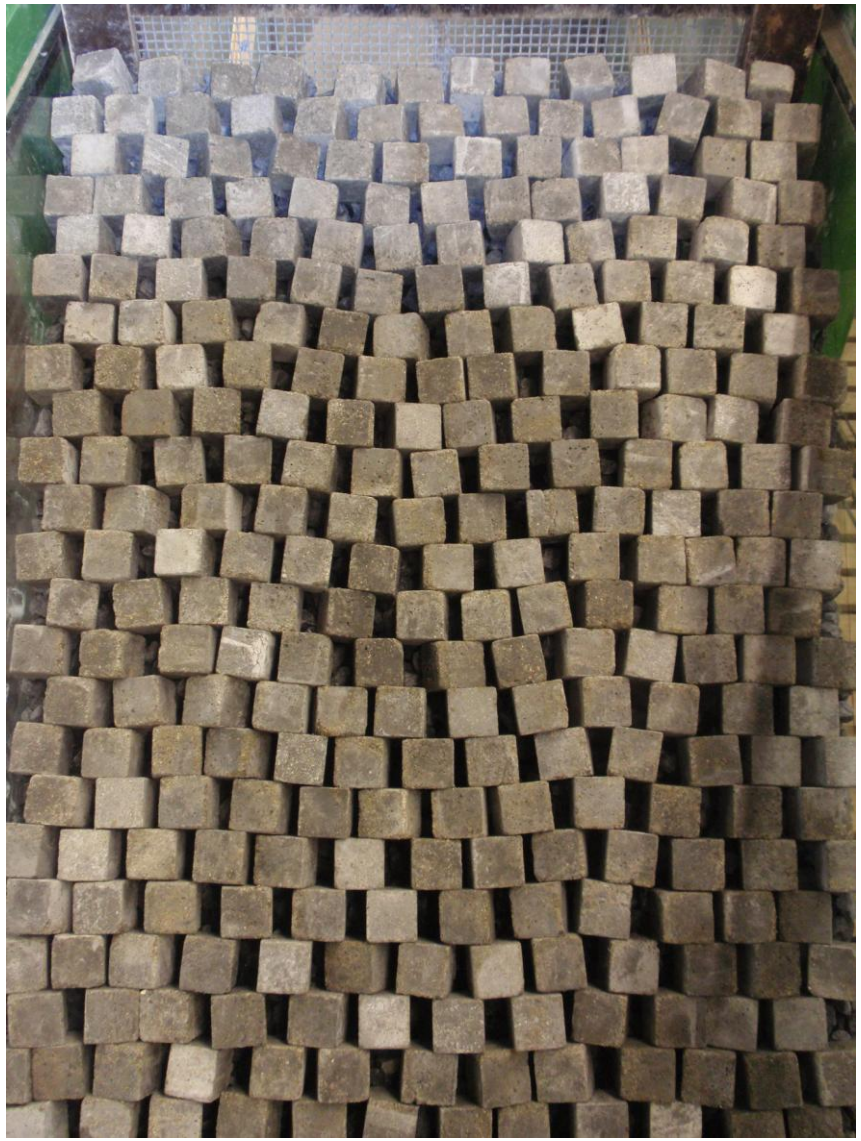

Figure G 5. Test serie B0

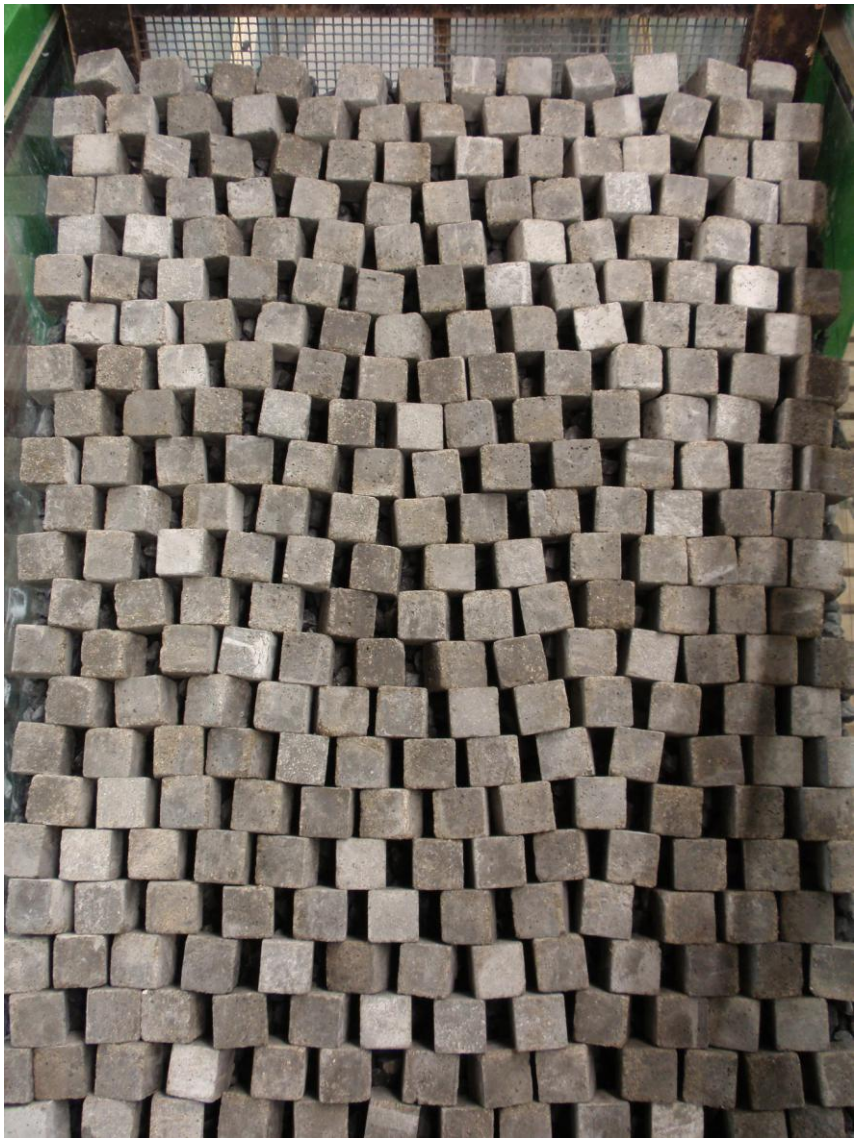

Figure G 6. Test serie B1

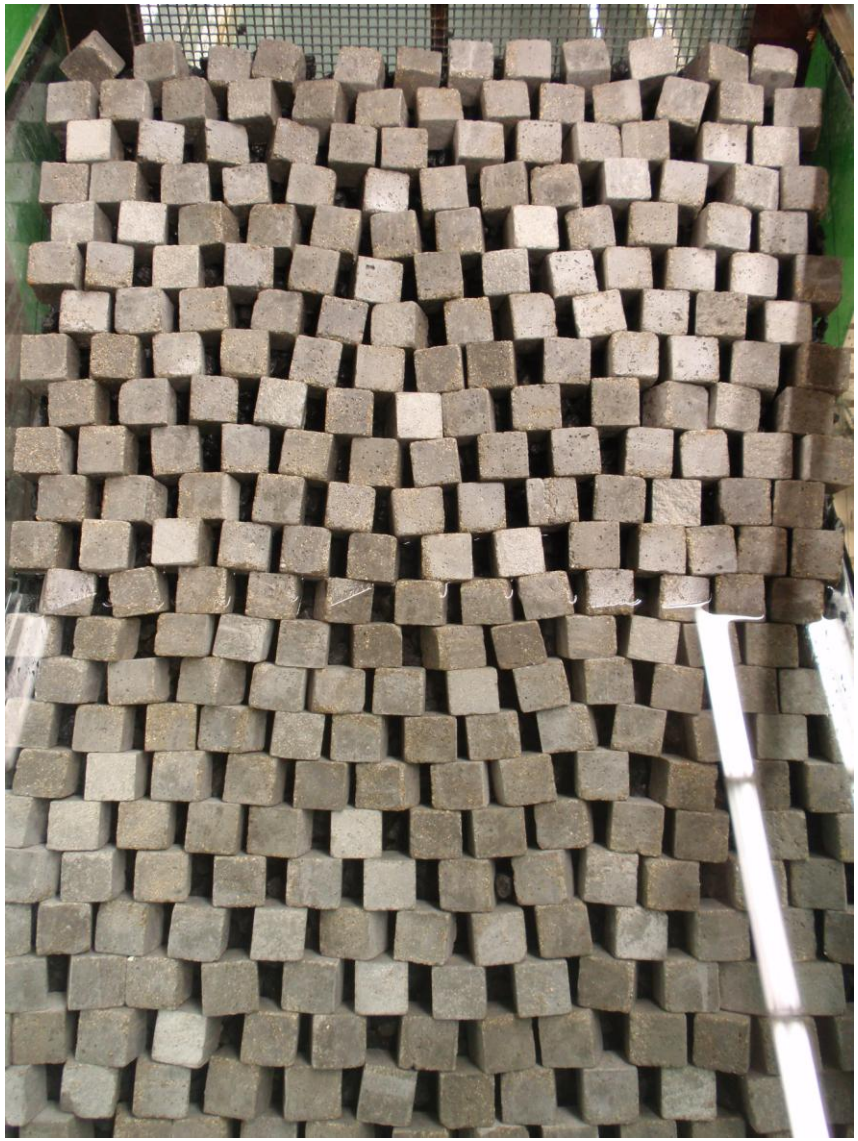

Figure G 7. Test serie B2

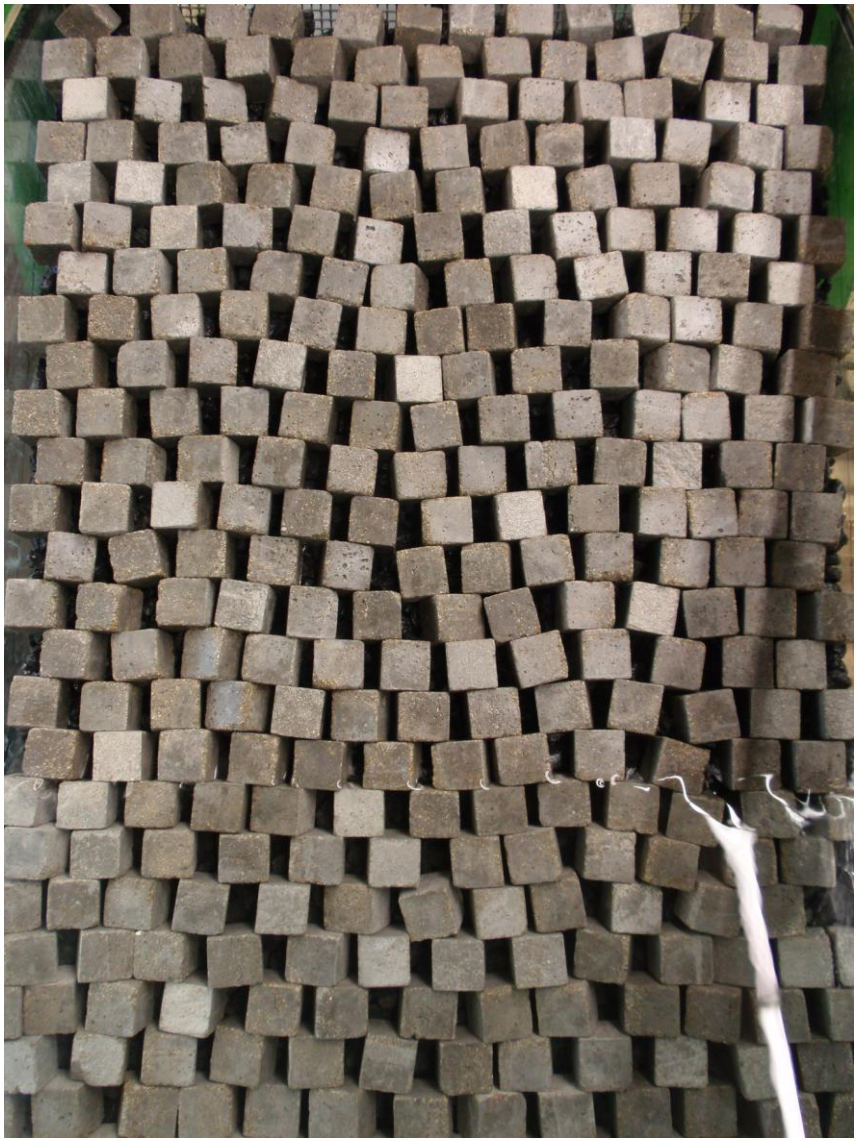

Figure G 8. Test serie B3

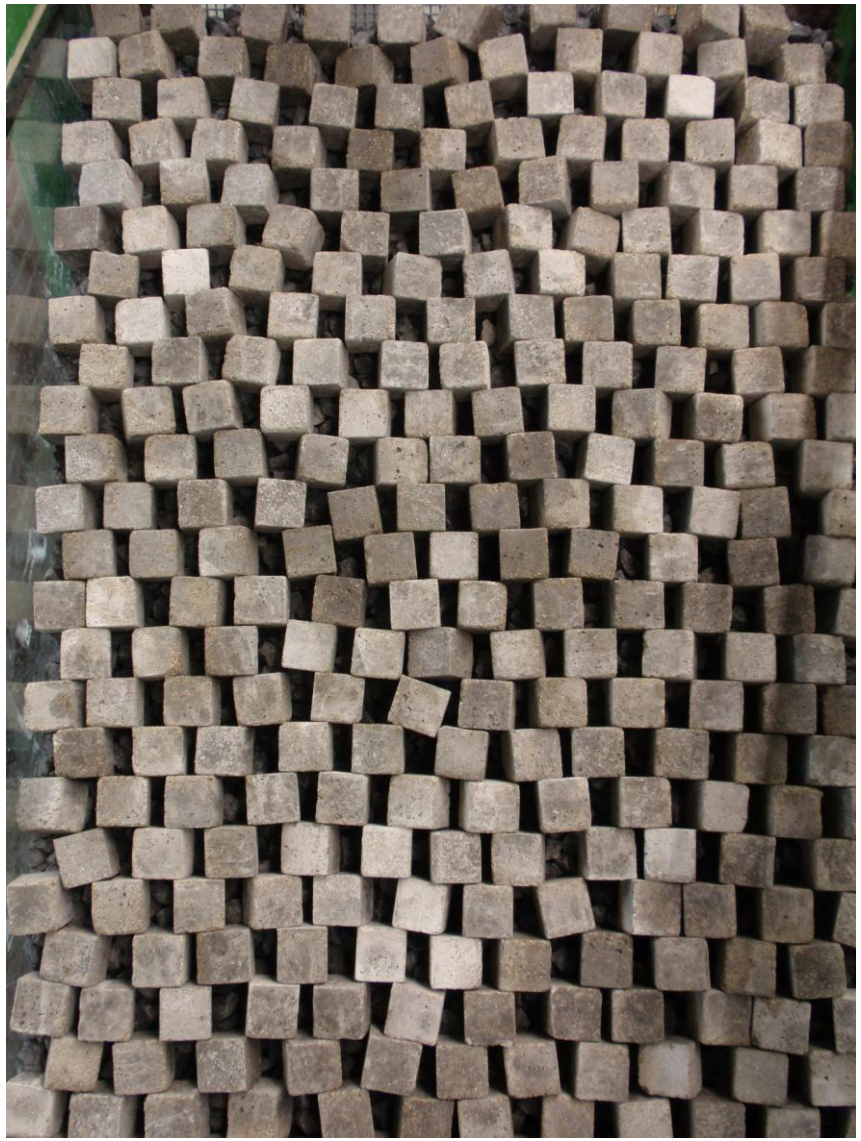

Figure G 9. Test serie C0

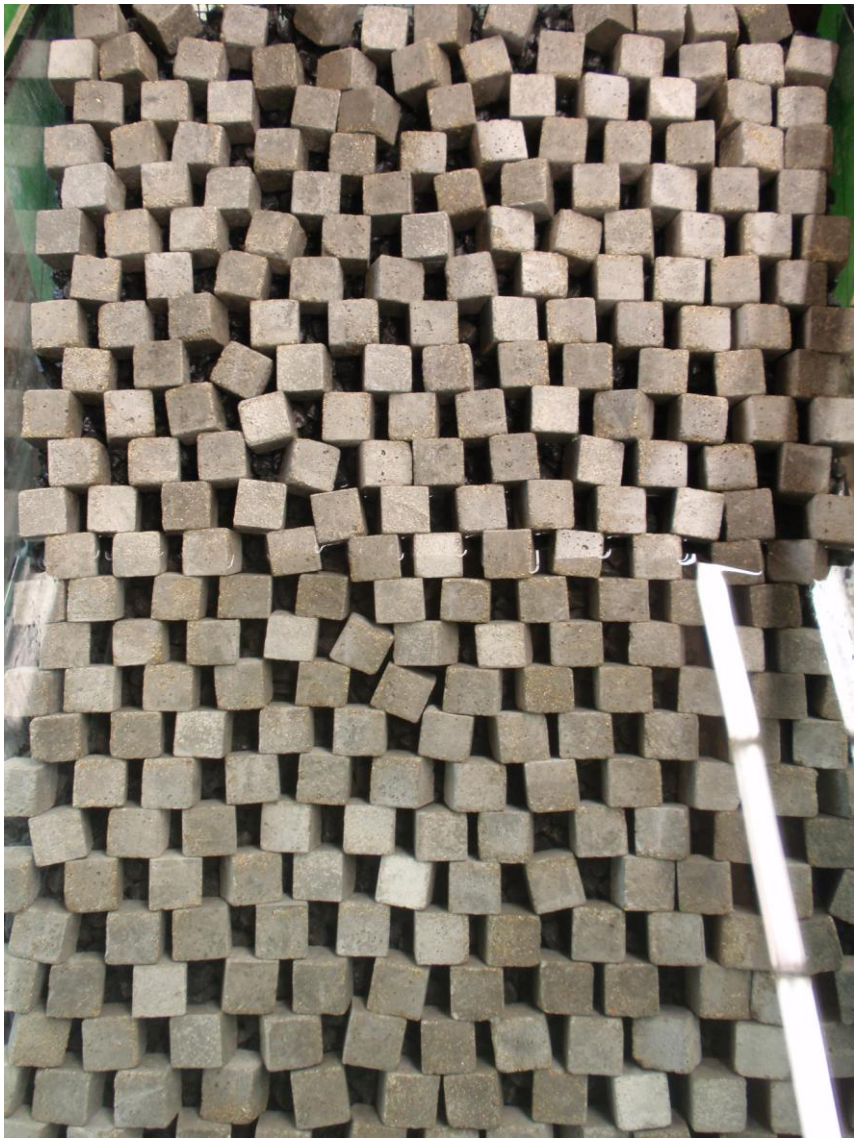

Figure G 10. Test serie C1

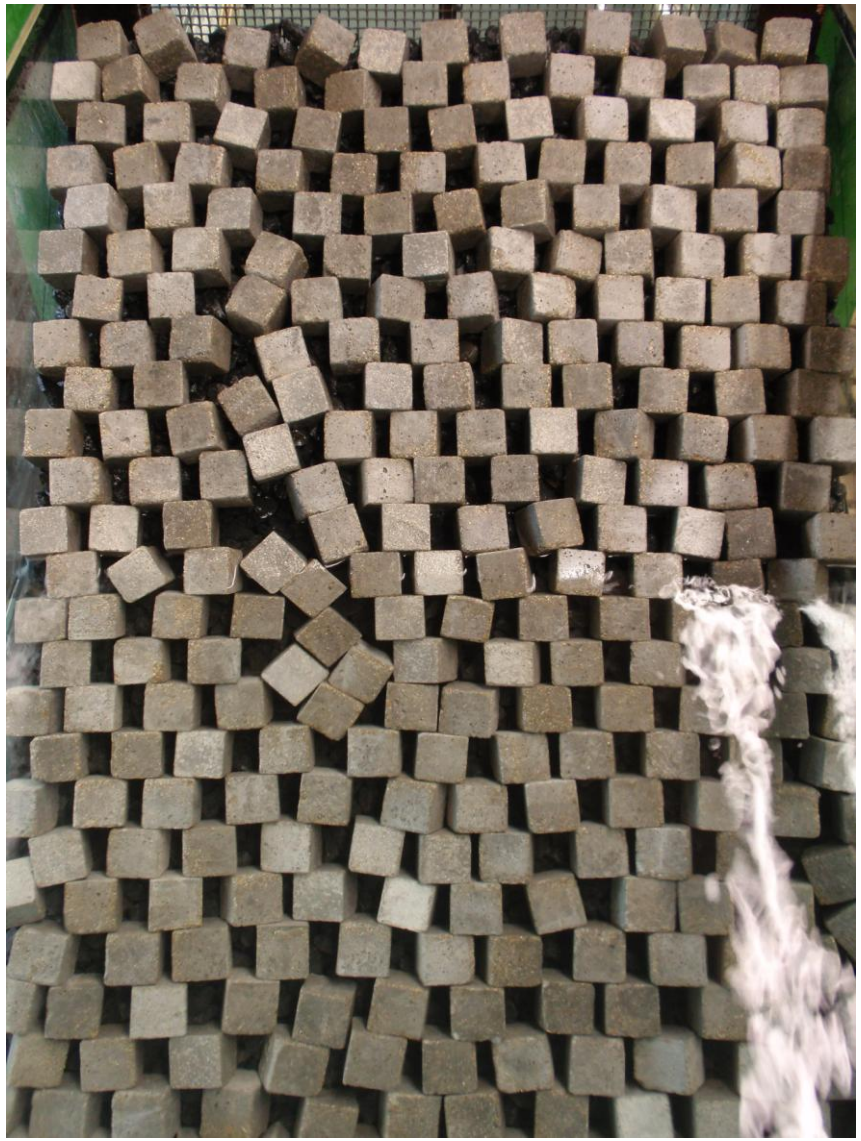

Figure G 11. Test serie C2

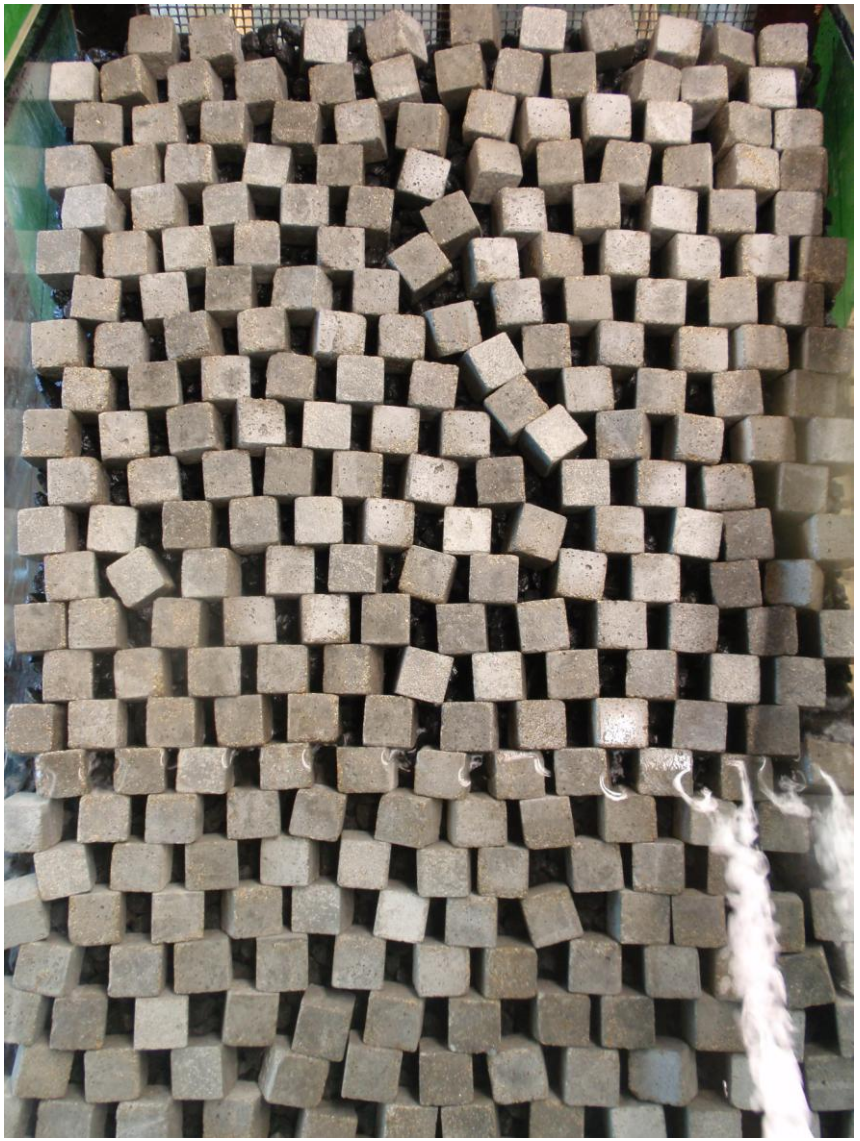

Figure G 12. Test serie C3

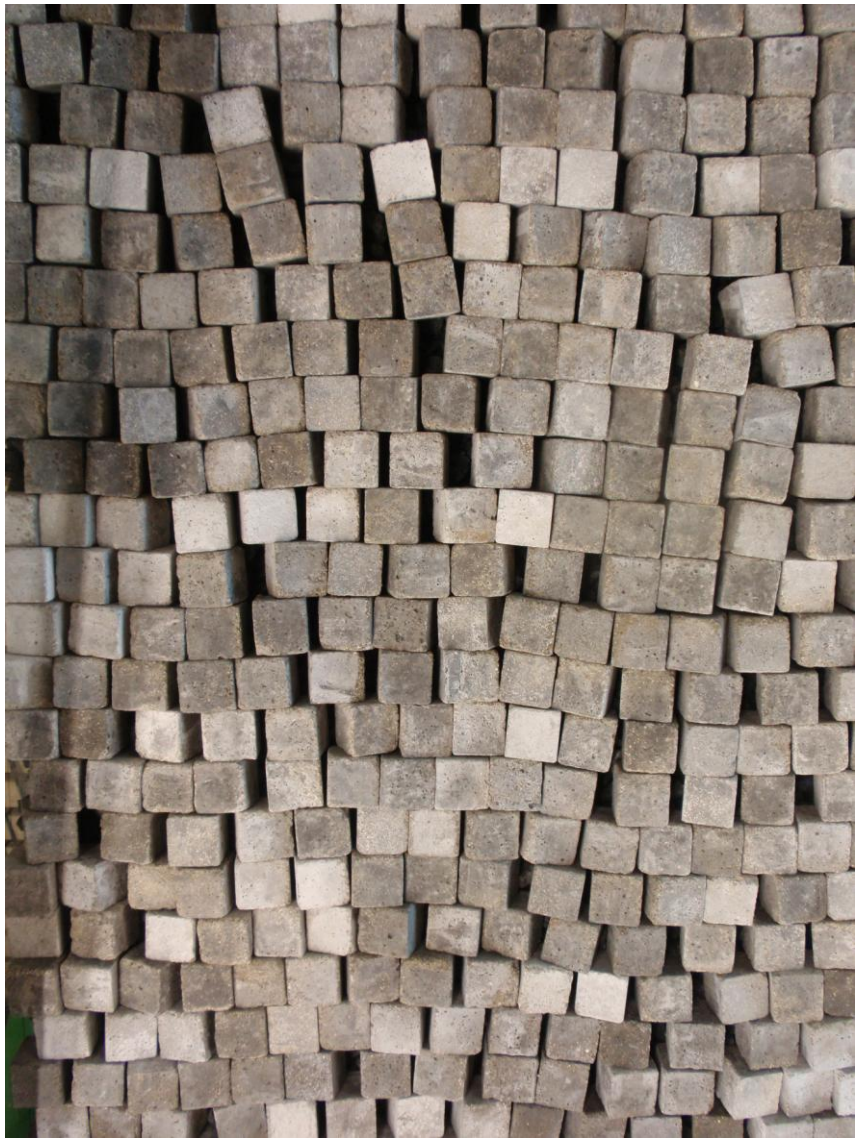

Figure G 13. Test serie D0

Figure G 14. Test serie D1

Figure G 15. Test serie D2

Figure G 16. Test serie D3

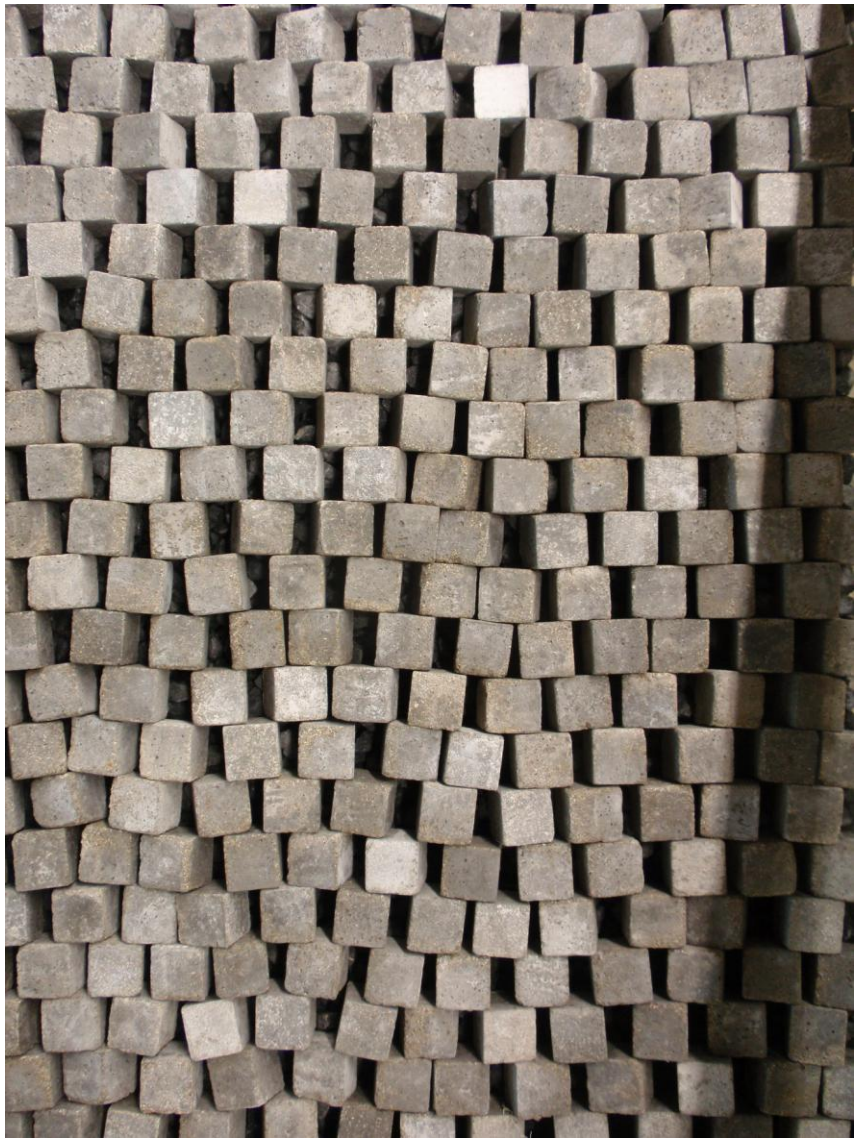

Figure G 17. Test serie E0

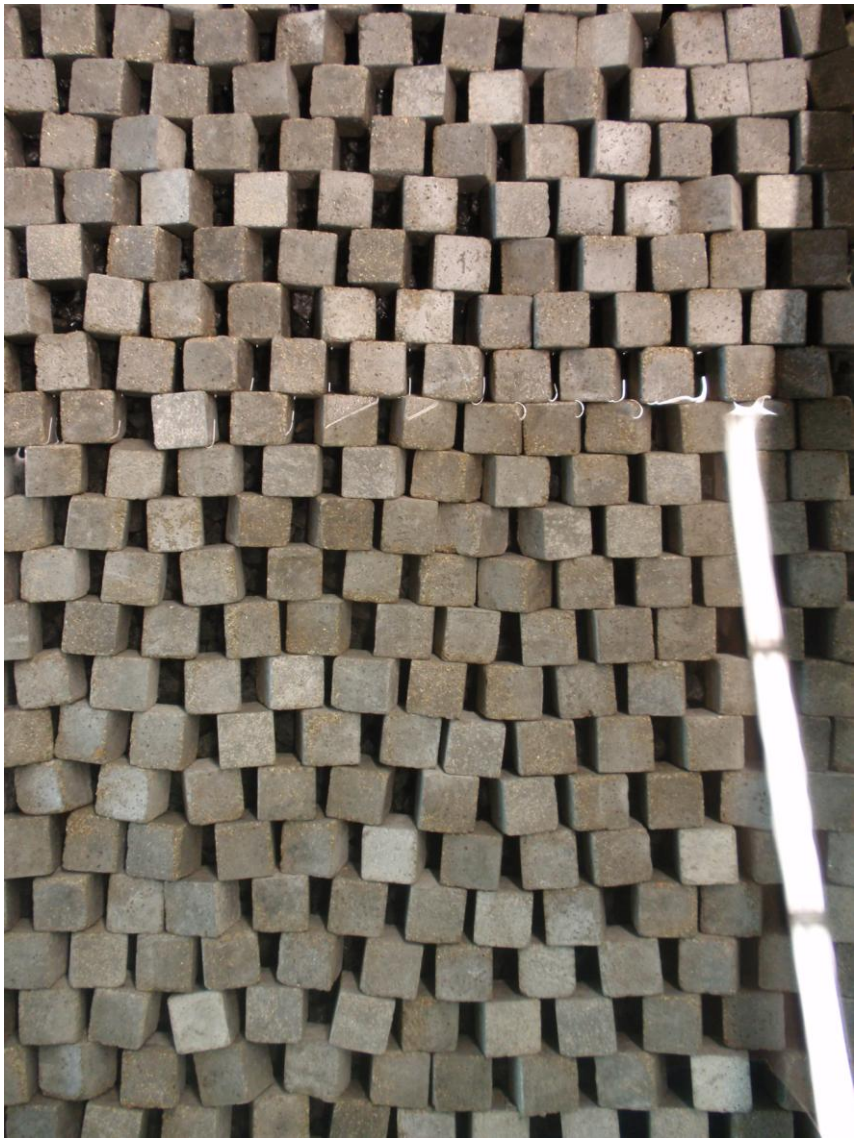

Figure G 18. Test serie E1

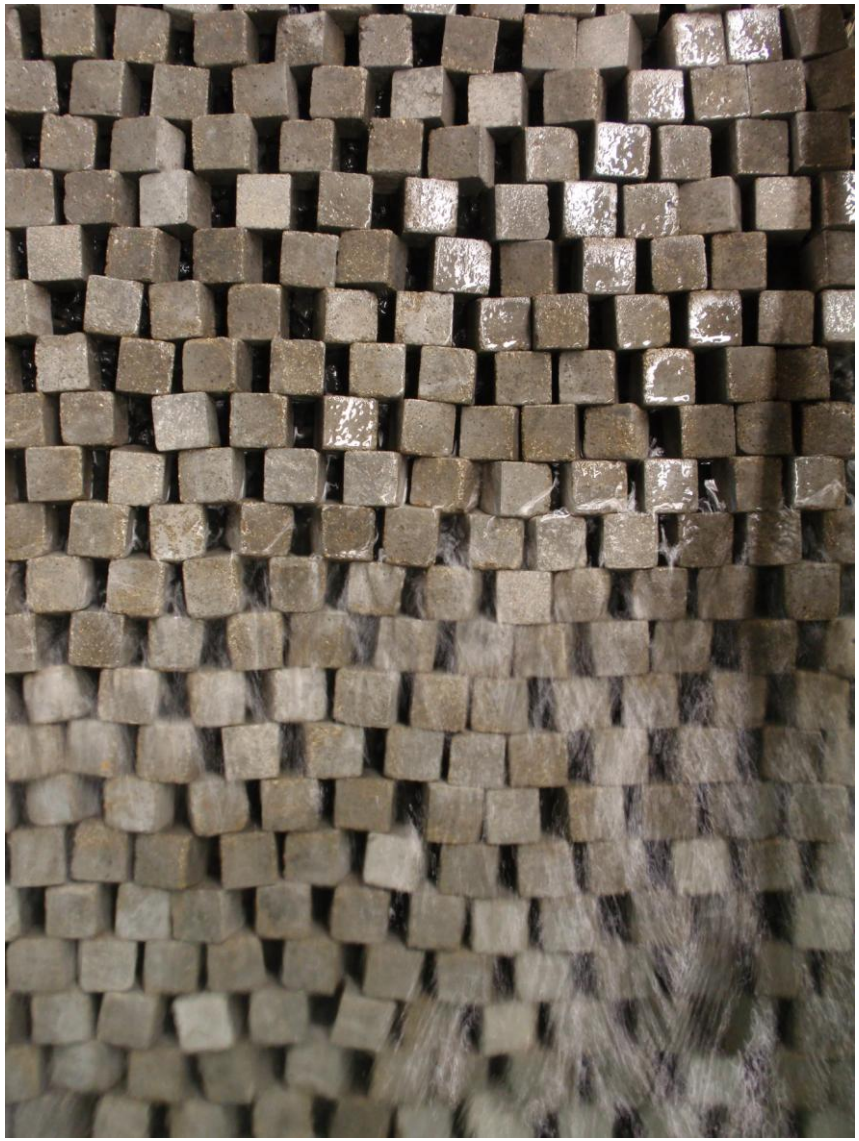

Figure G 19. Test serie E2

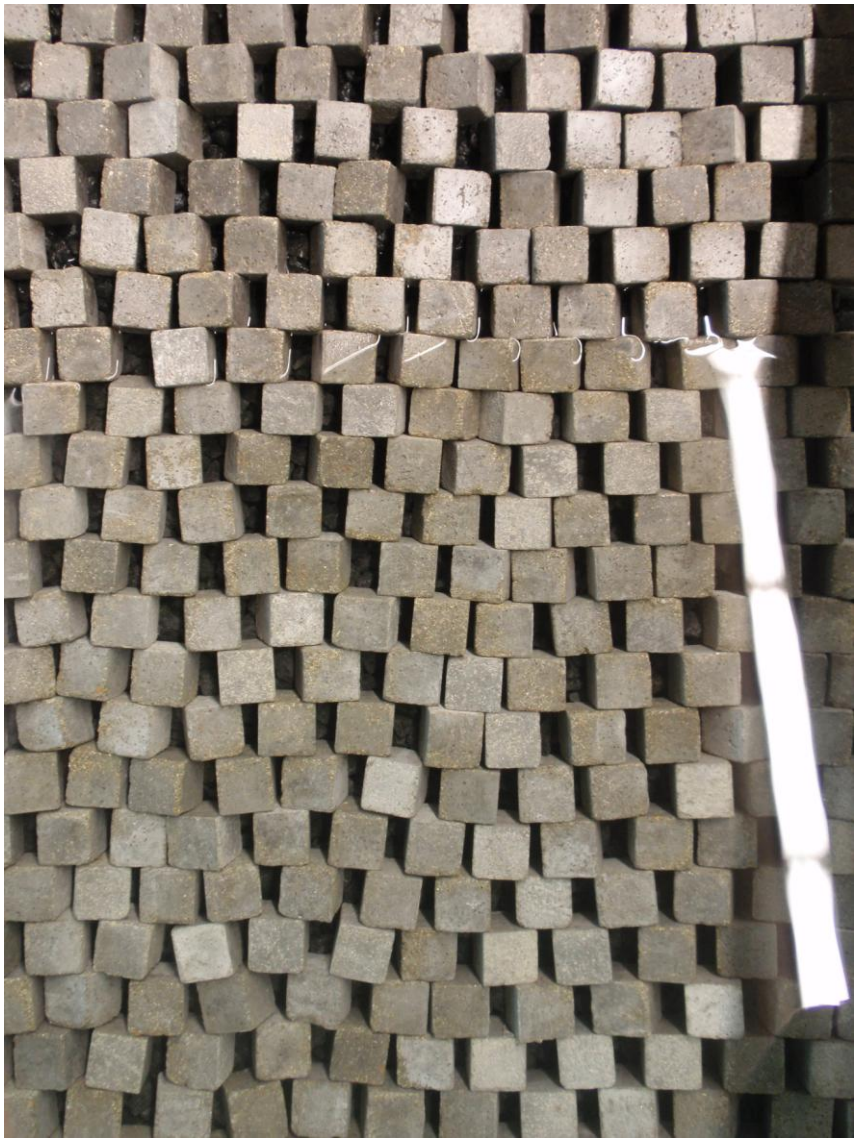

Figure G 20. Test serie E3

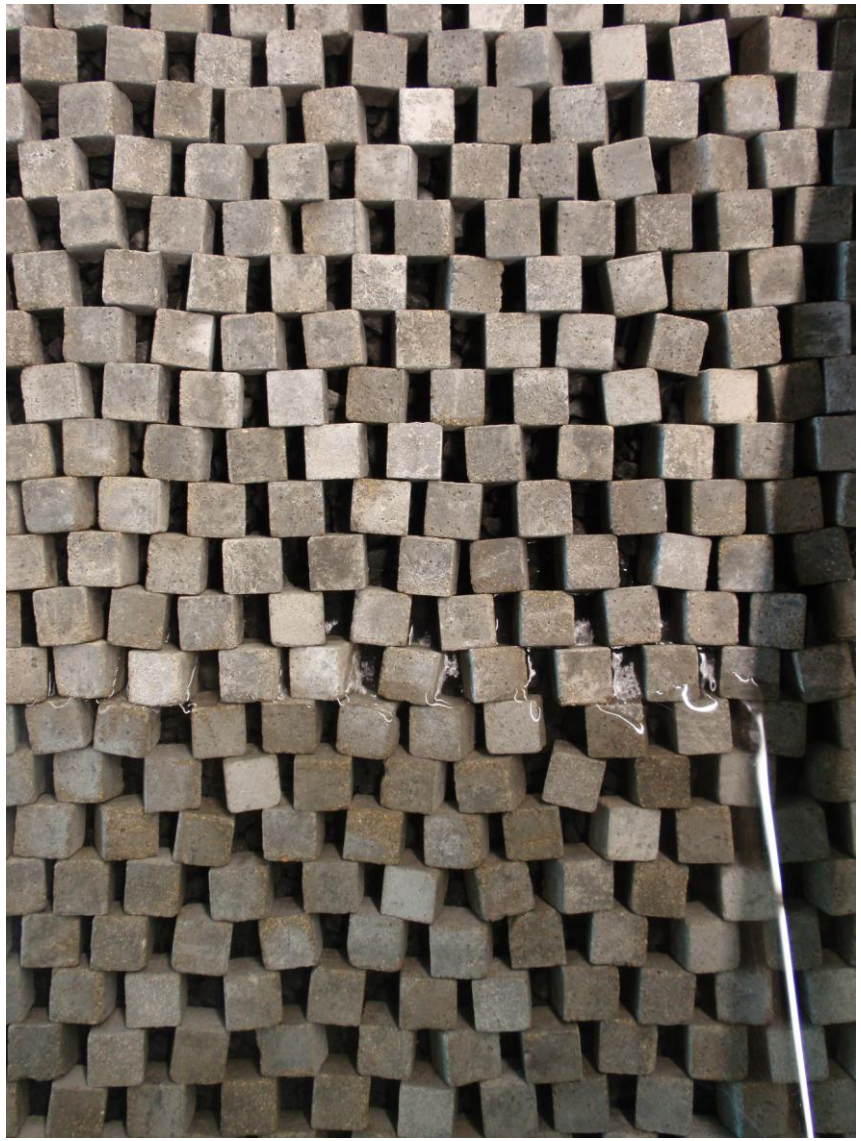

Figure G 21. Test serie F0

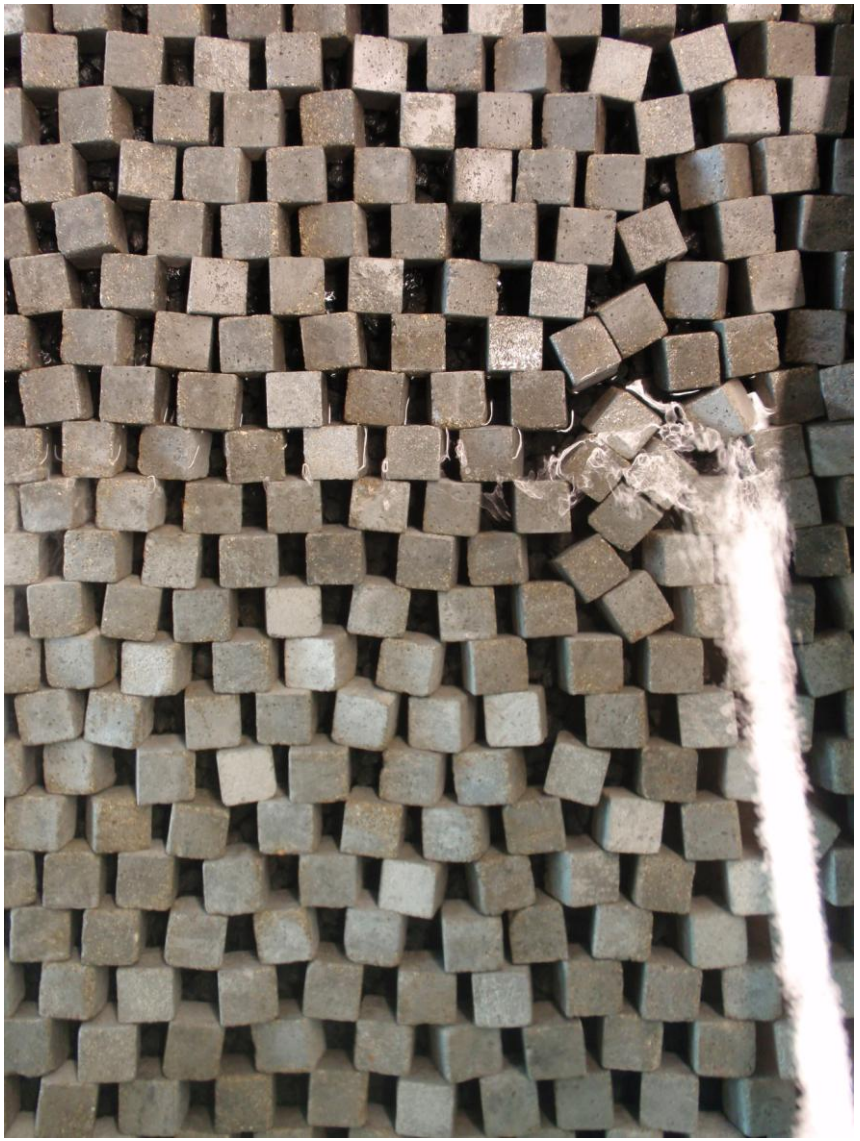

Figure G 22. Test serie F1

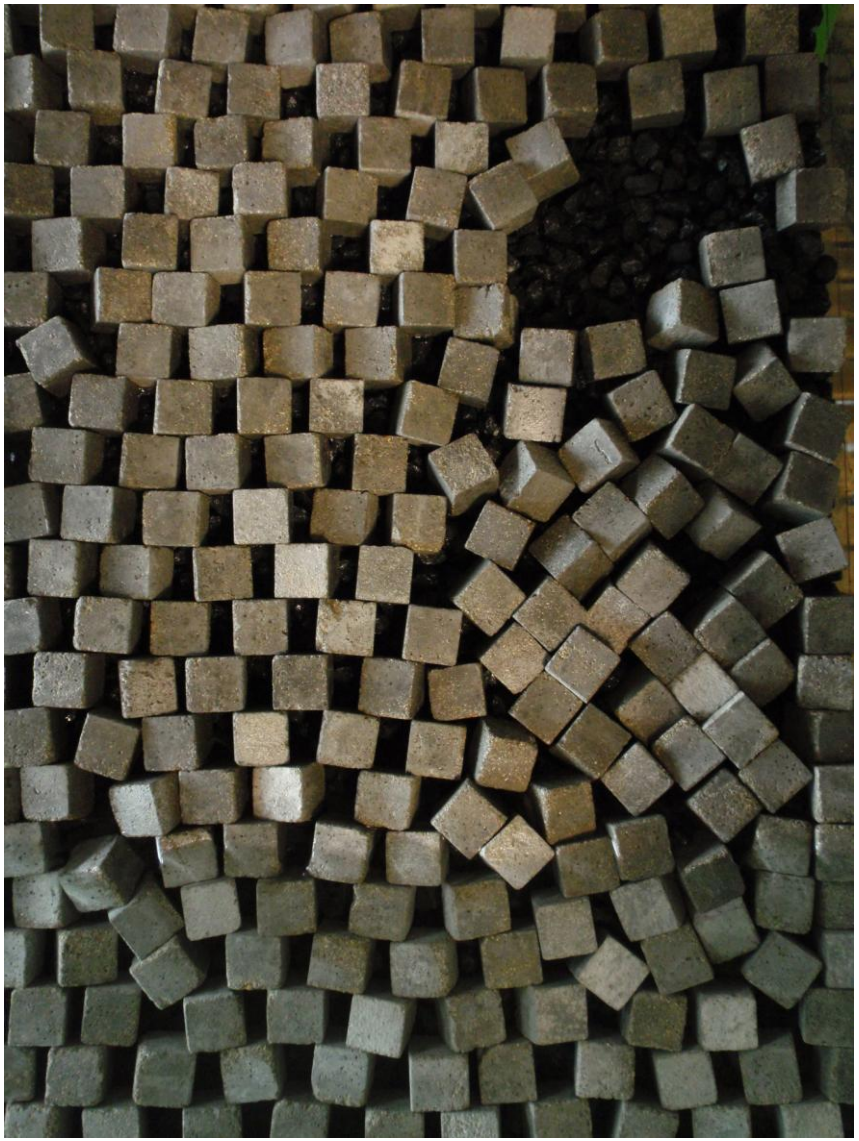

Figure G 23. Test serie F2

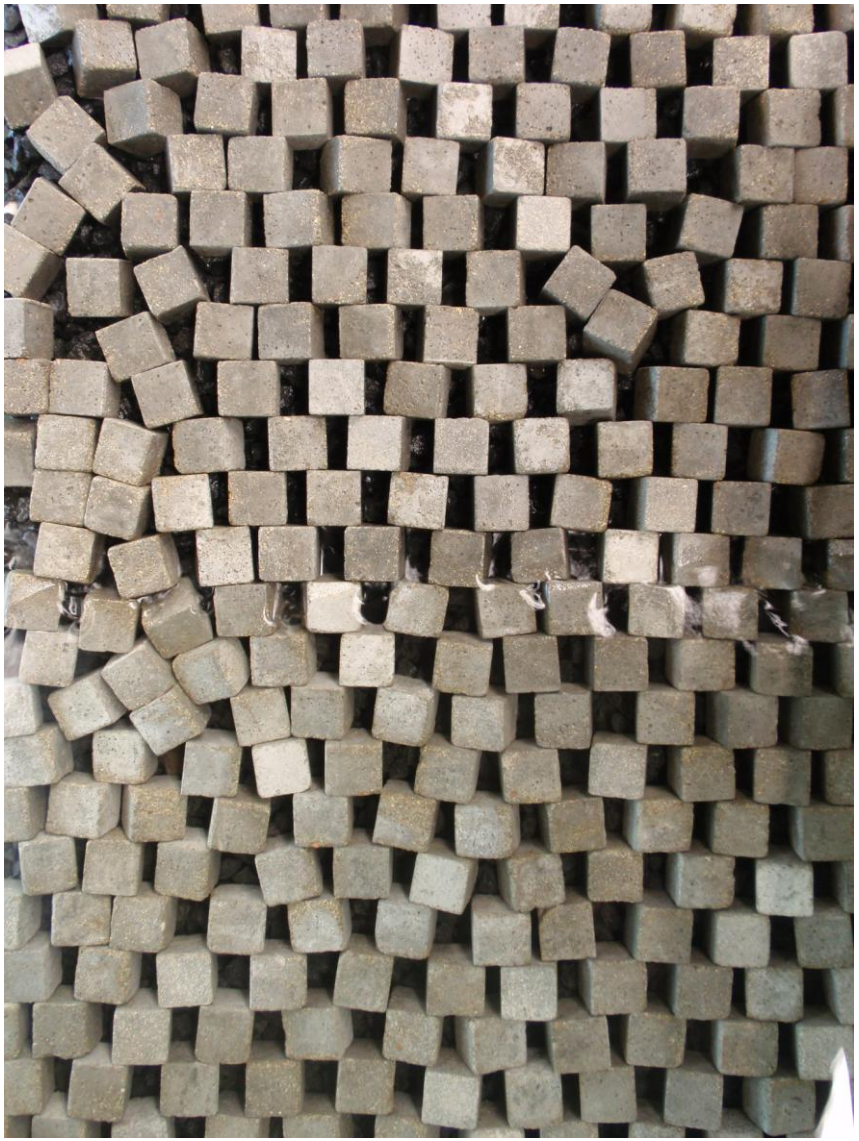

Figure G 24. Test serie F3

APPENDIX H; XI-RULE PLOTS

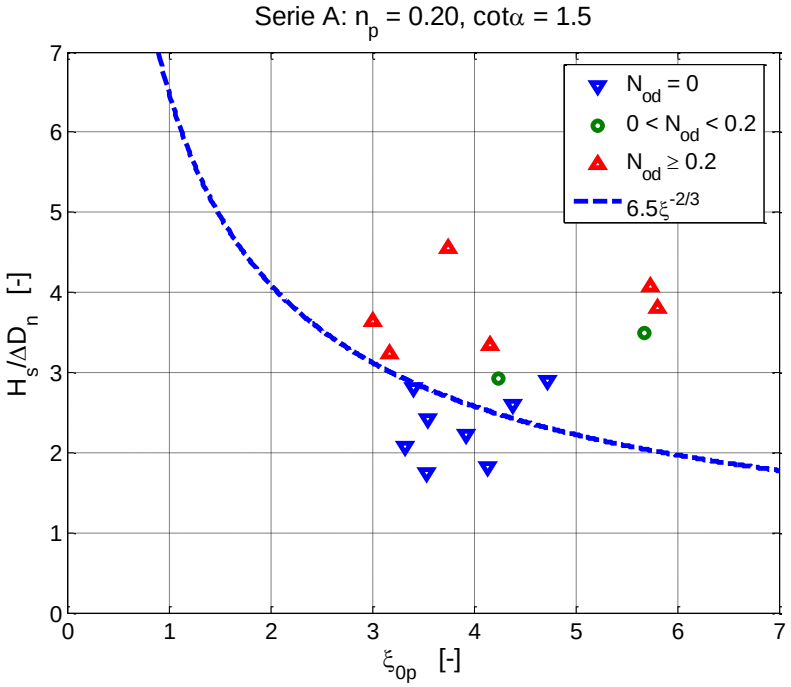

Figure H 1. Serie A.

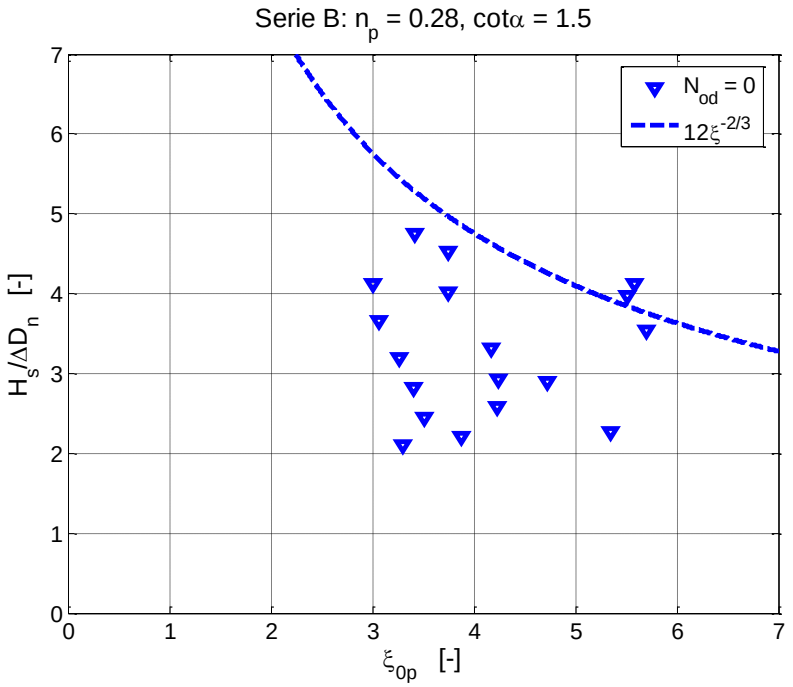

Figure H 2. Serie B.

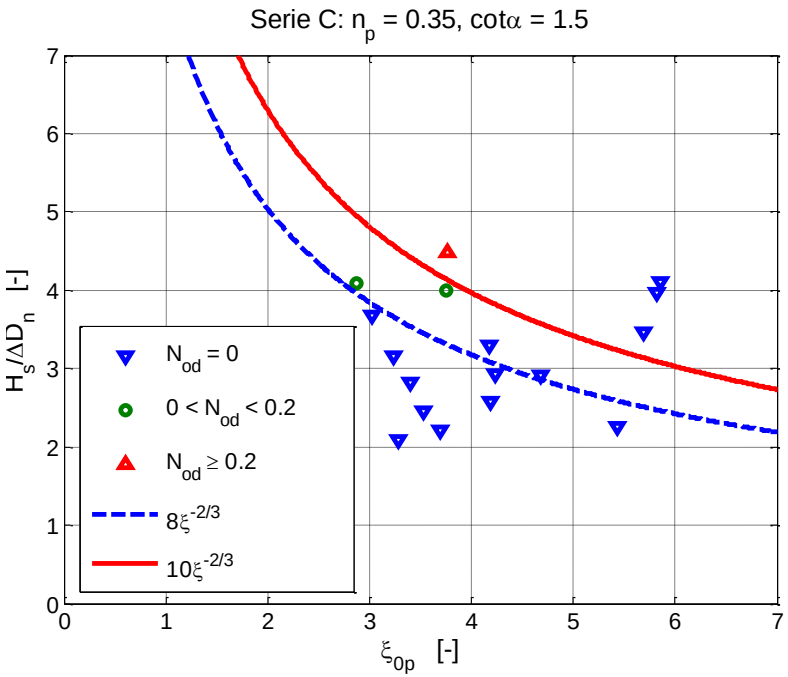

Figure H 3. Serie C.

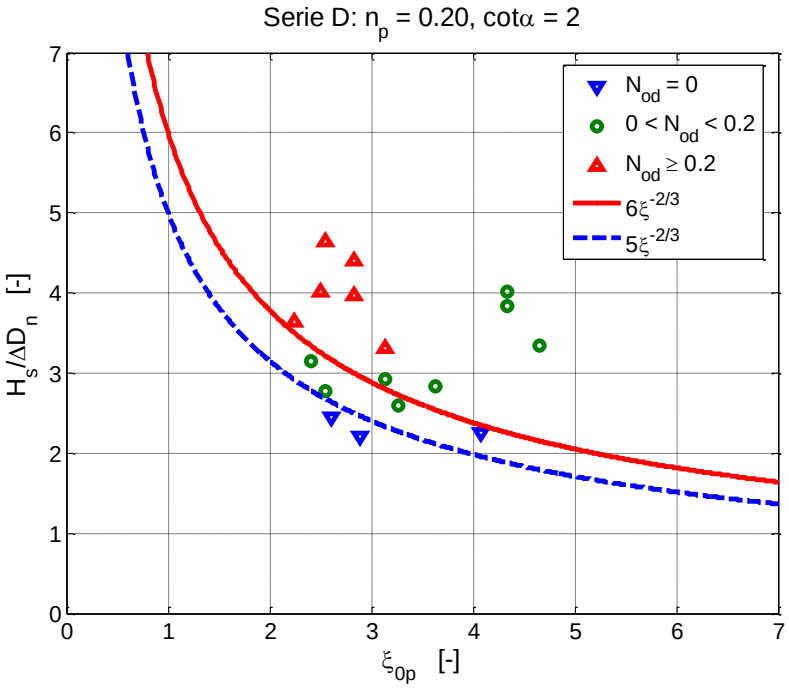

Figure H 4. Serie D.

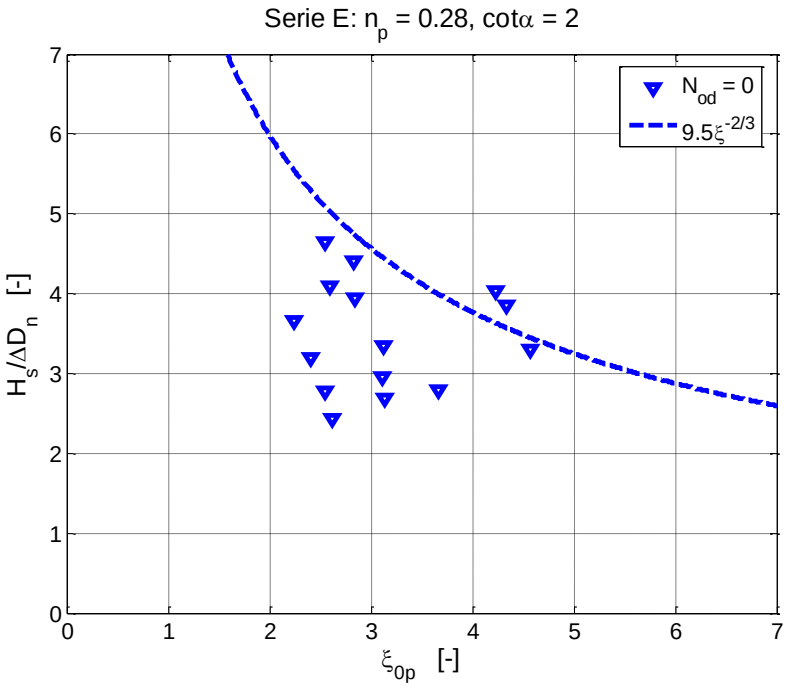

Figure H 5. Serie E.

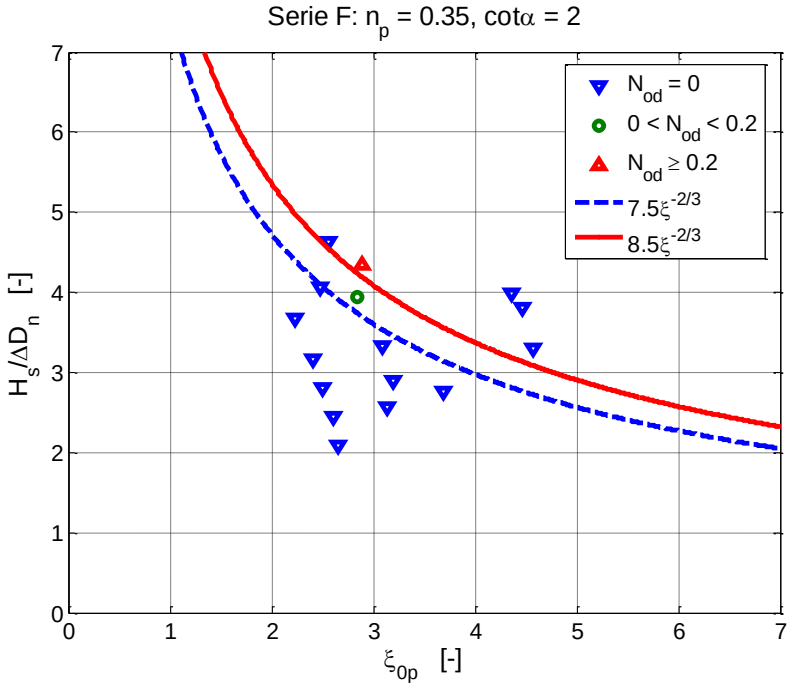

Figure H 6. Serie F.

APPENDIX I; PLOTS BASED ON FORMULAE

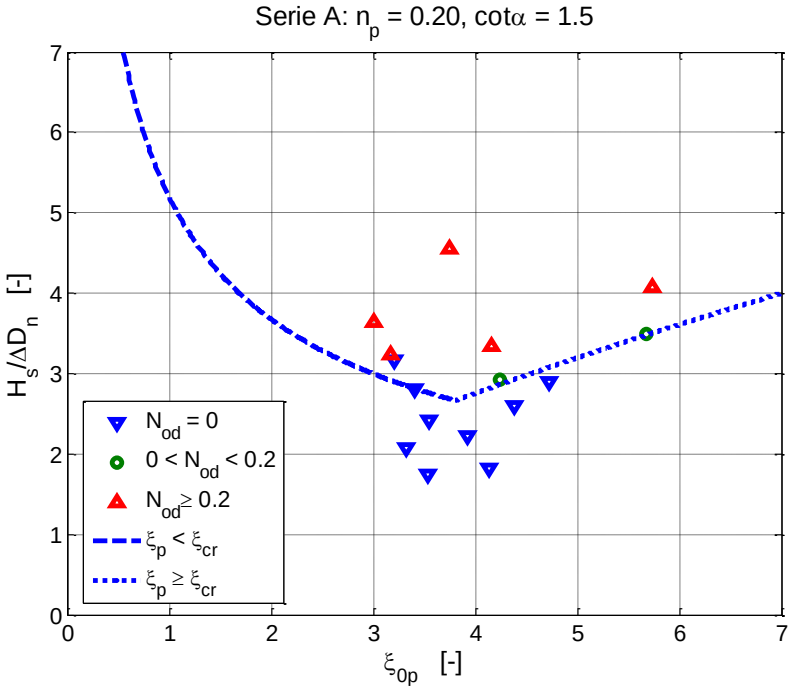

Figure I 1. Serie A.

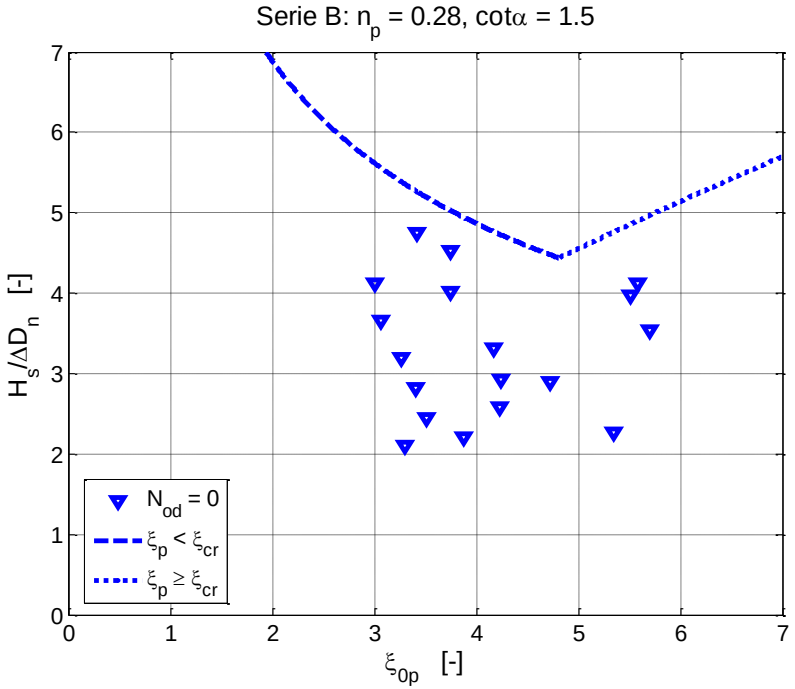

Figure I 2. Serie B.

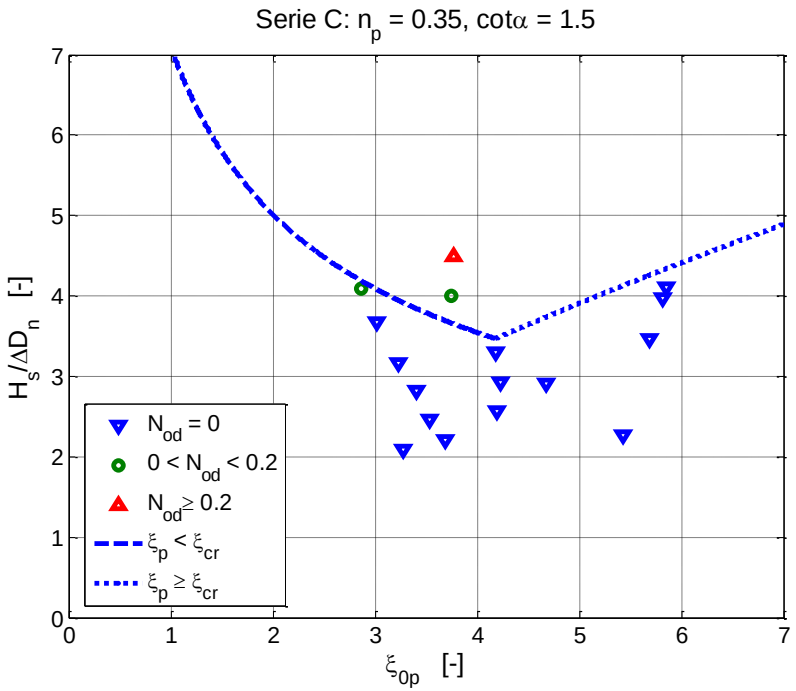

Figure I 3. Serie C.

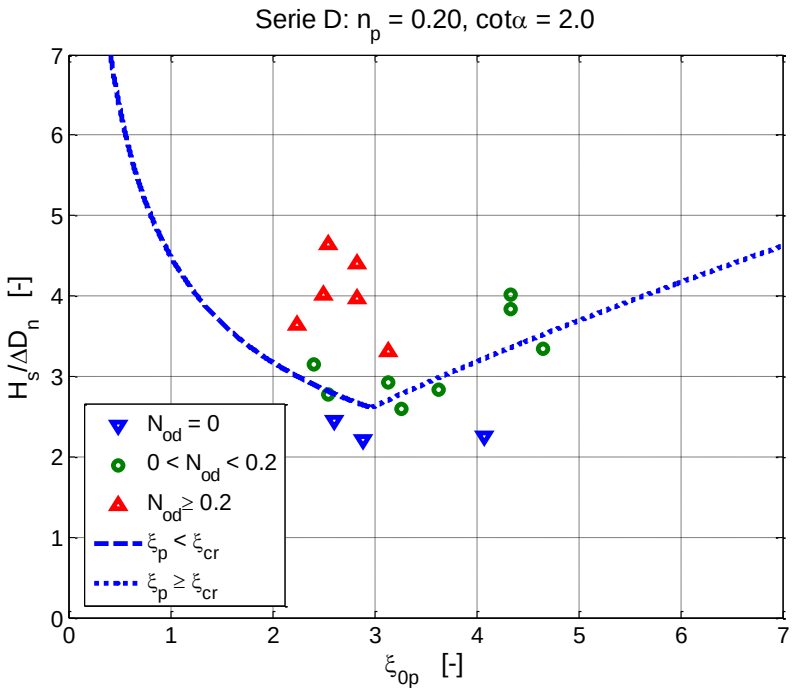

Figure I 4. Serie D.

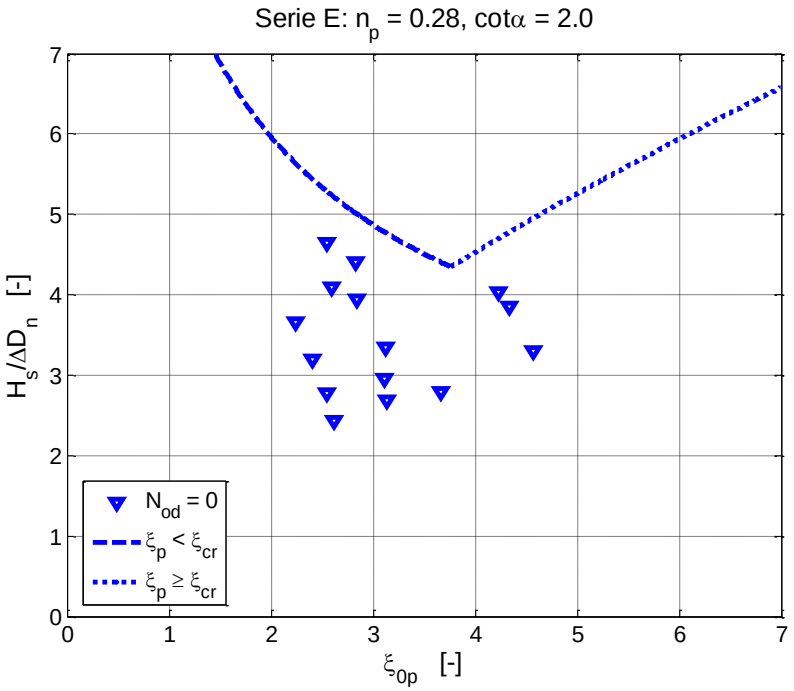

Figure I 5. Serie E.

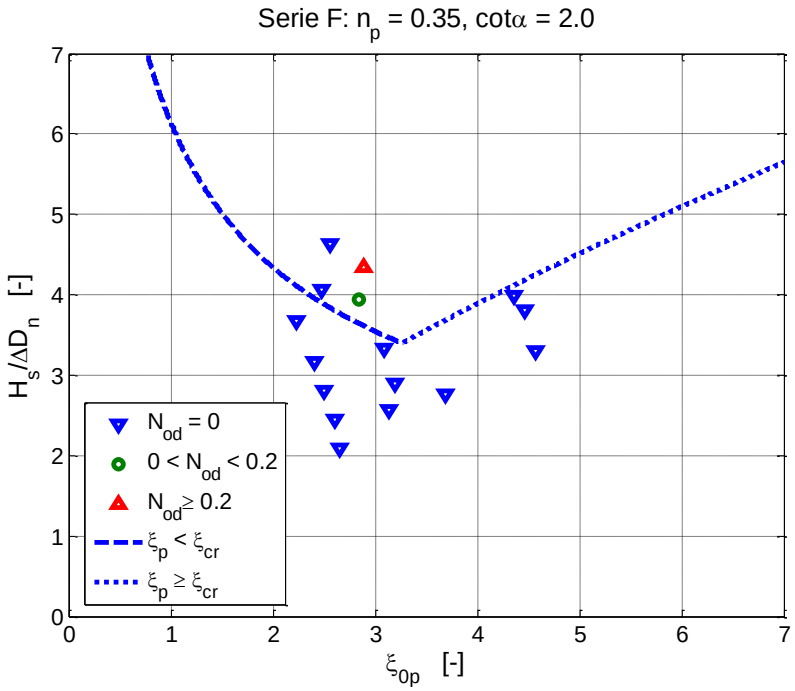

Figure I 6. Serie F.

APPENDIX J; PLOTTED GRAPHS ALL SERIES

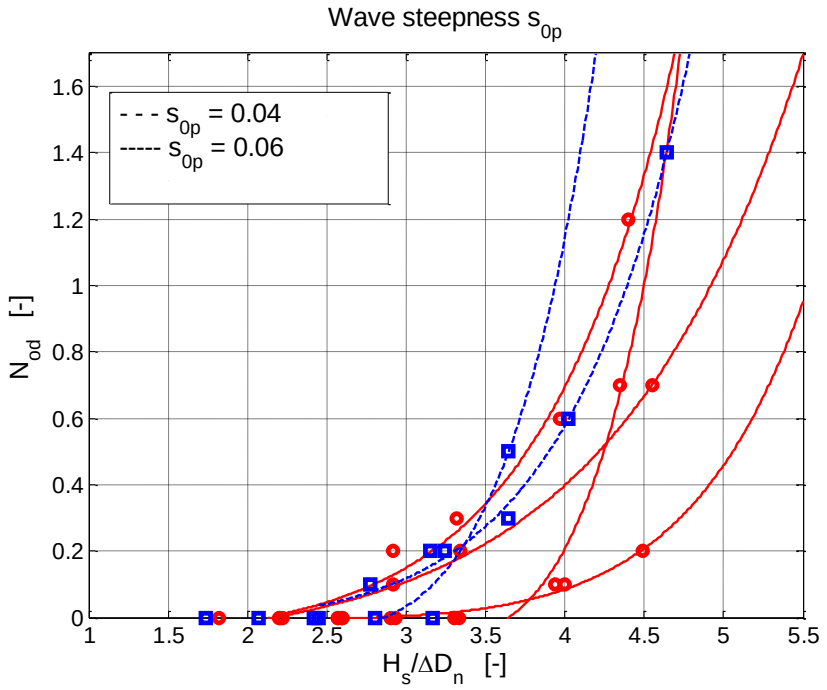

Figure J 1. Wave steepness

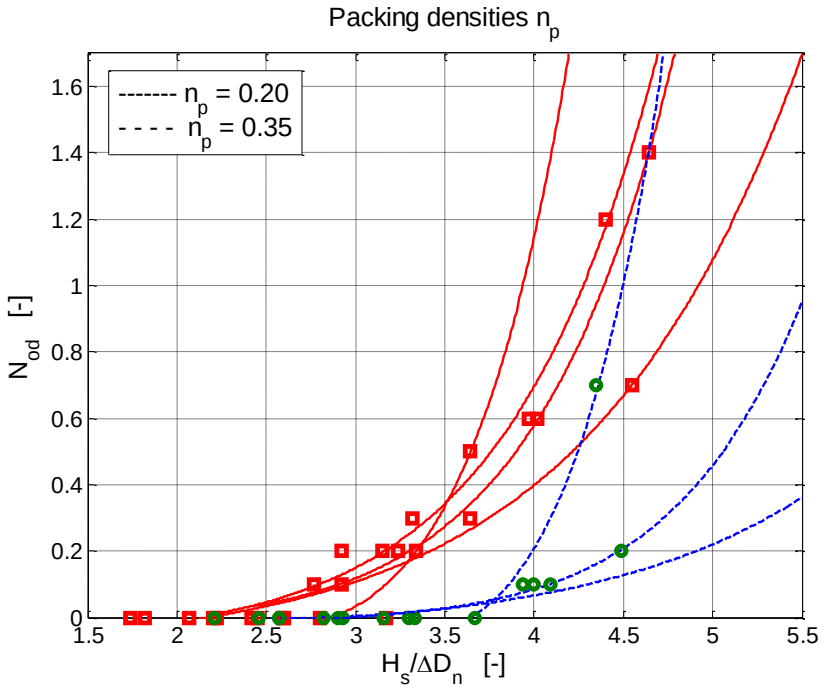

Figure J 2. Packing densities

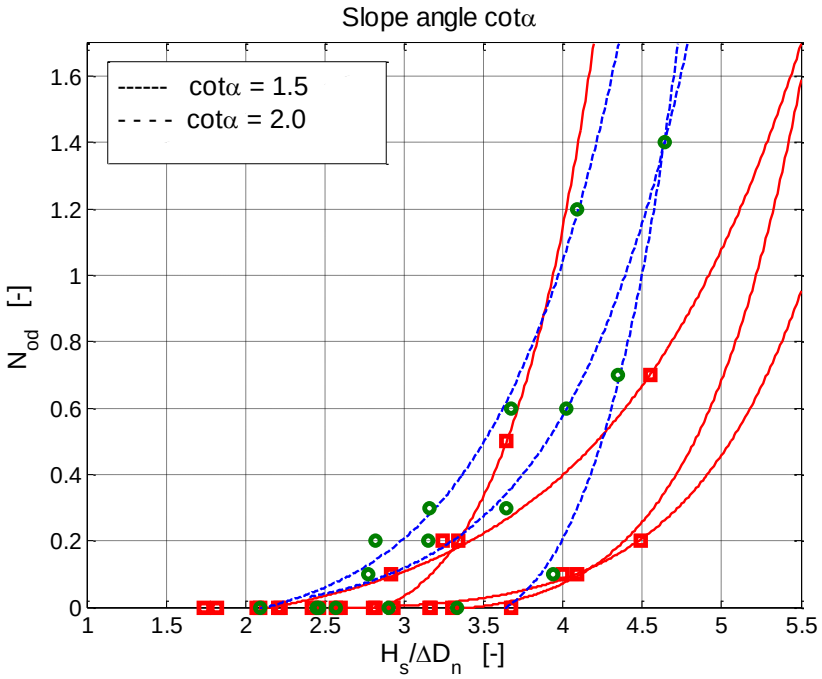

Figure J 3. Slopes